Receptor Kinases Regulating Rhizobial Infection

Erik Limpens

Promotor: prof. dr. A.H.J. Bisseling
Hoogleraar in de Moleculaire Biologie
Wageningen Universiteit

Co-promotor: dr. ir. R. Geurts
Universitair docent
Laboratorium voor Moleculaire Biologie
Wageningen Universiteit

Promotiecommissie:
prof. dr. H.P. Spaink, Universiteit Leiden
prof. dr. P.J.G.M. de Wit, Wageningen Universiteit
dr. R. Heidstra, Universiteit Utrecht
prof. dr. G.C. Angenent, Katholieke Universiteit Nijmegen

Dit onderzoek is uitgevoerd binnen de onderzoekschool Experimentele Plantwetenschappen.

Receptor Kinases Regulating Rhizobial Infection

Erik Limpens

Proefschrift

ter verkrijging van de graad van doctor
op gezag van de rector magnificus
van Wageningen Universiteit,
prof. dr. ir. L. Speelman,
in het openbaar te verdedigen
op vrijdag 18 juni 2004
des namiddags te vier uur in de Aula.

Receptor Kinases Regulating Rhizobial Infection

Limpens, Erik

Thesis Wageningen University, The Netherlands
With references - with summary in Dutch

ISBN 90-5804-059-0

Contents

Outline **7**

Chapter 1 **11**
Signaling in Symbiosis. *Current Opinion in Plant Biology* 2003, **6**: 343-350

Chapter 2 **27**
Microsynteny between pea and *Medicago truncatula* in the *SYM2* region**.**
Plant Molecular Biology 2002, **50**: 225-235

Chapter 3 **43**
RNA interference in *Agrobacterium rhizogenes* transformed roots of Arabidopsis and *Medicago truncatula*. *Journal of Experimental Botany* 2004, **55**: 983-992

Chapter 4 **61**
LysM domain receptor kinases regulating rhizobial Nod factor induced infection. *Science* 2004, **302**: 630-633

Chapter 5 **77**
Nod factor signaling inside

Chapter 6 **85**
NODULATION RECEPTOR KINASE controlling the switch from infection thread growth to bacterial release in nodule cells

Chapter 7 **103**
Concluding remarks

Nederlandse samenvatting **117**

Dankwoord **121**

Curriculum vitae **123**

List of publications **125**

Outline

Leguminous plants are able to establish a symbiotic interaction with nitrogen-fixing soil bacteria, generally called rhizobia. This host-specific interaction results in the formation of a completely new organ, the root nodule, where the bacteria are hosted intracellularly and are able to fix atmospheric nitrogen. A successful interaction requires the strict coordination of two processes: the formation of the nodule organ from root cortical cells and infection of this new organ by the bacteria through tubular structures, called infection threads, whose formation is started in the root hairs. To initiate these processes a molecular dialogue is required between the two partners. Upon perception of flavonoids secreted by the plant the rhizobia produce lipo-chitooligosaccharidic signalling molecules, the Nod factors, which are essential and in most cases sufficient for the induction of symbiotic responses in the host plant. These Nod factors have a common basic structure consisting of three to five β-1,4-linked *N*-acetyl-D-glucosamine subunits with an acyl chain linked to the non-reducing terminal sugar residue. Depending on the rhizobial species, the structure of the acyl chain can vary and specific decorations at the reducing and non-reducing terminal glucosamine residues can be present, which function as major determinants of the host-specificity of the interaction. Nod factors are biologically active at nano- to picomolar concentrations and their activity depends on their structure, which implies that they are perceived by specific receptors. The major goal of the research described in this thesis was to unravel the molecular basis of Nod factor perception. Therefore we focussed on the pea *SYM2* gene, which was proposed to be involved in Nod factor perception. In the pea accession Afghanistan a $SYM2^{A}$ allele was identified, which controls rhizobial infection in a Nod factor structure dependent manner. Only *Rhizobium leguminosarum* bv *viciae* strains that contain the bacterial nodulation gene, *nodX*, which specifically acetylates the reducing terminal sugar residue of pentameric Nod factors, are allowed to successfully infect pea plants containing the $SYM2^{A}$ allele from Afghanistan. This suggests that $SYM2^{A}$ is involved in recognizing these *nodX* modified Nod factors and it would be attractive to clone this gene. However, positional cloning in pea is severely hampered because of its large genome size (~5000 Mb) and it is difficult to transform this legume. Therefore we decided to use a synteny based positional cloning approach in the phylogenetically closely related model legume *Medicago truncatula* (Medicago).

In **Chapter 1** an overview is given of the different steps of nodulation with a focus on the molecular basis of Nod factor perception and transduction as it was known at the start of the research.

In **Chapter 2** the level of microsynteny between pea and Medicago was studied in the *SYM2* region. This resulted in the delineation of a ~350 kb physical BAC contig representing the *SYM2* orthologous region in Medicago. A conserved gene content was observed in the *SYM2* orthologous regions, which supports the idea that Medicago can be used as intergenomic vehicle to clone pea genes.

Because *SYM2* represent a natural occurring variation in pea, sequence analysis could not be used to identify the *SYM2* gene. Therefore we developed a reverse genetics approach in Medicago to identify genes involved in rhizobial infection. In **Chapter 3** we report the effective use of RNA interference (RNAi) via *Agrobacterium rhizogenes* mediated root transformation as a reverse genetic tool to knock down gene expression in the roots of both Arabidopsis and Medicago. *A. rhizogenes* mediated root transformation has the advantage that it is a relatively fast method to generate genetically transformed roots. It is further shown that the silencing signal does not spread to non co-transformed (lateral) roots and only inefficiently to the non-transgenic shoot. Furthermore, RNAi appeared to be cell-autonomous in the epidermis of Medicago roots.

In **Chapter 4** we used *A. rhizogenes* mediated RNAi to knock down candidate genes from the Medicago *SYM2* othologous region and examined their role in rhizobial infection. We survey-sequenced the *SYM2* orthologous region and strikingly many genes encoding receptor-like proteins appeared to be present. Knock down by RNAi of two genes, *LYK3* and *LYK4*, affected rhizobial infection. By using *Sinorhizobium meliloti* strains that are mutated in their *nod* genes, a block of infection thread formation due to knock down of *LYK3/4* was shown to be correlated to the structure of the produced Nod factors. The two identified genes encode LysM domain containing receptor-like kinases. The nature of the LysM domains together with the Nod factor structure dependent block of rhizobial infection strongly suggests that these genes represent Nod factor receptors.

The formation of a functional root nodule requires the tight coordination of the infection process by the bacteria and the formation of the nodule organ. In all mutants currently characterized the loss of (all) Nod factor responses in the epidermis is always correlated with the loss of the cortical cell division (nodule primordium) response. This led to the hypothesis that Nod factor signalling in the epidermis results in the generation of a secondary signal that subsequently triggers cortical cell division. In **Chapter 5** we show that the presence of an essential component of the Nod factor perception and transduction machinery, *NODULATION RECEPTOR KINASE* (*NORK*), exclusively in the epidermis is sufficient to trigger cortical cell divisions by external application of Nod factors. This shows that mitotic activation of cortical cells is triggered by Nod factors in a non cell-autonomous manner and implies the involvement of intercellular communication in Nod factor signalling.

Several lines of evidence indicate that the Nod factor perception and transduction machinery also plays a role in the nodule. In **Chapter 6** we show that *NORK* expression is highly upregulated in the nodule and the region where it is expressed coincides with rhizobial *nod* gene activity in the infection zone of the nodule where bacteria are released into the plant host cells. By mimicking allelic series of *NORK* via RNA interference and by expression of *35S::NORK* constructs in the mutant background we show that NORK controls the switch from infection thread growth to release of bacteria in the nodule. This suggests a role for the Nod factor perception and signaling machinery in this process.

Finally **Chapter 7** summarizes and discusses the results obtained by the research described in this thesis.

Chapter 1

Signaling in Symbiosis

Erik Limpens and Ton Bisseling

Current Opinion in Plant Biology 2003, **6**: 343-350

In recent years, the major focus in nodulation research has been on the genetic dissection of Nod factor signaling. Components of this pathway appear to be shared with signaling processes that are induced during the formation of mycorrhiza. With the cloning of orthologs of the *NIN* and *DMI2* genes from several legumes, the molecular characteristics of components of the Nod factor signaling pathway are now starting to be revealed. Orthologs of *HAR1*, a key player in the systemic autoregulatory mechanism controlling nodule numbers, have also been cloned recently. The mechanism by which nodulation is autoregulated is related to that by which fixed nitrogen inhibits nodulation. Genes that are involved in Nod factor signaling may be targets for mechanisms that suppress nodulation. If this is the case, it would bring two fascinating areas of symbiosis together.

Introduction

Plants are able to establish endosymbiotic interactions with several microorganisms. Among agriculturally and ecologically important symbioses are the interactions of plants with mycorrhizal fungi and nitrogen fixing bacteria. Most higher plants are able to form arbuscular mycorrhiza (AM), an endosymbiotic association of plant roots with zygomycete fungi of the order *Glomales*. During AM formation, fungal hyphae enter the root and grow towards the inner cortex where they penetrate the cortical cells and form highly branched feeding structures, the arbuscules. The fungi also form hyphae outside of the plant, greatly extending the root-soil interface to facilitate the uptake of nutrients such as phosphate (*1,2*).

In contrast to AM formation, the endosymbiosis with nitrogen fixing bacteria is limited to only a few plant families. The best-studied N-fixing symbiosis is formed by legumes (*Fabaceae*) and by gram-negative bacteria belonging to the genera *Azorhizobium*, *Bradyrhizobium, Mesorhizobium*, *Rhizobium* and *Sinorhizobium* (collectively called rhizobia). This interaction leads to the formation of a completely new organ, the root nodule, where the rhizobia are hosted intracellularly and fix atmospheric nitrogen that can be used by the plant (*3,4*). In both mycorrhizal and rhizobial symbioses the microorganisms are hosted intracellularly and a molecular dialogue between the two partners is required to coordinate the events leading to the symbiosis and to avoid host defense responses (*2-5*). However, the plant responses induced by rhizobia and mycorrhizal fungi seem to be very different and contrastive host ranges are involved. Nevertheless, genetic studies have shown that the signaling pathway that is involved in the formation of mycorrhizal-plant interactions has several steps in common with that activated by rhizobia (*1,6*). Furthermore, similar host genes are induced during the initial steps of the two interactions (*1*).

As legumes can establish symbiotic interactions with both mycorrhiza and rhizobia, they are ideal plants in which to study the signaling events that control these two endosymbiotic

systems. Most progress in understanding the molecular basis of the signaling cascade that leads to the symbiotic interactions has come from studies on the nodulation process in the two model legumes *Lotus japonicus* (Lotus) (*7*) and *Medicago truncatula* (Medicago) (*8*). In this review, we therefore focus mainly on the current information on signaling events that has been obtained from these two model systems.

Nodulation

The establishment of a nitrogen fixing symbiosis involves an infection process in which the rhizobia enter the plant via the root epidermis and induce the formation of a nodule by reprogramming root cortical cell development. A successful interaction requires the strict coordination of these two processes. In general the infection process starts with curling of root hairs (Figure 1c), which is thought to be caused by a gradual and constant reorientation of the growth direction of the root hair (*9*). The bacteria become entrapped within the pocket of the curl, the plant cell wall is locally degraded, the cell membrane invaginates and new material is deposited by both plant and bacteria. A tip growing tubular structure, the infection thread (Figure 1c), is formed in this way and will grow to the base of the root hair and subsequently into the cortex (*10,11*). Before the infection thread reaches the cortex, cortical cells dedifferentiate, enter the cell cycle and are reprogrammed to form a primordium. In addition to the cortical cells, pericycle cells are activated leading to some divisions as well as to the induction of *EARLY NODULIN40* (*ENOD40*) expression (*4*). When the infection thread reaches this primordium, the bacteria enter the primordial cells via an endocytosis-like process in which droplets of the infection thread are released into the plant cell. Once inside the plant cytoplasm the bacteria (which are surrounded by the plant derived peribacteroid membrane) differentiate into bacteroids that fix nitrogen (*12*).

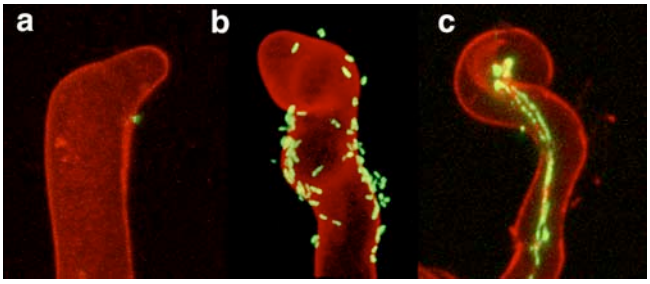

Figure 1. Morphological responses in Medicago root hairs upon inoculation with *S. meliloti* expressing *GFP*. (a) Typical root hair deformation showing reinitiated tip growth with an altered growth direction. Cell walls are counterstained with propidium iodine(red). One fluorescent bacterium is visible at the point of redirected tip growth. (b) A root hair with multiple attached fluorescent bacteria that has undergone several changes in growth direction. No bacterium has gained the dominance necessary to determine the position of the curl. (c) Curled root hair containing two infection threads.

Root-hair curling only occurs in few hairs in the zone of the root that is susceptible to rhizobia, whereas most root hairs within this zone show altered growth behaviour, resulting in so-called root hair deformations (Figure 1a,b) (*13*). These deformations are the result of isotropic growth, by which the tip of the hair swells, followed by a reinitiation of tip growth with an altered growth direction (*14*). Although many bacteria can be attached to a single hair (Figure 1b), it is probable that one or only a few bacteria induce the curling (*15,16*). The growth direction of the hairs needs to be constantly redirected towards the bacteria in order for them to become entrapped (e.g. Figure 1a), which makes it probable that bacteria provide a positional cue. Rhizobia have been shown to secrete signaling molecules, the so-called Nod factors (see below), that are essential for the induction of many plant responses (*3,4*). These Nod factors are shown to concentrate in the root hair cell wall and are almost immobile (*17*), suggesting that Nod factors secreted by one or a few bacteria could provide such a positional cue to the root hair.

Nod factors

Nod factors are essential and in most cases even sufficient to induce (early) responses in their legume hosts (*3,4*). Nodulation research has therefore focused especially on the perception of these molecules and on their signal transduction. Nod factors are first produced by the rhizobia upon recognition of certain plant components. Of these, flavonoids especially are able to activate the bacterial transcriptional regulator NodD, which induces the expression of the rhizobial nodulation genes (*nod*) that are involved in the synthesis and secretion of the Nod factors (*18*). Nod factors generally consist of a β-1,4-linked N-aceteyl-D-glucosamine (GlcNAc) backbone of 4 or 5 residues of which the non-reducing terminal residue is substituted at the C2 with an acyl chain. Depending on the rhizobial species and its combination of *nod* genes, the structure of the acyl chain can vary and specific substitutions at the reducing and non-reducing terminal glucosamine residues can be present. The structure of the acyl chain as well as the presence of substitutions are important for their biological activity and are a major determinant of host specificity. The major Nod factor produced by *Sinorhizobium meliloti*, the microsymbiont of Medicago, consists of four GlcNAc residues, an acyl chain of 16 C-atoms with two unsaturated bonds (C16:2), an acetyl group at the non-reducing terminal sugar residue and a sulphate group at the reducing end (*18*). Especially the sulphate decoration of the *S. meliloti* Nod factor is required for the induction of most symbiotic responses in Medicago (*19*).

Genetic dissection of Nod factor signaling

A genetic approach has been used to unravel the mechanisms underlying Nod factor perception and transduction. Several genetic loci that are essential for the early steps in nodulation have been identified especially in pea (*20*) and in the two model legumes, Lotus

and Medicago. Although in most cases it is still unclear whether these loci are orthologous, we will name them according to the Medicago nomenclature (e.g. *DOES NOT MAKE INFECTIONS* [*DMI*]). We have shown the Medicago genes in Figure 2 and the pea and Lotus genes with a similar function are mentioned in the legend of this figure.

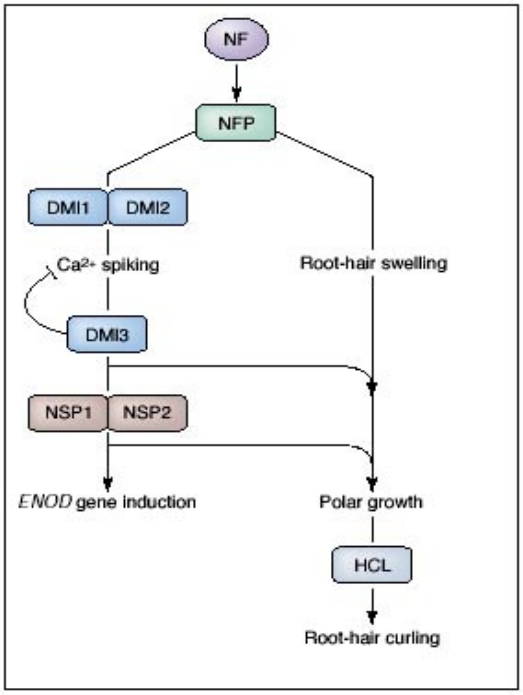

Figure 2. Genetical dissection of the Nod factor (NF) signaling pathway in Medicago (Mt) root hairs. Modified from (*2-7,22,23,30,31*). Mutants of Lotus (Lj) and pea (Ps) that have phenotypes similar to those of Medicago Nod factor signaling mutants are mentioned. The *Mtnfp* (and by analogy *Pssym10, Ljsym1* and *Ljsym5*) mutants are blocked in all Nod factor induced responses, although a normal mycorrhizal interaction can be established by these mutants. The corresponding gene products are good candidates for proteins that are involved directly in Nod factor perception. Although the scheme indicates that Nod factors are percieved by one receptor, multiple receptors are most likely involved. *Mtdmi2* (which are orthologous to *Ljsym2(SYMRK)* and *Pssym19*) and *Mtdmi1* (analogous to *Ljsym4* and *Pssym8*) still respond to Nod factor treatment by swelling of root hairs tips, but show only very limited outgrowth of branches. The root hair deformation response (characterized by root hair swelling and redirected polar growth) is therefore drawn as a separate branch. Because *Mtdmi2* and *Mtdmi1* mutants do not show a Nod factor induced calcium spiking response, they are placed upstream of *MtDMI3* mutants (which are analogous to *Ljsym30, Pssym9* and *Pssym30*). *Mtdmi3* mutants respond with calcium spiking although their root hair deformations are limited to swellings. *Mtdmi1, Mtdmi2* and *Mtdmi/3* mutants (and their analogous mutants in Lotus and pea) do not form normal mycorrhizal interactions. MtDMI1, MtDMI2 and MtDMI3 therefore represent components of a common signaling pathway that is triggered by both mycorrhiza and rhizobia. The precise role of calcium spiking in this pathway is not yet known, and could represent a separate branch. The *Mtnsp1* and *Mtnsp2* mutants are impaired for their abilities to induce *ENOD* gene expression (such as *ENOD11, RHIZOBIUM-INDUCED PEROXIDASE [RIP1]*), with *Mtnsp2* showing the more severe effect (*30*). Root hair deformation is also affected in these mutants. They respond to Nod factor treatment with limited redirected outgrowth of branches, indicating that the induction of polar outgrowth by Nod factors is impaired. This evidence, together with the fact that mycorrhization can still take place in these mutants, places *Mtnsp1* and *Mtnsp2* downstream of *Mtdmi3* in a nodulation specific pathway. The *hcl* mutant is blocked in its ability to control root hair curling. All other Nod factor induced epidermal responses, including the deformation of root hairs, remain unaffected in this mutant. In this scheme, *HCL* is positioned downstream of *NSP* in the Nod factor transduction pathway, but could be involved in a separate pathway, that is not involved in Nod factor perception.

The *dmi1, dmi2* and *dmi3* class of Medicago mutants is blocked in almost all early steps of nodulation as well as in mycorrhization (*6*). The root surface of these mutants can be colonized by AM fungi but the interaction is blocked at the appressorium stage. Upon inoculation with rhizobia or Nod factors the only detectable morphological response is the swelling of root hair tips. Hence, the induction of root-hair swellings does not depend on DMI1, DMI2 and DMI3, whereas the efficient induction of tip growth leading to deformed hairs depends on these proteins. The *dmi* mutants are defective in both the *Rhizobium* and AM

symbiosis, indicating that a part of the Nod factor signaling pathway is shared with a pathway induced by a signaling molecule that is secreted by AM fungi (*1,6,7*). This fungal signal molecule, the so-called Myc factor, has not yet been characterized, but recent studies demonstrate that AM fungi indeed produce a diffusible signal molecule that can induce responses in the legume host (*21*).

Approximately 10 minutes after the application of Nod factor, a calcium spiking response is triggered in the root hairs of all legumes tested to date (*22,23*). Although the precise role of calcium spiking during nodulation is not yet clear, this response has been useful in positioning the *DMI* genes in the signaling pathway. Calcium spiking is not induced by Nod factors in *dmi1* and *dmi2* mutants, whereas the *dmi3* mutant does show this response (*22*). This indicates that *DMI1* and *DMI2* act upstream of *DMI3* in the signaling pathway. Furthermore, the induction of calcium spiking in *dmi3* mutants is up to ten times more responsive to Nod factors than this response in wild-type plants (*24*). Besides being essential for Nod factor signal transduction downstream of calcium spiking, *DMI3* therefore appears to be involved in a negative feedback loop that regulates this response.

As *DMI1* and *DMI2* act in an early step of both nodulation and mycorrhization, it seems possible that they could play a role in the perception of Nod and Myc factors. *DMI2*, and its orthologs from pea, alfalfa (*NODULATION RECEPTOR KINASE* [*NORK*]) and Lotus (*SYMBIOSIS RECEPTOR-LIKE KINASE* [*SYMRK*]), is the only host gene involved in these early signaling steps to be cloned to date (*25,26*). *DMI2* encodes a receptor-like kinase (RLK) that contains a characteristic extracellular domain with three leucine-rich repeats (LRRs), a transmembrane domain and an intracellular serine/threonine kinase domain. This overall structure indicates a role for DMI2 in perception of an extracellular signal and further signal transduction.

It seems unlikely that a single receptor, such as DMI2, is sufficient for the perception of both Nod and Myc factors for a number of reasons. First, the morphological responses that are induced by mycorrhizal fungi and rhizobia are different; for example, Nod factors induce root hair deformation whereas AM fungi do not. Second, even though Myc factors (whose structure remains unknown) and Nod factors induce similar genes (e.g. *MtENOD11; 1,6*), Nod factors require DMI1, DMI2 and DMI3 for *MtENOD11* induction whereas Myc factors do not (21). Furthermore, Nod factors induce *MtENOD11* in the epidermis, whereas Myc factors induce the expression of this gene in the root cortex (*21*). Myc factors and Nod factors must therefore be percieved by different receptors and are able to activate different pathways. Nevertheless, the induction of some *ENOD* genes does seem to involve the same pathway components in both symbioses; for example, the induction of *PsENOD12* is blocked in pea *Pssym8* mutants (which are most likely orthologs of *dmi1*) that have been inoculated with either rhizobia or AM fungi (*1*). Along this line it seems probable that a mutation in a Nod

factor receptor gene, active upstream of *DMI1* and *DMI2,* would not affect the mycorrhizal interaction, whereas it would eliminate all Nod factor induced responses including calcium spiking and root hair deformation/swelling. Indeed, two such loci (*LjSYM1* and *LjSYM5*) have been found in Lotus, as has one in pea (*PsSYM10*) and one in Medicago (*NOD FACTOR PERCEPTION*; *NFP*) (*2-4,7,23,27*). The cloning of these genes will clarify whether they are indeed involved in the perception of Nod factors.

Myc- and Nod-factor induced signaling appear to converge at or above *DMI1* and *DMI2*. How these proteins can integrate the two signaling pathways is therefore an intriguing question. A hint to how this could be achieved comes from the functioning of LRR type receptors in plants and animals. The LRR-RLKs form one of the largest groups of receptors in the plant kingdom with 174 members identified in Arabidopsis, and have been shown to play a role in development and defense against pathogens (*28*). A paradigm for signal transduction by this kind of receptor molecules is the formation of receptor complexes by heterodimerizing or interacting with other extra- and intracellular proteins. After binding of a ligand they induce a phosphorylation cascade involving MAP-kinases (*28*). A candidate protein for a function in a complex with DMI2 could be encoded by the genetically identified *NFP* gene (and/or by *LjSYM1* and *LjSYM5* or *PsSYM10*). As mentioned above, these proteins are good candidates for involvement in Nod factor perception. The binding of Nod factors to these proteins in complex with DMI2 could then trigger further signal transduction, whereas the Myc factor would then bind to another complex containing DMI2.

Genetic studies have also identified a set of mutants that are blocked in Nod factor signal transduction downstream of the calcium spiking response and *DMI3* (Figure 2). These mutants are still able to establish a normal mycorrhizal association and so these genes play a role in a nodulation specific signal transduction pathway. In all of these mutants, root hair deformation is induced but proper curling does not take place, and infection is blocked as a result.

In Medicago, the *nodulation-signaling pathway* mutants (*nsp1* and *nsp2*) are blocked in Nod factor induced cortical cell activation and infection (*6,30*). In contrast to *dmi3*, the *nsp* mutants are still able to develop root hair deformations beyond the root hair swelling stage, albeit somewhat less efficiently than the wild type. The induction of gene expression appears to be slightly different in the two mutants, but both *nsp* mutants have a markedly reduced ability to induce expression of early nodulin genes, such as *MtENOD11* (*6,30*). The induction of *MtENOD11* is strongly impaired in the rhizobia-inoculated *nsp* mutants, without affecting mycorrhization of these mutants. These findings are in line with the different pattern of expression of *MtENOD11* in both symbiotic interactions, as well as with the strict requirement for *DMI1, DMI2* and *DMI3* for Nod factor induced *MtENOD11* induction, but not for Myc factor induced *MtENOD11* expression (*21*). All of these observations show that *MtENOD11* is

activated in both symbiotic interaction but the underlying activation mechanisms must be different in each interaction.

In Medicago, a mutant called *hair curling* (*hcl*) has been identified that is specifically blocked in the process of root hair curling. Nod factor induced responses such as calcium spiking, root hair deformations, cortical cell divisions and *ENOD* gene induction are all unaffected in this mutant (*31*). The *HCL* gene is therefore positioned downstream of *NSP* in the Nod factor signaling pathway, although it could represent an independent path.

Another mutant that has defective hair curling, *nodule inception* (*nin*) has been identified in Lotus (*32*). In contrast to *HCL,* however, *NIN* is also required for cortical cell activation. *LjNIN,* was the first gene that is involved in Nod factor signaling to be cloned (*32*). The *NIN* ortholog from pea (*Pssym35*) was also cloned recently using a comparative mapping approach (*33*). *NIN* encodes a putative transcription factor that has a typical DNA binding/dimerization domain in the carboxy-terminal half of the protein and two putative membrane spanning helices. The DNA binding/dimerization domain shows strong homology to a region of the MID (minus dominance) proteins of *Chlamydomonas reinhardtii*, which regulate sexual reproduction in response to nitrogen starvation (*32*). As root nodulation is also regulated by nitrogen this may hint at the evolutionairy conservation of this type of regulators. Expression analysis has shown that *LjNIN* is expressed at low levels in cotyledons, leafs, stems and roots, and is strongly upregulated in nodules (*32*). *NIN* is especially active in the meristematic region of pea nodules (*33*). In addition to having a clear role in the infection process, *LjNIN* also seems to be essential for the induction of cortical cell divisions, a function that also could be required in the nodule meristem. Although calcium spiking and *ENOD* gene induction have not been tested in the *nin* mutants, the phenotypic characteristics of these mutants suggest that *NIN* is positioned at or just downstream of the Medicago *NSP* genes in the Nod factor signaling pathway.

Biochemical approach to study Nod factor perception and transduction

In addition to the genetic dissection of Nod factor signaling (described above), biochemical approaches have been used to identify Nod factor binding proteins and to study Nod factor induced signaling events. These studies are only briefly summarized here and are reviewed more extensively in (*3,4,34*).

Two different Nod factor binding sites, NFBS1 and NFBS2, have been identified in *Medicago* species (*34*). Although these molecules bind Nod factors they do not discriminate between biologically active *S.meliloti* Nod factors that contain the O-sulfate at the reducing end or an inactive molecule that lacks this substitution. This lack of specificity makes it unlikely that NFBS1 and/or NFBS2 are specific Nod factor receptors. They could, however, be part of a

Nod factor binding complex (*34*). It is of interest, therefore, to know whether the binding activity of NFBS1 and NFBS2 is lost in the putative Nod factor receptor mutants (e.g. *nfp*).

A candidate gene approach has also been used in attempts to identify Nod factor binding proteins. The most promising candidate revealed in this way was a lectin-nucleotide phosphohydrolase (*LNP*) from the legume *Dolichos biflorus* that can bind Nod factors. *DbLNP* has no sequence homology to conventional lectins and has an apyrase activity that catalyses the hydrolysis of phosphoanhydride bonds of nucleoside di- and triphophates (*35*). The best indication that this lectin is involved in early steps of nodulation came from studies where roots where pre-treated with an antibody against LNP. This pre-treatment blocked both root hair deformation and nodulation by the appropriate rhizobial species (*35*). Homologs of *LNP* have also been identified in other legumes including Medicago and Lotus (*34,36*), and hence the tools are available to integrate these lectin studies with the genetic approach.
Electrophysiological studies have provided insight into the early signaling events that are evoked by Nod factors in root epidermal cells (*37-39*). These early events include changes in ion fluxes, which occur within seconds/minutes after Nod factor application. Such ion fluxes result, for example, in cytoplasmic alkalinization and in a marked increase in calcium influx at the root hair tip. This is followed by an efflux of chloride ions, which depolarizes the plasma membrane, and by a potassium efflux that balances the charge to stop depolarization. About 6-10 minutes after Nod factor application a regular oscillation of calcium (calcium spiking) occurs in the perinuclear region (*37*). Although the precise role of these induced ion changes is not yet clear, they are useful assays in the dissection of Nod factor signal transduction.

Further insight into Nod factor signaling has come from pharmacological studies, in which chemicals have been used in attempts to mimic or block Nod factor induced responses. Mastoporan, an agonist of trimeric G-proteins in animal systems, induces both root hair deformation (*40*) as well as *ENOD12* expression in a manner similar to that of Nod factors (*41*). This evidence, as well as data from other sources, suggests that trimeric G-proteins are involved in Nod factor signaling (*40,41*). Furthermore, both mastoporan and Nod factors activate phosholipid signaling, causing an increase in the concentrations of phosphatidic acid and diaglycerol pyrophosphate (DGPP) but not of other phospholipids (*40*). The application of phospholipase C (PLC) and phospholipase D (PLD) antagonists blocked Nod factor induced *ENOD12* expression as well as root hair deformations and the increase in phosphatidic acid, showing that phospholipid signaling is essential for some of the Nod factor induced responses (*40*).

Mtannexin is a Nod factor induced gene belonging to the family of annexin genes that encode calcium- and phospholipid-binding proteins, providing further evidence for the involvement of phospholipid signaling in nodulation. This gene is transcriptionally activated in both outer (cortical) and inner (mainly endodermal) cell layers of the root in response to Nod factor

treatment (*42*), suggesting that phospholipid signaling also plays a role in these inner cell layers of the root.

More than one Nod factor receptor

Figure 2 indicates that Nod factors are perceived by a single receptor. Several studies indicate, however, that the perception mechanism for Nod factors is complex and involves multiple receptors or a receptor with multiple activities. A few examples are described below.

Threshold concentrations of Nod factors for the induction of various responses can differ. For example, calcium spiking in root hairs is induced about 10 min after the addition of Nod factor at concentrations as low as 1-10 pM. Calcium spiking in root hairs is preceded by a fast (within 1-3 min) biphasic calcium influx, initially near the tip of the cell and then near the nucleus. The threshold Nod factor concentration for this response, however, is more than 1 nM (*43*). This different Nod factor concentration dependence for responses that are induced in the same cells suggests either that there is a single receptor with multiple activities or that multiple receptors control the earliest steps of Nod factor signaling.

Cytoplasmic alkalinization of Medicago root hairs is the only epidermal response that can be induced in this host by non-sulphated and sulphated Nod factors. When this response has been induced by (non-)sulphated Nod factor, the plants become desensitized and a second dose of the same Nod factor has no effect. When treatment with non-sulphated Nod factor follows a treatment with sulphated Nod factors (or *vice versa*), however, there is an additive effect. Hence, it seems that non-sulphated and sulphated Nod factors are recognized by different receptors (*44*).

The structure–function relationship for various Nod factors is not identical for the different responses that they induce. For example, the infection process places more stringent demands on Nod factor structure than any other response. The *S. meliloti nodF/nodL* mutant, which makes Nod factors that lack an acetate group at the non-reducing end and contain a C18:1 acyl chain (in stead of C16:2), is able to induce root hair deformations, curling, *ENOD* induction and cortical cell divisions (*45*). However, infection threads are not induced by this mutant. These observations led to the proposal of two Nod factor perception mechanisms (*45*); the first involving a highly stringent receptor that controls bacterial entry and the second involving a non-stringent Nod factor receptor that is involved in the induction of other epidermal responses. Similar observations were made in vetch (*46*) and pea. In the latter, natural variation has been exploited to identify an allele in the pea accession Afghanistan (*SYM2*^{A}), whose presence requires that a specific substitution (acetate or fucose) at the reducing end of the Nod factor produced by *Rhizobium leguminosarum* biovar *viciae* is present to allow a successful infection (*4)*. The Medicago region that includes a putative

SYM2 homolog has been identified (*47*), and molecular characterisation of the Medicago ortholog should provide insight in the molecular basis of the “multiple perception” mechanism.

Regulation of nodule numbers

So far we have discussed how a signal from the microsymbiont is perceived by the host and how this perception leads to responses by which the nodulation process is set in motion. Mutants that have completely lost the ability to form nodules are an important tool in exploring these processes. However, wild type plants can also loose their ability to form nodules; striking examples involve plants in which nodule number is controlled by the autoregulation process or plants growing in conditions that include a fixed nitrogen source like ammonia or nitrate. After the inoculation of wild type plant, nodules are typically formed in the susceptible region of the root. When the root system grows, new regions that can be infected are continuously formed. Once nodules are formed on a root system, however, a systemic response is induced that blocks nodulation in the newly formed root regions. In this way, the host plant controls the nodule number, keeping profit (N-fixation) and costs (carbon sources and so on) in balance. In the presence of a fixed nitrogen source, there is no requirement for nodule formation, and as a consequence all responses to rhizobia and their Nod factors are blocked. Autoregulation and repression of nodulation by fixed nitrogen are probably controlled (in part) by a similar mechanism since autoregulation mutants are insensitive to nitrate.

Several autoregulation mutants have been isolated, especially in pea and soybean, that have no autoregulatory ability and root systems that become fully covered with nodules upon inoculation (*48-50*). Physiological studies of such mutants have shown that autoregulation involves a long distance communication between shoot and root. This work was based on grafting studies which showed that, in several cases, the grafting of a mutated shoot onto a wild type root caused hypernodulation of the wild type root.

The *HYPERNODULATION ABERRANT ROOT* (*HAR1*) gene, which is involved in the long distance communication controlling nodule numbers, was recently positionally cloned from Lotus (*48,49*). This gene is orthologous to the autoregulatory receptor kinase gene of soybean (*GmNARK*) (*50*) and to *Sym29* of pea (*48,49*). The *NARK/HAR1* gene encodes a RLK that consists of extracellular LRRs (19 *in GmNARK* and 21 in *HAR1*) and an intracellular serine/threonine kinase domain. This structure places the protein in the LRR1 class of receptor like kinases, which also includes DMI2 (*28*). It also suggests that the protein has roles in perception of a signal from the root and in the generation of an autoregulation signal by which nodulation is stopped (*51*).

The molecular mechanism by which the formation of nodules is suppressed by fixed nitrogen or during autoregulation is unknown. The effect of a fixed nitrogen source on the early responses induced by Nod factors has, however, been studied in some detail in several legumes. These studies showed that a fixed nitrogen source completely blocks Nod factor induced deformation of root hairs, *ENOD12* induction, cortical cell division and infection thread formation (e.g. *13,52*). So, most of the early steps of nodulation are blocked by fixed nitrogen. Such a general block of Nod factor responses would be achieved most effectively if key regulatory genes (as depicted in Figure 2) or their encoded products were targeted by the suppressing mechanism. As the mechanisms of autoregulation and the suppression of nodulation by exposure to fixed nitrogen appear to be controlled by a similar mechanism, it is likely that the autoregulatory signal also affects such key regulators.

Conclusion and perspectives

The recognition of mycorrhiza and rhizobia, and further signal transduction leading to an effective symbiosis, appears to be complex and may be controlled by multiple receptors and signaling pathways. Genetic analysis of signal transduction in symbiosis has been the main focus of nodulation research in the past couple of years. The molecular characterization of the identified mutants is just beginning to reveal some of the key players (e.g. MtDMI2 and LjNIN). These key players are likely targets for nodulation suppression mechanisms, such as those involved in the autoregulation of nodulation and the response to fixed nitrogen, which appear to be related. In the near future, the cloning of more symbiosis related genes will be markedly speeded up by the genomic approaches that have been initiated for the model legumes Lotus and Medicago. These include the construction of physical maps, the sequencing and transcription profiling of the genomes of these legumes and their microsymbionts, and the development of efficient targeted induced local lesions in genomes (TILLING) facilities. The availability of legume genes that are part of genetic networks that control Nod factor induced responses or the systemically induced autoregulation of nodulation will also provide the tools to reveal whether and how these networks are interconnected.

Acknowledgements

We thank René Geurts for providing Figure 1 and critical reading of this manuscript. E.L. is supported by the Dutch Organization for Scientific Research (NWO).

References

1 Albrecht C, Geurts R, Bisseling T: **Legume nodulation and mycorrhizae formation; two extremes in host specificity meet.** *EMBO J* 1998, **18**:281-288.

2 Kistner C, Parniske M: **Evolution of signal transduction in intracellular symbiosis.** *Trends Plant Sci* 2002, **7**:511-518.

3 Oldroyd GED: **Dissecting symbiosis: Development in Nod factor signal transduction.** *Ann Bot* 2001, **87**:709-718.

4 Geurts R, Bisseling T: ***Rhizobium* Nod factor perception and signalling.** *Plant Cell* 2002, supplement: S239-S249.

5 Mithöfer A: **Suppression of plant defence in rhizobia-legume symbiosis.** *Trends Plant Sci* 2002, **7**:440-444.

6 Catoira R, Galera C, De Billy F, Penmetsa RV, Journet EP, Maillet F, Rosenberg C, Cook D, Gough C, Dénarié J: **Four genes of *Medicago truncatula* controling components of a Nod factor transduction pathway.** *Plant Cell* 2000, **12**:1647-1666.

7 Stougaard J: **Genetics and genomics of root symbiosis.** *Curr Opin Plant Biol* 2001, **4**:328-335.

8 Cook DR**: *Medicago truncatula* – a model in the making!** *Curr Opin Plant Biol* 1999, **2**:301-304.

9 Emons AMC, Mulder B: **Nodulation factors trigger an increase of fine bundles of subapical actin filaments in *Vicia* root hairs: Implication for root hair curling around bacteria.** In *Biology of Plant-Microbe Interactions*. Vol 2. Edited by De Wit PJGM, Bisseling T and Stiekema JW. St. Paul, Minnesota: The International Society of Molecular Plant-Microbe Interaction; 2000:272-276.

10 Hadri A-E, Spaink HP, Bisseling T, Brewin NJ: **Diversity of root nodulation and rhizobial infection processes.** In: *The Rhizobiaceae,* Edited by Spaink HP, Kondorosi A, Hooykaas PJJ. Dordrecht, The Netherlands: Kluwer Academic Publishers; 1998:347-360.

11 Timmers ACJ, Auriac MC, Truchet G: **Refined analysis of early symbiotic steps of the *Rhizobium-Medicago* interaction in relationship with microtubular cytoskeleton rearrangements.** *Development* 1999, **126**:3617-3628.

12 Oke V, Long SR: **Bacteroid formation in the *Rhizobium*-legume symbiosis.** *Curr Opin Microbiol* 1999, **2**:641-646.

13 Heidstra R, Geurts R, Franssen H, Spaink HP, Van Kammen A, Bisseling T: **Root hair deformation activity of nodulation factors and their fate on *Vicia sativa.*** *Plant Physiol* 1994, **105**:787-797.

14 De Ruijter NCA, Rook MB, Bisseling T, Emons AMC: **Lipochito-oligosaccharides re-initiate root hair tip growth in *Vicia sativa* with high calcium and spectrin-like antigen at the tip.** *Plant J* 1998, **13**:341-350.

15 Gage DJ, Margolin W: **Hanging by a thread: invasion of legume plants by rhizobia.** *Curr Opin Microbiol* 2000, **3**:613-617.

16 Gage DJ: **Analysis of infection thread development using *GFP*- and *dsRED*-expressing *Sinorhizobium meliloti.*** *J Bacteriol* 2002, **184**:7042-7046.

17 Goedhardt J, Hink MA, Visser AJ, Bisseling T, Gadella TW jr: **In vivo fluorescence correlation microscopy (FCM) reveals accumulation and immobilization of Nod factors in root hair cell walls.** *Plant J* 2000, **21**:109-119.

18 Spaink HP: **Root nodulation and infection factors produced by rhizobial bacteria.** *Annu Rev Microbiol* 2000, **54**:257-288.

19 Gressent F, Drouillard S, Mantegazza N, Samain E, Geremia RA, Canut H, Niebel A, Driguez H, Ranjeva R, Cullimore J, Bono JJ: **Ligand specifictiy of a high-affinity binding site for lipo-oligosaccharidic Nod factors in *Medicago* cell suspension cultures.** *Proc Natl Acad Sci USA* 1999, **96**:4704-4709.

20 Borisov AY, Barmicheva EM, Jacobi LM, Tsyganov, VE, Voroshilova VA, Tikhanovich IA: **Pea (*Pisum sativum* L.) mendelian genes controlling development of nitrogen-fixing nodules and arbuscular mycorrhizae.** *Czech J Genet Plant Breeding* 2000, **36**:106-110.

21 Kosuta S, Chabaud M, Lougnon G, Gough C, Dénarié J, Barker DG, Bécard G: **A diffusible factor from arbuscular mycorrhizal fungi induces symbiosis-specific *MtENOD11* expression in root of *Medicago truncatula*.** *Plant Physiol* 2003, **131**:952-962.

22 Wais RJ, Galera C, Oldroyd G, Catoira R, Penmetsa RV, Cook D, Gough C, Dénarié J, Long SR: **Genetic analysis of calcium spiking responses in nodulation mutants of *Medicago truncatula.*** *Proc Natl Acad Sci USA* 2000, **97**:13407-13412.

23 Walker SA, Viprey V, Downie JA: **Dissection of nodulation signaling using pea mutants defective for calcium spiking induced by Nod factors and chitin oligomers.** *Proc Natl Acad Sci USA* 2000, **97**:13413-13418.

24 Oldroyd GE, Mitra RM, Wais RJ, Long SR: **Evidence for structurally specific negative feedback in the Nod factor signal transduction pathway.** *Plant J* 2001, **28**:191-199.

25 Endre G, Kereszt A, Kevei Z, Mihacea S, Kaló P, Kiss GB: **Cloning of a receptor kinase gene regulating symbiotic nodule development.** *Nature* 2002, **417**:962-966.

26 Stracke S, Kistner C, Yoshida S, Mulder L, Sato S, Kaneko T, Tabata S, Sandal N, Stougaard J, Szczyglowski K, Parniske M: **A plant receptor-like kinase required for both bacterial and fungal symbiosis.** *Nature* 2002, **417**:959-962.

27 Amor BB, Shaw SL, Oldroyd GED, Maillet F, Penmetsa RV, Cook D, Long SR, Dénarié J, Gough C: **The *NFP* locus of *Medicago truncatula* controls an early step of Nod factor signal transduction upstream of a rapid calcium flux and root hair deformation.** *Plant J* 2003, **34**:495-506.

28 Shiu S-H, Bleecker AB: **Receptor-like kinases from *Arabidopsis* form a monophyletic gene family related to animal receptor kinases.** *Proc Natl Acad Sci USA* 2001, **98**:10763-10768.

29 Asai T, Tena G, Plotnikova J, Willmann MR, Chiu WL, Gomez-Gomez L, Boller T, Ausubel FM, Sheen J: **MAP kinase signalling cascade in Arabidopsis innate immunity.** *Nature* 2002, **415**:977-983.

30 Oldroyd ED, Long SR: **Identification and characterization of *Nodulation-Signaling Pathway 2*, a gene of *Medicago truncatula* involved in Nod factor signaling.** *Plant Physiol* 2003, **131**:1027-1032.

31 Catoira R, Timmers ACJ, Maillet F, Galera C, Penmetsa RV, Cook D, Dénarié J, Gough C: **The *HCL* gene of *Medicago truncatula* controls *Rhizobium*-induced root hair curling.** *Development* 2001, **128**:1507-1518.

32 Schauser L, Roussis A, Stiller J, Stougaard J: **A plant regulator controlling development of symbiotic root nodules.** *Nature* 1999, **402**:191-195.

33 Borisov AY, Madsen LH, Tsyganov VE, Umehara Y, Voroshilova VA, Batagov AO, Sandal N, Mortensen A, Schauser L, Ellis N, Tikhonovich IA, Stougaard J: **The *Sym35* gene required for root nodule development in pea is an ortholog of *Nin* from *Lotus japonicus*.** *Plant Physiol* 2003, **131**:1009-1017.

34 Cullimore JV, Ranjeva R, Bono JJ: **Perception of lipo-oligosaccharidic Nod factors in legumes.** *Trends Plant Sci* 2001, **6**:24-30.

35 Etzler ME, Kalsi G, EwingNN, Roberts NJ, Day RB, Murphy JB: **A Nod factor binding lectin with apyrase activity from legume roots.** *Proc Natl Acad Sci USA* 1999, **96**:5856-5861.

36 Navarro-Gochicoa MT, Camut S, Niebel A, Cullimore JV: **Expression of the apyrase-like *APY1* genes in roots of *Medicago truncatula*is induced rapidly and transiently by stress and not by *Sinorhizobium meliloti* or Nod factors.** *Plant Physiol* 2003, **131**:1124-1136.

37 Cárdenas L, Holdaway-Clarke TL, Sánchez F, Quinto C, Feijó JA, Kunkel JG, Hepler PK: **Ion changes in legume root hairs responding to Nod factors.** *Plant Physiol* 2000, **123**:443-451.

38 Felle HH, Kondorosi E, Kondorosi A, Schultze M: **The role of ion fluxes in Nod factor signaling in *Medicago sativa*.** *Plant J* 1998, **13**:455-464.

39 Felle HH, Kondorosi E, Kondorosi A, Schultze M: **Elevation of the cytosolic free [Ca^{2+}] is indispensable for the transduction of the Nod factor signal in alfalfa.** *Plant J* 1999, **121**:273-279.

40 Den Hartog M, Musgrave A, Munnik T: **Nod factor-induced phosphatidic acid and diacylglycerol pyrophosphate formation: A role for phospholipase C and D in root hair deformation.** *Plant J* 2001, **25**:55-65.

41 Pingret JL, Journet EP, Dedieu A, De Billy F, Truchet G, Barker DG: ***Rhizobium* Nod factor signaling. Evidence for a G protein-mediated transduction mechanism.** *Plant Cell* 1992, **10**:659-672.

42 De Carvalho-Niebel F, Timmers AC, Chabaud M, Defaux-Petras A, Barker DG: **The Nod factor-elicited annexin *MtAnn* is preferentially localised at the nuclear periphery in symbiotically activated root tissues of *Medicago truncatula*.** *Plant J* 2002, **32**:343-352.

43 Shaw SL, Long SR: **Nod factor elicits two separable calcium responses in *Medicago truncatula* root hair cells.** *Plant Physiol* 2003, **131**:976-984.

44 Felle HH, Kondorosi E, Kondorosi A, Schultze M: **Rapid alkalinization in alfalfa root hairs in response to rhizobial lipochitooligosaccharide signals.** *Plant J* 1996, **10**:295-301.

45 Ardourel M, Demont N, Debellé F, Maillet G, De Billy F, Promé JC, Dénarié J, Truchet G: ***Rhizobium meliloti*** **lipoligosaccharide nodulation factors: different structural requirements for bacterial entry into target root hair cells and induction of plant symbiotic developmental responses.** *Plant Cell* 1994, **6**:1357-1347.

46 Walker SA, Downie JA: **Entry of *Rhizobium leguminosarum* bv. *Viciae* into root hairs requires minimal Nod factor specificity, but subsequent infection thread growth requires *nodO* or *nodE.*** *Mol Plant-Microbe Interact* 2000, **13**:754-762.

47 Gualtieri G, Kulikova O, Limpens E, Kim DJ, Cook DR, Bisseling T, Geurts R: **Microsynteny between pea and *Medicago truncatula* in the *SYM2* region.** *Plant Mol Biol* 2002, **50**:225-235.

48 Krusell L, Madsen LH, Sato S, Aubert G, Genua A, Szczyglowski K, Duc G, Kaneko T, Tabata S, de Bruijn F, Pajuelo E, Sandal N, Stougaard J**: Shoot control of root development and nodulation is mediated by a receptor-like kinase.** *Nature* 2002, **420**: 422-426.

49 Nishimura R, Hayashi M, Wu G-J, Kouchi H, Imaizumi-Anraku H, Murakami Y, Kawasaki S, Akao S, Ohmori M, Nagasawa M, Harada K, Kawaguchi M: ***HAR1*** **mediates systemic regulation of symbiotic organ development.** *Nature* 2002, **420**:426-429.

50 Searle IR, Men AE, Laniya TS, Buzas DM, Iturbe-Ormaetxe I, Carroll BJ, Gresshoff PM: **Long-distance signaling in nodulation directed by a *CLAVATA1*-like receptor kinase.** *Science* 2003, **299**:109-112.

51 Van Brussel AAN, Tak T, Boot KJM, Kijne JW: **Autoregulation of root nodule formation: signals of both symbiotic partners studied in a split-root system of *Vicia sativa* subsp. *nigra.*** *Mol Plant-Microbe Interact* 2002, **15**:341-349.

52 Heidstra R, Nilsen G, Martinez-Abarca, Van Kammen A, Bisseling T: **Nod factor induced expression of leghemoglobin to study the mechanism of NH_4NO_3 inhibition on root hair deformation.** *Mol Plant-Microbe Interact* 1997, **10**: 215-220.

Chapter 2

Microsynteny between pea and *Medicago truncatula* in the *SYM2* region

---

Gustavo Gualtieri, Olga Kulikova, Erik Limpens, Dong-Jin Kim, Douglas R. Cook,
Ton Bisseling & René Geurts

Plant Molecular Biology 2002, **50**: 225-235

The crop legume pea (*Pisum sativum*) is genetically well characterized. However, due to its large genome it is not amenable to efficient positional cloning strategies. The purpose of this study was to determine if the model legume *Medicago truncatula*, which is a close relative of pea, could be used as a reference genome to facilitate the cloning of genes identified based on phenotypic and genetic criteria in pea. Towards this end, we studied the level of microsynteny between the *SYM2* region of pea and the orthologous region in *M. truncatula*. Initially, a marker tightly linked to *SYM2* was isolated by performing differential RNA display on near isogenic pea lines. This marker served as the starting point for construction of a BAC physical map in *M. truncatula*. A fine structure genetic map, based on eight markers from the *M. truncatula* physical map, indicates that the two genomes in this region share a conserved gene content. Importantly, this fine structure genetic map clearly delimits the *SYM2*-containing region in pea and the *SYM2*-orthologous region in *M. truncatula*, and should provide the basis for cloning *SYM2*. The utility of the physical and genetic tools in *M. truncatula* to dissect the *SYM2* region of pea should have important implications for other gene cloning experiments in pea, in particular where the two genomes are highly syntenic within the region of interest.

Introduction

The legume sub-family of Papilionoideae contains many agronomically important species, including soybean (*Glycine max*), alfalfa (*Medicago sativa*) and pea (*Pisum sativum*). A unique property that contributes to the agronomic importance of these species is their capacity to establish a symbiosis with rhizobia, resulting in the formation of nitrogen-fixing root nodules. Several of these crop legumes are genetically well characterized, but due to their large genomes or complex ploidy they are not amenable to efficient positional cloning strategies. An example is pea, from which many genes have been identified based on phenotype and genetically mapped. Among these are about 30 *SYM* genes which are essential for the formation of nitrogen-fixing root nodules (*1*). At present none of these pea *SYM* genes have been cloned, mainly because pea has a large genome and is recalcitrant for transformation studies. For such reasons, two legume species, *Medicago truncatula* (*2*) and *Lotus japonicus* (*3*), have been proposed as model systems for the study of legume biology.

It has been shown that closely related species can have (syntenic) genomes in which several genes have similar map positions (For reviews see: *4*-*7*). In cases where the level of synteny in a region of interest is high (micro-syntenic), an inter-species positional cloning strategy can be envisaged. This approach would have greatest utility when the genome of the target species has a relatively large and/or complicated genome, and the genome of the reference species is relatively simple. This strategy has been successfully used for cloning a gene in Syrian hamster by making use of the available molecular genetic data of mouse and human

(*8*). In plants, synteny studies have focused primarily on species belonging to the Poaceae and Brassicaceae, respectively. Detailed studies of small gene-rich segments revealed that within both families closely related species have a conserved order of their genes. However, even in very closely related species this co-linearity is not absolute, often due to small rearrangements.

Synteny studies in legumes are rather limited. By comparative mapping it was shown that within the Phaseoleae, mungbean (*Vigna radiata*), cowpea (*Vigna unguicalata*) and common bean (*Phaseolus vulgaris*) exhibit large conserved linkage blocks (*9,10*). Similarly, within the Vicieae tribe, pea and lentil (*Lens culinaris*), exhibit a conserved genetic structure (*11*). Comparisons of species that are phylogentically more distant reveal that syntenic regions are often reduced to short linkage blocks. For example, although soybean and *Arabidopsis thaliana* exhibit local synteny of certain mapped genes, the genomes are highly diverged at a global level (*12*). *M. truncatula* is a member of the Trifoleae tribe, and is closely related to other temperate legumes such as pea (*13*). However, *M. truncatula* is distinguished by its relatively small genome, and the recent development of significant genetic and genomic tools (*2*). These factors suggest that *M. truncatula* could serve as an important reference genome for the map-based cloning of genes from Papilionoideae species with more complex genomes and less tractable molecular-genetic properties.

Linkage group I of pea contains two regions with several symbiotic genes (i.e. *NOD3*, *SYM2*, leghemoglobin and *ENOD7*, and a second region containing *SYM5*, *SYM18*, *SYM19*, and *ENOD40*) (*14-18*). Mutations in some of these genes produce unique phenotypes that have not been observed in mutants of the model legume species; therefore, it is of interest to use pea as a means to clone these genes. If *M. truncatula* and pea have a similar gene content around the loci of interest, an inter-species map-based-cloning approach might be feasible.

To test this hypothesis, we focused on the *SYM2* locus of pea. *SYM2* was first identified in the pea accession ‘Afghanistan’ where it has been shown to control infection by *Rhizobium* in a Nod factor structure dependent manner (*19,20*). Nod factors are the rhizobial signal molecules that are involved in the induction of various host responses. To understand the molecular mechanism by which *SYM2* regulates the infection process it will be essential to clone this gene. To determine whether tools available for the model legume *M. truncatula* could contribute to the cloning of this gene, we first isolated a molecular marker that is tightly linked to *SYM2*. Since the phenotype of *SYM2* suggests that the gene is transcribed in root hairs (*20*), we compared root hair RNA populations of a parental line and an introgression line containing the *SYM2* region of 'Afghanistan' pea by differential RNA display (*21*). This strategy produced a genetic marker tightly linked to *SYM2* that was used to isolate *M. truncatula* BAC clones and initiate a chromosome walk. Several *M. truncatula* genes located on this physical map were identified and used to construct a comparative map of pea and *M.*

truncatula in this genomic region. The results presented here show that *M. truncatula* and pea share a conserved genome structure throughout the *SYM2* region, and thus support the proposal that *M. truncatula* can serve as an intergenomic cloning vehicle to characterize the *SYM2* locus.

Results

Isolation of cDNA based markers linked to the pea SYM2 locus

To isolate markers that are tightly linked to *SYM2* we used the pea introgression line BC-*SYM2*, which contains the *SYM2*^{A} allele of the accession 'Afghanistan' within a cv. Sparkle background. The introgressed region in this line was previously mapped to a position between markers cDNA164 and OPA1, corresponding to a 5.8 cM region spanning the *SYM2* locus (Fig.1). Root hair RNA of the parental line Sparkle and the introgression line BC-*SYM2* was compared by differential RNA display. Analysis of approximately 15,000 bands resulted in 65 differential cDNA fragments that were cloned. Seventeen of these clones were polymorphic between BC-*SYM2* and Sparkle, suggesting that the clones originate from Afghanistan DNA present in the Sparkle background.

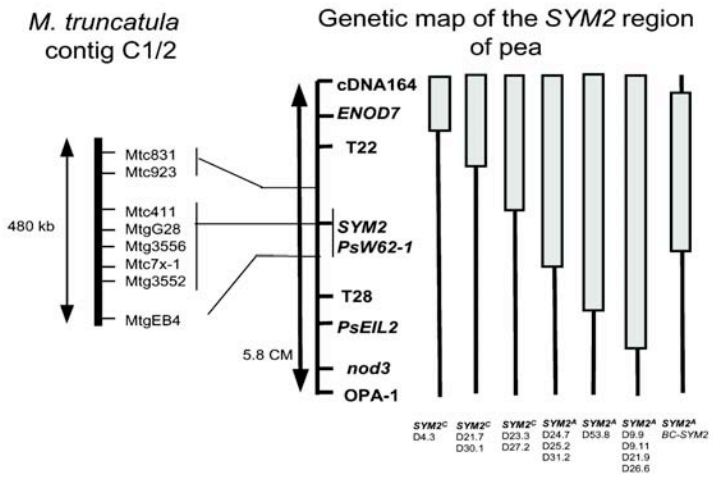

Figure 1. Genetic map of a region of 5 cM around the *SYM2* locus of pea and the physical map of the orthologous region in *M. truncatula*. The region between the *SYM2* flanking markers OPA-1 and ENOD7 is dissected by a RIL population of 13 lines (numbered with a 'D' code). Furthermore the *SYM2*^{A} introgression line BC-*SYM2* is shown. In both, the introgressed Afghanistan DNA is marked as a gray box. Markers T22, T28 and W62 are identified using differential RNA display. A 480 kb BAC contig of the *SYM2* orthologous region of *M. truncatula* (C1/C2) is constructed by using *PsW62-1* as probe in the initial screen and subsequently extended by chromosome walking. Eight markers physically linked in *M. truncatula* are also clustered in pea and can be genetically divided into 3 groups located in a 0.5-1 cM region.

To determine linkage between these markers and *SYM2*, we constructed Recombinant Inbred Lines (RILs) that specifically dissect a region of about 5 cM around the *SYM2* locus

(Figure 1 and *material and methods*). The RILs were initially genotyped with the molecular marker ENOD7 and the phenotypic marker NOD3 (*nod3* conditions a supernodulation phenotype; *22*), which define a 5 cM interval that contains *SYM2*. Thirteen individuals from the RIL population were recombinant between ENOD7 and NOD3. Eight RILs (numbers: D9.9, D9.11, D21.9, D24.7, D25.2, D26.6, D31.2 and D53.8) contain the $SYM2^{A}$ allele of the accession 'Afghanistan', whereas the other five RILs (numbers D4.3, D21.7, D23.3, D27.2, and D30.1) contain the $SYM2^{C}$ allele originating from the *nod3* mutant (Figure 1). One of the 17 cDNA clones, named W62, was tightly linked with *SYM2*, as no cross-overs between this clone and *SYM2* were identified within the 13 RILs. Two additional clones, named T22 and T28, also mapped within the *ENOD7*/*NOD3* region, but did not show tight linkage to *SYM2* (Figure 1). The linkage of W62 to *SYM2* was confirmed by using two segregating populations composed of 112 F2 individuals (for populations see: *23*). This analysis also failed to identify recombination between W62 and *SYM2*.

A pea root hair cDNA library was screened with W62 as probe. DNA sequencing suggested that the cDNAs originated from two homologous genes. One of these genes, designated *PsW62-1*, contained a 3' UTR that was 100% identical with W62. The second gene was 89% identical to *PsW62-1* at the nucleotide level and was designated *PsW62-2*. Gene-specific PCR markers were constructed to genetically map *PsW62-1* and *PsW62-2.* Analysis of the pea RILs and *SYM2*-introgression lines using these markers demonstrated that only *PsW62-1* is tightly linked to the *SYM2* locus (data not shown).

Identification and analysis of PsW62-1 homologous regions in the M. truncatula genome

To identify the *SYM2* orthologous region in *M. truncatula,* a *M. truncatula* 5X BAC library (*24*) was screened with *PsW62-1* as probe. Eleven distinct BAC clones were isolated by this approach (shown in black in Fig. 2), which is in agreement with Southern blot analysis indicating the existence of multiple W62 homologs in *M. truncatula.* Construction of contigs by AFLP and restriction/hybridization fingerprinting showed that these BAC clones comprise three non-overlapping contigs, designated C1, C2 and C3. Hybridization of these contigs with *PsW62-1* revealed three C1 and one C3 strongly hybridizing restriction fragments, whereas C2 contained a single fragment that weakly hybridized with *PsW62-1* (Fig. 2). The three BAC contigs were extended by hybridization screening of high density BAC filter arrays with contig end subclones (C2), or by PCR based screenings of a multiplex DNA copy of the *M. truncatula* BAC library with primers designed from BAC-end sequences (C1, C3) (shown in gray Fig.2).

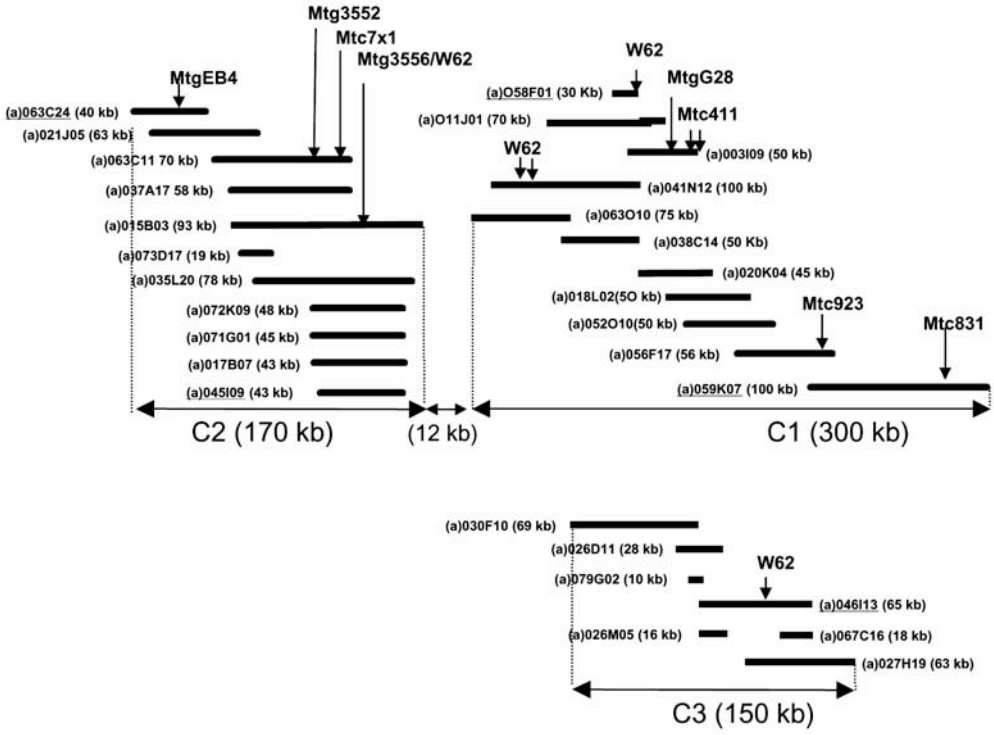

Figure 2. BAC contigs of *M. truncatula* harboring *PsW62-1* homologous sequences. The three contigs obtained after hybridization with *PsW62-1* (shown in black) were extended by chromosome walking (shown in gray) resulting in C1 (300 kbp), C2 (170 kbp) and C3 (150 kbp). The position of all fragments strongly hybridizing with the cDNAs and the fragments corresponding to the contig subclones are shown. *PsW62-1* weakly hybridizes in C2 to a single restriction fragment that corresponds to Mtg3556. Note that in C1 *PsW62-1* hybridizes to three restriction fragments located in two widely separated contig regions, while *Mtc411* strongly hybridizes to 2 fragments of C1. The clones used for FISH analysis are underlined. The 12 kbp gap between C1 and C2 was bridged by 3 BAC clones (b)048B15, (b)031F21 and (b)022J24 (clones not shown in drawing) identified in a second BAC library (Cook, unpublished).

The three BAC contigs were genetically mapped in *M. truncatula* by means of PCR markers generated from BAC-end sequences of clone (a)058F01 (C1 marker DK006-R), clone (a)045I09 (C2 marker DK039-R), and clone (a)046I13 (C3 marker DK003-R) (table 1). Analysis of these markers in an F2 population composed of 93 individuals revealed that all 3 contigs are located on linkage group V between the markers rip1 and MtEIL2-1 (Fig. 3). Genetic comparison of 4 additional markers, more widely distributed on the respective pea and *M. truncatula* linkage groups, indicates broader conservation of pea linkage group I and *M. truncatula* linkage group V. Thus, the symbiotic markers *ENOD40* (18), leghemoglobin (*LB1*), the ethylene-insensitive 3 (*EIN3*) homologs *MtEIL2-1/PsEIL2* (24), and DK355-L/Fr19 (generated from the *M. truncatula* BAC clone (a)008H08) map in a conserved order in both species (Fig 3), showing that these linkage groups are syntenic.

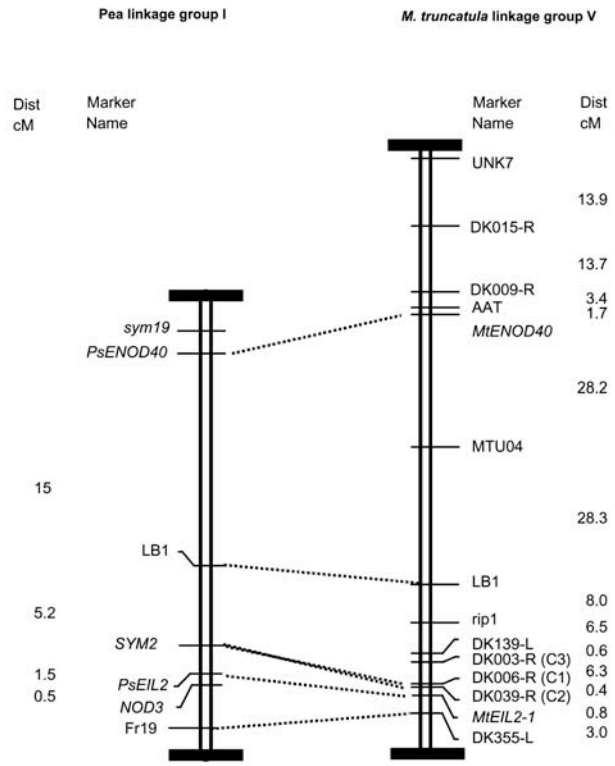

Figure 3. Comparison of the *SYM2* region of pea (linkage group I) and the orthologous region in *M. truncatula* (linkage group V). Macro synteny is found in a region between ENOD40 and the markers Fr19/DK355-L, the latter are generated from the BAC clone (a)008H08. The linkage map of pea is composed using a F2 segregating population as described in Kozik *et al*., (23) (for markers PsENOD40, LB-1 and SYM2) as well as data obtained with RILs dissecting the *ENOD7-nod3* region (SYM2, PsEIL2, nod3 and Fr19; no standard errors). Fr19 is located distal to NOD3 by which no genetic distance could be determined.

As shown in Figure 3, each of the contigs (C1, C2 and C3) map to the lower arm of *M. truncatula* linkage group V. DK006-R (C1) and DK039-R (C2) are relatively closely linked (0.6±0.6 cM distance), while DK003-R (C3) maps 6.8±2.9 cM above C1/C2. The order of the 3 contigs was further established using two-color fluorescence *in situ* hybridization (FISH) on pachytene chromosomes (Fig 4a). To determine the orientation of the tightly linked contigs C1 and C2 on chromosome 5 we performed FISH using two clones from both contigs (Fig 4b,c). The results show that BAC clone (a)058F01 of C1 and (a)045I09 of C2 flank the gap between C1 and C2, while BAC clones (a)059K07 of C1 and (a)063C24 of C2 define the centromere and telomere proximal ends, respectively, of the region. To estimate the size of the gap between C1 and C2, we used cytogenetic methods and physical map information to calculate the degree of chromatin condensation in this region (*25*). According to the physical mapping data (Fig 2), the centers of clones (a)058F01 and (a)059K07 are separated by 150 kbp, while FISH data indicate that the centers of these clones are separated 0.5 µm. Thus, the chromatin density in this region is predicted to be 300 kbp/µm, which is in good agreement with estimates for euchromatic portions of the *Arabidopsis thaliana* genome (*25,26*). Similar analysis of the hybridization signals of clones (a)058F01 of C1 and clone (a)045I09 of C2 indicate that the centers of these two clones are also separated by about 0.5 µm, or approximately 150 kbp. Based on the fingerprints of C1 and C2, approximately 120 kbp is cloned between the centers of (a)058F01 and (a)045I09, and thus the gap between C1 and C2 is estimated at 30-40 kbp.

Table 1: *Medicago truncatula* genetic marker information.

Marker name	Template Sequence *	Primer sequence	Polymorphism#	CAPS profile (bp) A17 allele	A20 Allele	Genetic distance (cM)	Standard error
ENOD40	X80262	AACCAATGCCACTTTTCACTTTGCCTCC AGACTCTTGCGAGTGCTACCATTTGACC	length	136	177	27.2	5.3
LB1	X57732	TTTTAAAGAATATAATGGCTTGTGGAGG GGAGCGAAAATGTTACCTAAAATTAAG	CAPS VspI	210	170, 140	7.5	2.2
rip1	U16727	GCAATGCGTTGCTAGGGATTAATGATGTGACC AGTTTATAAAGAGTAACACACATCTCACC	CAPS SspI	37, 59, 81, 134, 320	53, 81, 171, 320	5.7	2.6
DK003-R	AQ841082	TCTGCGGTCATGAGGTGGTT GATATATAGGTGATTTGGTTTCTACTAA	length	350	900	6.8	2.9
DK006-R	AQ841074	GAACATAACCCCGAAGTGGAT GAGTTTGGGAACAAAATTAGTATGAT	length	450	420	0.6	0.6
DK039-R	AQ841114	CAATTACTAGATCTATTTTATTTTCAAGC ACCACAAGCAGAGGGAGGATAGT	CAPS DraI	370 , 80	450	0.6	0.6
EIL2-1	BH153075	GGAGCATCCATAGCCACTGTTG TATCTTTTATTTCGGTATTCATCTCCA	CAPS FokI	160, 145	305	2.4	1.2
DK355-L	AQ917302	AACTAACTCTAAGATGCCACATTATAGGCT CAAAACATTCATCCGCCTATMCCACCTCA	CAPS MslI	25 , 175	200		

*Template sequences are identified by sequence accession number.
#CAPS: cleaved amplified polymorphic sequence, including restriction enzyme.

To confirm this prediction, and to complete the physical map spanning C1 and C2, we screened high density filter arrays prepared from a second, >20-fold coverage BAC library of *M. truncatula* (Cook *et al*., unpublished). Screening was conducted on a subset of the library using C1 and C2 contig end subclones as probe. Three clones [(b)048B15, (b)031F21 and (b)022J24] were recovered that hybridized to flanking sequences from each of contigs C1 and C2. BAC DNA fingerprinting confirmed that these new clones bridged C1 and C2, and the size of the gap was determined to be 12 kbp based on long template PCR (Roche) using BAC (b)022J24 as template. Thus, the total length of the C1/C2 contig is 480 kbp. The combination of cytogenetic data and physical map information for BACs (a)058F01 and (a)045I09 establishes that the degree of chromatin condensation in this region is roughly 132 kbp/0.5 µm kbp per micron, in good agreement with the previous measurement of 150kbp/0.5 µm for BACs (a)058F01 and (a)059K07. Thus FISH analysis on pachytene chromosomes of

M. truncatula gives distance estimates in close agreement with those provided by physical mapping.

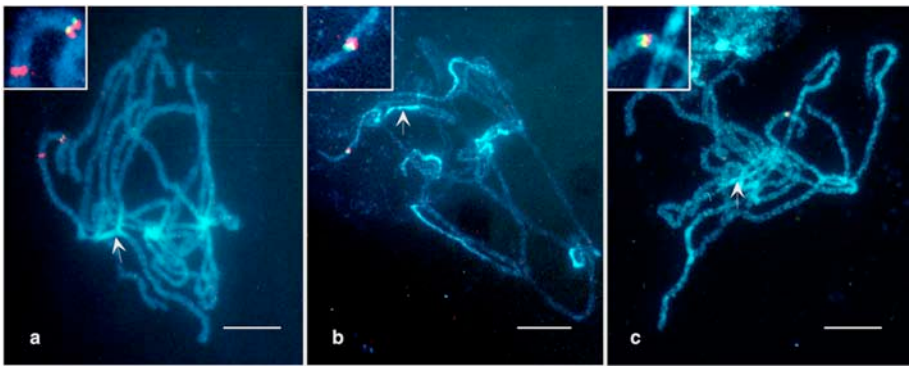

Figure 4. Two-color FISH pachytene chromosomes of *M. truncatula* A17. The DAPI stained chromosomes have bright fluorescent heterochromatin around the centromeres (pericentromeric heterochromatin). The hybridization with BACs of the 3 contigs as probe was performed in 2 rounds; (**a**) first BAC (a)058F01 (green) of C1, BAC (a)045I09 (red) of C2, and secondly (a)027H19 (red) of C3 are used as probes. (**b**) BAC (a)059K07 (red) and BAC (a)058F01 (green) of C1 and (**c**) BAC (a)045I09 (green) and BAC (a)063C24 (red) are used to determine the orientation of the contigs C1 and C2. Yellow fluorescence indicates co-localization of green and red signals. The position of the centromere of chromosome 5 is indicated with an arrow. Bar = 10 µm.

Identification of the SYM2 orthologous region in M. truncatula

To study whether C1/C2 or C3 represents the *M. truncatula* genomic region that is orthologous to the pea *SYM2* region we used RFLP mapping in pea. The initial analysis focused on C1/C2 since the map position in *M. truncatula* of this contig is comparable to the map position of *SYM2* in pea with respect to the *MtEIL2-1* and DK355-L/Fr19 loci (Fig. 3). We isolated 4 genomic subclones from C1/C2 as well as 4 *M. truncatula* cDNAs representing genes located on C1/C2 that could be used as an RFLP marker in pea (Table 2). The 8 clones represent different regions of the C1/C2 contig as shown diagrammatically in Figure 2. Two clones, named Mtc411 and Mtg3552, weakly hybridized with contig C3, while the remaining 6 clones hybridized only to C1/C2. The 8 *M. truncatula* clones were mapped in pea using the RILs and the introgression line BC-*SYM2*. In all cases the most strongly hybridizing band showed linkage to the *SYM2* locus of pea. The five central-most markers from contig C1/C2 (i.e., Mtg3556, Mtg3552, MtgG28, Mtc7x1 and Mtc411; see Fig. 1 and 2) were invariantly linked to *SYM2*, while recombination events were identified between *SYM2* and markers located at the ends of contig C1/C2 (i.e., Mtc831/ Mtc923 and MtgEB4 respectively, Fig. 1 and 2). These results, shown diagrammatically in Figure 1, suggest that the syntenic counterpart of the pea *SYM2* region is fully-contained within the C1/C2 region of *M. truncatula*. Moreover, they demonstrate that the recombination intervals are in the same order in pea as in *M. truncatula*. Physical map analysis indicates that the upper limit of the *SYM2*-like region in *M. truncatula* is approximately 350 kbp.

Table 2: RFLP markers used in pea generated from the *M. truncatula* BAC contig C1/C2.

Marker name*	Corresponding BAC clone	Pea RIL with recombination between marker and *SYM2*
Mtc831	(a)059K07	D23.3, D27.2
Mtc923	(a)056F16	D23.3, D27.2
Mtc411	(a)003I09	none
MtgG28	(a)003I09	none
Mtg3556	(a)015B03	none
Mtc7x1	(a)045I09	none
Mtg3552	(a)045I09	none
MtgEB4	(a)063C24	BC-SYM2

*cDNA clones are designated “Mtc” and genomic clones are designated “Mtg”.

Discussion

Previous studies in both animals and plants have led to the generalization that the level of synteny between two genomes is correlated with phylogenetic distance (e.g. *27*). *Medicago truncatula* and pea belong to closely related tribes within the Papilionoid subfamily of legumes, and thus it seemed likely that these two genomes would exhibit significant conservation of gene content and order. Using a set of genetic markers that are widely distributed on pea linkage group I and *M. truncatula* linkage group V, we have determined that these two linkage groups are syntenic. A specific region of these linkage groups was analyzed in greater detail to test whether the genomes of these two legumes might also be micro syntenic. Nine markers (*8 M. truncatula* subclones and *PsW62-1*) that are physically linked in *M. truncatula*, in a region spanning about 480 kbp (0.5- 1.0 cM), are also clustered in pea. Genetic analysis using pea recombinant inbred lines allowed us to position these markers into three adjacent recombination intervals, spanning a region of 0.5-1 cM. Importantly, the order of these three groups in pea is identical to that established for *M. truncatula*, demonstrating that both the content and order of the pea and *M. truncatula* genomes are largely conserved in this region.

Despite that fact that both pea and *M. truncatula* are diploid species with similar numbers of chromosomes (7 and 8, respectively), the pea genome contains nearly 10X the amount of DNA found in *M. truncatula*. From a genetic perspective, the two genomes are approximately 2-fold different, with 500 to 600 cM in *M. truncatula* (DJ Kim, unpublished) and 1200-1700 cM in pea (*28*). In both species the *SYM2* region defined in this manuscript spans approximately

0.5-1.0 cM. Due to the lack of physical map information for pea we are unable to determine if the physical to genetic distance is comparable, or not, between the two species in the *SYM2* interval. However, a potentially analogous comparison has been made for the *adh* locus of maize and sorghum (*Sorghum bicolor*), two species that are also closely related and differ 3.5X in genome size. Tikhonov *et al*. (*29*) determined that gene density of the *adh* locus in maize was 9 genes in 225 kbp, but only 70 kbp in sorghum. Thus, for the *adh* region of these two grass species, gene density was correlated with genome size.

Although reports on synteny-based cloning approaches are still limited, this strategy was used successfully to characterize the mammalian circadian mutation *tau* in Syrian hamster (*8*). A synteny based cloning approach requires that the target genome regions contain the same genes and that their order is generally conserved between the two species. However, even in highly syntenic genomes, orthologous genes can be absent. For example, the barley stem rust resistance gene *rpg1* is apparently absent from rice (*30*), despite the fact that barley and rice are highly syntenic.

In the present analysis, Southern hybridization experiments revealed that the copy number of the genes present in the *SYM2* region in pea and *M. truncatula* is not identical. In pea, only a single copy of W62 is present in the *SYM2* region, whereas in *M. truncatula* 4 copies can be detected (of which one is weakly hybridizing). Such differences in copy number are also observed in species that are highly syntenic like mouse and human (*31*), and in clusters of resistance genes in closely related plant species (e.g. *32,33*). Although construction of a corresponding physical map for pea, and complete sequencing of this region in both species, would allow a more detailed comparison of genome micro-structure at the *SYM2* locus, our present data clearly demonstrate that the gene content and overall structure of this region is conserved between pea and *M. truncatula*. We have also determined that macro-synteny is conserved throughout a significant portion of the corresponding linkage group in both species. We conclude, therefore, that detailed analysis of the *M. truncatula* genome will have significant utility for study of the pea genome.

It remains to be demonstrated that *M. truncatula* has a functional *SYM2* ortholog. Nevertheless, the conservation of genome structure between these two species was extremely useful to develop a detailed genetic map around *SYM2* in pea. In particular we were able to define a 0.5-1.0 cM interval of the pea genome that contains *SYM2*, and to delimit a 350kb orthologous region in *M. truncatula*. Our current focus is to sequence this region of *M. truncatula* and search for the *SYM2* ortholog using the “candidate gene approach”.

Materials and Methods

Differential RNA display

Differential RNA display was performed with cv Sparkle and the Sparkle introgression line BC-*SYM2* that contains the *SYM2*^{A} region of Afghanistan pea (*17,34*). Root hairs were harvested from 5 day old seedlings of cv Sparkle and BC-*SYM2* (*35*). Total RNA was isolated according to Pawlowski *et al.* (36) followed by a DNaseI (Promega) treatment. The differential display was performed according to Bauer *et al*. (*37*). Differential cDNAs were isolated from the acrylamide gel and collected in siliconized eppendorf tubes. The fragments were incubated in 100 µl TE (pH9.0) for 10 min at room temperature and subsequently boiled for 20 min. The supernatant was filtered through a glass wool filter. The DNA was ethanol precipitated in the presence of 0.3M Na-acetate (pH5.2), 50 ng glycogen and subsequently re-dissolved in 10 µl H_2O. This DNA was used as template in a PCR reaction using identical conditions as for the RNA display. The reaction mixture was separated on a 1.5% agarose gel, and DNA fragments were isolated using a gel extraction kit (MBI Fermentas) and cloned in pGEM-T (Promega). In several cases more than one clone was obtained from an excised DNA band, therefore the number of cloned fragments was determined as described by Callard *et al.* (*38*).

M. truncatula BAC library screening and construction of contig physical maps

Bacterial Artificial Chromosome (BAC) clones of *M. truncatula* genotype A17 hybridising with *PsW62-1* were identified by screening high-density filter arrays obtained from the Clemson University Genomics Institute (http://www.genome.clemson.edu). BAC DNA was isolated according to Nam *et al.* (*24*). Contigs were constructed by a combination of AFLP and restriction/hybridisation BAC DNA fingerprinting. These analyses resulted in arrays of overlapping BAC clones that formed contigs and defined different regions within each contig. Chromosome walking was conducted either by screening high density nylon arrays of BAC clones with subclones obtained from the ends of the contigs, or by PCR-screening of a multiplexed DNA copy of the *M. truncatula* BAC library with primers designed from BAC-end sequences (24). BAC clones derived from the original 5X BAC library (24) were designated with the prefix "(a)", and those obtained from the new library were designated with the prefix "(b)".

Genetic and FISH mapping in M. truncatula

The *M. truncatula* markers DK003-R, DK006-R and DK039-R are based on the BAC-end sequences of BAC clones (a)046I13, (a)058F01 and (a)045I09, respectively. Details of the genetic markers used in this study are given in Table 2. Briefly, CAPS (cleaved amplified polymorphic sequences) or length polymorphism markers were mapped on a F2 population of 93 plants from a cross between genotype A17 X A20. Polymorphic DNAs were resolved on a 1.5% agarose gel and visualised by ethidium bromide staining. Marker order and genetic distance was calculated using Map Manager (39). FISH mapping on pachytene chromosomes was done according to Kulikova *et al.* (*25*).

Pea Recombinant Inbred lines

A set of recombinant inbred lines (RILs) (Fig.1) was used to map markers in the vicinity of *SYM2*. The RILs were constructed by crossing the Rondo-*SYM2*^{A} introgression line A54 with the Rondo super-nodulating mutant Nod3 (*22*). The *NOD3* locus is located approximately 2 cM to the south of *SYM2* (Geurts; unpublished) and can be used as a phenotypic marker. The *SYM2*^{A} intogression line A54 was generated by crossing Rondo with Afghanistan and subsequently using Rondo as the recurrent parent for 4 back crosses and selecting for the *SYM2*^{A} phenotype. A54 contains an introgressed region spanning from marker cDNA267 to cDNA164, so including *SYM2*^{A} (Fig.1; *23*). 882 F2 plants of the cross A54 x Nod3 were screened for a super-nodulating phenotype upon inoculation with *Rhizobium leguminosarum.* bv *viciae* 248.pMW1071(*nodX*), a strain that nodulates plants with either the *SYM2*^{A} allele or the allele of cultivated peas (*SYM2*^{C}) like Rondo and Sparkle (*23*). 190 supernodulating plants were selected, from which 13 contained an Afghanistan *ENOD7* allele, a marker that is located 1.5 cM to the south of the *SYM2* locus (*15*).

These 13 plants were selfed and F3 plants homozygous for Afghanistan ENOD7 were inoculated with *R. leguminosarum* bv *viciae* 248, a strain that does not nodulate plants homozygous for *SYM2*^{A} (*20*). Five lines were super-nodulated (numbers D4.3, D21.7, D23.3, D27.2, and D30.1) whereas the others (numbers: D9.9, D9.11, D21.9, D24.7, D25.2, D26.6, D31.2 and D53.8) formed only a few nodules (0-10 nodules). The latter lines are homozygous for *nod3* as well as *SYM2*^{A}. These lines were crossed with the *SYM2*^{A} introgression line A569 (*23*) and the nodulation phenotype of the F1 plants confirmed that the lines are homozygous for *SYM2*^{A}.

Isolation of RFLP markers

M. truncatula cDNAs which served as RFLP markers in pea were isolated from a *M. truncatula* root hair cDNA library (*40*) using digested BAC clone inserts as probes. Subclones of the contigs were made from specific regions by using the physical map as a guide. *PsW62-1 and PsW62-2* were isolated from a pea root hair cDNA library constructed by Strategene in lambda ZAPII vector system, using equal amounts of poly(A)+ RNA isolated from root hairs of uninoculated and 48 h inoculated with *R. leguminosarum* bv *viciae* 248 of 6 days old cv Finale plants.

Mapping in pea

The *M. truncatula* and pea markers were mapped using the set of RILs and the *SYM2*^{A} introgression lines BC-*SYM2* (17,34), A543, A569 and 2 F2 segregating populations (*15,23*). RFLPs for the following markers were visualised using the indicated restriction enzymes: BamHI for Mtc923 (AF323013) and MtgEB4; EcoRI for Mtg3552, PscLRR52 and Mtg3556; HaeIII for W62 (AF327039), MtgG28, T22 (AF327041), T28 (AF327040) and PsEIL2; and HindIII for Mtc411, Mtc7x1 Mtc831, LB-1, ENOD40 and Fr19. For the marker ENOD7, allele specific primers were used in the forward direction [i.e., SCRE7A-f "TAGAGAAACCAATGAGAA" for the Afghanistan ENOD7 allele (AF323102), and SCRE7R-f "TAGAGAAACCAATGAGGC" for the Rondo ENOD7 allele (AF323101)] in combination with a common reverse primer ENOD7-r "TAATAACTACATGGTCCC". For marker OPA1 allele specific primers were used in the forward direction [i.e., SCR-A1AFG "CAGGCCCTTCCTACAAAAGAGATA" for the Afghanistan OPA-1 allele (AF327037), and SCR-A1R"GAGGCCAGGTTCAGGTAT" for the Rondo OPA-1 allele (AF327038)] in combination with a common reverse primer SCR-A1 "CAGGCCCTTCCTACAAAAGAGATA".

Acknowledgements

The root hair enriched *M. truncatula* cDNA library was generously provided by Sharon Long. This work was supported by grants form the Human Frontiers Science Organization (RG-0327) to T.B. and D.C., the EU (QLG-CT-2000-30676) to T.B., the Dutch Organization for Scientific Research (NWO-ALW) to E.L., and the US National Science Foundation (9872664) to D.C. and D.K.

References

1 Borisov AY, Barmicheva EM, Jacobi LM, Tsyganov VE, Voroshilova VA, Tikhanovich IA**: Pea (*Pisum sativum* L.) mendelian genes controlling development of nitrogen-fixing nodules and arbuscular mycorrhizae.** *Czech J. Genet. Plant Breeding* 2000, **36**:106-110.

2 Cook DR: ***Medicago truncatula* - a model in the making!** *Curr Opin Plant Biol* 1999, **2**:301-304.

3 Jiang Q, Gresshoff PM: **Classical and molecular genetics of the model legume *Lotus japonicus*.** *Mol Plant Microbe Interact* 1997, **10**:59-68.

4 Bennetzen JL: **Comparative sequence analysis of plant nuclear genomes: microcolinearity and its many exceptions.** *Plant Cell* 2000, **12**:1021-1030.

5 Devos KM, Gale MD: **Genome relationships: the grass model in current research.** *Plant Cell* 2000, **12**:637-646.

6 Paterson AH, Bowers JE, Burow MD, Draye X, Elsik CG, Jiang CX, Katsar CS, Lan TH, Lin YR, Ming R, Wright RJ: **Comparative genomics of plant chromosomes.** *Plant Cell* 2000, **12**:1523-1540.

7 Schmidt R: **Synteny: recent advances and future prospects.** *Curr opinion Plant Biol* 2000, **3**:97-102.

8 Lowrey PL, Shimomura K, Antoch MP, Yamazaki S, Zemenides PD, Ralph MR, Menaker M, Takahashi JS: **Positional syntenic cloning and functional characterization of the mammalian circadian mutation *tau*.** *Science* 2000, **288**:483-492.

9 Menancio-Hautea D, Fatokun CA, Kumar L, Danesh D, Young ND: **Comparative genome analysis of mungbean (*Vigna radiata* L. Wilczek) and cowpea (*Vigna unguiculata* L. Walpers) using RFLP mapping data.** *Theor Appl Genet* 1993, **86**:797-810.

10 Boutin S, Young ND, Olson T, Yu ZH, Schoemaker RC, Vallejos CE: **Genome conservation among three legume genera detected with DNA markers.** *Genome* 1995, **38**:928-937.

11 Weeden NF, Muehlbauer FJ, Ladizinsky G: **Extensive conservation of linkage relationships between pea and lentil genetic maps.** *J Heredity* 1992, **83**:123-129.

12 Grant G, Cregan P, Schoemaker RC**: Genome organization in dicots: genome duplication in *Arabidopsis* and synteny between soybean and *Arabidopsis*.** *Proc. Nat. Acad. Sci. USA* 2000, **97**:4168-4173.

13 Doyle JJ: **DNA data and legume phylogeny: a progress report.** In: MD Crisp and JJ Doyle (Ed.) Advances in legume systematics, seven; Phylogeny The Royal Botanic Gardens, Kew, Britain 1995, p 11-30.

14 Weeden NF, Kneen BE, LaRue TA: **Genetic analysis of *sym* genes and other nodule-related genes in *Pisum sativum*.** In: Gresshoff, Roth, Stacey and Newton (Ed.) Nitrogen fixation: achievements and Objectives, Chapman and Hall New York 1990, 323-330.

15 Kozik A, Matvienko M, Scheres B, Paruvangada VG, Bisseling T, Van Kammen A, Ellis THN, LaRue TA, Weeden NF: **The pea early nodulin gene *PsENOD7* maps in the region of linkage group I containing *sym2* and leghemoglobin.** *Plant Mol Biol* 1996, **31**:149-156.

16 Temnykh SV, Kneen BE, Weeden NF, LaRue TA: **Localization of *nod-3*, a gene conditioning hypernodulation, and identification of a novel translocation in *Pisum sativum* L. cv. Rondo.** *J Heredity* 1995a, **86**:303-305.

17 Temnykh SV, Weeden NF, LaRue TA: ***Sym*-2 and *nod*-3 are independent but closley linked genes influencing nodule development in pea.** *Pisum Genet* 1995b, **27**:26-28.

18 Schneider A, Walker SA, Poyser S, Sagan M, Ellis TH, Downie JA: **Genetic mapping and functional analysis of a nodulation-defective mutant (*sym19*) of pea (*Pisum sativum* L.).** *Mol Gen Genet* 1999, **262**:1-11.

19 Firmin JL, Wilson KE, Carlson RW, Davies AE, Downie J: **Resistance to nodulation of c.v. Afghanistan peas is overcome by *nodX*, which mediates an *O*-acetylation of the *Rhizobium leguminosarum* lipo-oligosaccharide nodulation factor.** *Mol. Microbiol* 1993, **10**:351-360.

20 Geurts R, Heidstra R, Hadri AE, Downie A, Franssen H, Van Kammen A, Bisseling T**: Sym2 of *Pisum sativum* is involved in a Nod factor perception mechanism that controls the infection process in the epidermis.** *Plant Physiol* 1997, **115**:351-359.

21 Liang P, Pardee AB: **Differential display of eukaryotic messenger RNA by means of the polymerase chain reaction.** *Science* 1992, **257**:967-971.

22 Jacobsen E, Feenstra WJ: **A new mutant with efficient nodulation in the presence of nitrate.** *Plant Sci Letters* 1984, **33**:337-344.

23 Kozik A, Heidstra R, Horvath B, Kulikova O, Tikhonovich I, Ellis THN, Van Kammen A, Bisseling T: **Pea lines carrying *sym1* or *sym2* can be nodulated by *Rhizobium* strains containing *nodX*; *sym1* and *sym2* are allelic.** *Plant Sci* 1995, **108**:41-49.

24 Nam YW, Penmetsa RV, Endre G, Uribe P, Kim D, Cook DR: **Construction of a bacterial artificial chromosome library of *Medicago truncatula* and identification of clones containing ethylene-response genes.** *Theor Appl Genet* 1999, **98**:638-646.

25 Kulikova O, Gualtieri G, Geurts R, Kim DJ, Cook DR, Huguet T, De Jong H, Franz PF, Bisseling T: **Integration of the FISH-pachytene and genetic maps *of Medicago truncatula***. *Plant J* 2001, **27**:49-58.

26 Fransz P, Armstrong S, Alonso-Blanco C, Fischer TC, Torrez-Ruiz RA, Jones G: **Cytogenetics for the model system *Arabidopsis thaliana*.** *Plant J* 1998, **13**:867-876.

27 Rossberg M, Theres K, Acarkan A, Herrero R, Schmitt T, Schumacher K, Schmitz G, Schmidt R: **Comparative sequence analysis reveals extensive microcolinearity in the lateral suppressor regions of the tomato, *Arabidopsis*, and *Capsella* genomes.** *Plant Cell* 2001, **13**:979-988.

28 Ellis THN, Turner L, Hellens RP, Lee D, Harker CL, Enard C, Domoney C, Davis DT: **Linkage map of pea.** *Genetics* 1992, **130**:649-663.

29 Tikhonov AP, SanMiguel PJ, Nakajima Y, Gorenstein NM, Bennetzen JL, Avramova Z: **Colinearity and its exceptions in orthologous *adh* regions of maize and sorghum.** *Proc Natl Acad Sci USA* 1999, **96**:7409-7414.

30 Han F, Kilian A, Chen JP, Kudrna D, Steffenson K, Yamamoto K, Matsumoto T, Sasaki T, Kleinhofs A: **Sequence analysis of a rice BAC covering the syntenous barley *Rpg1* region.** *Genome* 1999, **42**:1071-1076.

31 Dehal P, Predki P, Olsen AS, Kobayashi A, Folta P, Lucas S, Land M, Terry A, Ecale Zhou CL, Rash S, Zhang Q, Gordon L, Kim J, Elkin C, Pollard MJ, Richardson P, Rokhsar D, Uberbacher E, Hawkins T, Branscomb E, Stubbs L: **Human chromosome 19 and related regions in mouse: conservative and lineage-specific evolution.** *Science* 2001, **293**:104-111.

32 Parniske M, Hammond-Kosack KM, Golstei C, Thomas CM, Jones DA, Harrison K, Wulff BBH, Jones JDG: **Novel disease resistance specificities result from sequence exchange between tandemly repeated genes at the Cf-4/9 Locus of Tomato.** *Cell* 1997, **91**:821-832.

33 Parniske M, Jones JD: **Recombination between diverged clusters of the tomato *Cf-9* plant disease resistance gene family.** *Proc Natl Acad Sci USA* 1999, **96**:5850-5855.

34 Kneen BE, LaRue TA, Weeden NF: **Genes reported to affect symbiotic nitrogen fixation by peas.** *Pisum Newslett* 1984, **16**:31-34.

35 Gloudemans T, Bhuvaneswari TV, Moerman M, Van Brussel AAN, Van Kammen A, Bisseling T: **Involvement of *Rhizobium leguminosarum* nodulation genes in gene expression in pea root hairs.** *Plant Mol Biol* 1989, **12**:157-167.

36 Pawlowski K, Kunze R, de Vries S, Bisseling T: **Isolation of total, poly(A) and polysomal RNA from plant tissues.** In: Gelvin, SB Schilperoort RA (eds) *Plant Molecular Biology Manual*. Kluwer Academic Publishers. Dordrecht 1994, pp D5 1-13.

37 Bauer D, Muller H, Reich J, Riedel H, Ahrenkiel O, Wartoe P, Strauss M: **Identification of differentially expressed mRNA species by an improved display technique (DDRT-PCR).** *Nucleic Acids Res* 1993, **21**:4272-4280.

38 Callard D, Lescure B, Mazzolini L: **A method for the elimination of false positives generated by mRNA differential display technique.** *Biotechniques* 1994, **16**:1096-1103.

39 Manly KF, Cudmore Jr. RH, Meer JM: **Map Manager QTX, cross-platform software for genetic mapping.** *Mammalian Genome* 2001, **12**:930-932.

40 Covitz PA, Smith LS, Long SR: **Expressed sequence tags from a root-hair-enriched *Medicago truncatula* cDNA library.** *Plant Physiol* 1998, **117**:1325-1332.

Chapter 3

RNA interference in *Agrobacterium rhizogenes* transformed roots of Arabidopsis and *Medicago truncatula*

Erik Limpens, Javier Ramos, Carolien Franken, Vered Raz, Bert Compaan, Henk Franssen, Ton Bisseling and René Geurts

Journal of Experimental Botany 2004, **55**: 983-992

RNA interference (RNAi) is a powerful reverse genetic tool to study gene function. The data presented here show that *Agrobacterium rhizogenes* mediated RNAi is a fast and effective tool to study genes involved in root biology. The Arabidopsis gene *KOJAK*, involved in root hair development, was efficiently knocked down. *A. rhizogenes* mediated root transformation is a fast method to generate adventitious, genetically transformed roots. In order to select for co-transformed roots a binary vector was developed that enables selection based on *DsRED1* expression, with the additional benefit that chimaeric roots can be discriminated. The identification of chimaeric roots provided the opportunity to examine the extent of systemic spread of the silencing signal in the composite plants of both Arabidopsis and *Medicago truncatula*. It is shown that RNA silencing does not spread systemically to non co-transformed (lateral) roots and only inefficiently to the non-transgenic shoot. Furthermore, evidence is presented which shows that RNAi is cell autonomous in the root epidermis.

Introduction

In plants several reverse genetic techniques are being used to study the function of genes of interest, such as tagged mutants, targeted induced local lesions in genomes (TILLING), co-suppression and antisense suppression. Recent studies have shown that the formation of double stranded RNA (dsRNA) can lead to effective and sequence-specific degradation of homologous mRNA in a post-transcriptional fashion. Evidence for the involvement of dsRNA in mediating gene silencing was first discovered in *Caenorhabditis elegans*, and was termed RNA interference (RNAi) (*1*). Since then it has become clear that dsRNA can effectively suppress gene expression in a wide array of organisms including nematodes, insects, mammals and plants (*2,3*). In retrospect, the phenomenon of RNAi was already known in plants as post-transcriptional gene silencing (PTGS), where introduction of transgenes (co-suppression) or infection with manipulated viruses (Virus Induced Gene Silencing or VIGS) resulted in post-transcriptional silencing of homologous endogenous genes (*4,5*). RNAi is considered to be an ancient and ubiquitous antiviral system of eukaryotic organisms that has evolved before the divergence of plant and animals (*6*). The process of RNAi can be divided into a few steps. It is initiated by the production of double stranded RNA, which is recognized and cleaved by a nuclease, named DICER, to produce 21-25 nucleotide-long small interfering RNAs (siRNAs). In turn these siRNAs are incorporated into a second enzyme complex, called the RNA induced silencing complex or RISC, which is responsible for the specific degradation of homologous mRNAs in the cytoplasm (*7,8*). Currently RNAi is an important tool in the analysis of gene function in both plants and animals. Especially in *C. elegans* RNAi has been developed to 'genomics' scales (*9-11*), and also in Arabidopsis genome-wide RNAi efforts are underway.

In plants several different approaches are being used to trigger RNAi in living cells. RNAi can be triggered by generating stable transgenic plants that express RNAs capable of forming a double stranded hairpin (*12-14*). In *Nicotiana benthamiana* RNAi has been applied using *Agrobacterium tumefaciens* mediated transient expression (*15*) and in cereals, biolistic delivery of dsRNA to leaf epidermal cells by particle bombardment, resulted in interference with the function of endogenous genes at the single cell level (*16*). Also viruses can be manipulated to produce dsRNA intermediates of endogenous genes, which will be targeted for degradation after infection of the plant by the virus (*5*).

Most of these studies have mainly focused on targeting genes in the aerial parts of the plant. Recently it was shown that RNAi can also be used to effectively silence (trans) genes in primary transformed roots of the legumes *Medicago truncatula* (Medicago) (*17*) and *Lotus Japonicus* (*18*) by using *Agrobacterium rhizogenes* mediated transformation. *A. rhizogenes* generates adventitious, genetically transformed roots at the site of inoculation in many dicots and can be manipulated to co-transfer the T-DNA of a binary vector that contains the transgene of interest (*19*). Upon expression of the *root locus* (*rol)* genes carried on the Ri T-DNA, roots are formed of which a certain number will be co-transformed with the T-DNA of the binary vector (*20*). *A. rhizogenes* mediated root transformation has been described for a number of legumes. The transformed roots are morphologically indistinguishable from untransformed roots and in case of legumes they can be nodulated by *Rhizobium* bacteria and infected by mycorrhizal fungi. *A. rhizogenes* mediated transformation offers a fast alternative to generate genetically transformed roots, especially in species where generating stable transgenic lines is very time consuming. Furthermore, this method has the advantage that root cultures can be clonally propagated without the requirement of additional plant hormones.

Here it is shown that *A. rhizogenes* mediated RNAi is a fast and effective tool to study the function of genes involved in root biology, not only in legumes but also in Arabidopsis. An Arabidopsis gene, *KOJAK (CSLD3) (21,22)*, involved in root hair development was efficiently targeted by *A. rhizogenes* mediated RNAi. As selection marker for co-transformed roots the gene coding for the fluorescent protein *Ds*RED1, was used as nondestructive selectable marker. This marker offers the additional advantage to discriminate chimaeric and homogeneously transformed roots and allowed a close examination of the extent of systemic spreading of the silencing signal. RNA silencing did not spread to non co-transformed (lateral) roots and only with limited efficiency to the non-transgenic shoot of composite plants. Furthermore, evidence is presented which shows that RNA silencing is induced cell autonomously in the root epidermis.

Results

A. rhizogenes mediated root transformation in Arabidopsis and Medicago using the pRedRoot binary vector

A. rhizogenes mediated root transformation results in the formation of adventitious roots that are co-transformed with the gene of interest as well as roots lacking this gene. To interpret RNAi experiments it is essential to identify those roots that contain the transgene of interest. Recently it was shown for Medicago that selection on co-transformation can be done using kanamycin resistance (*23*). However, in our hands this selection does not effectively discriminate chimaeric roots (data not shown). Therefore the binary vector pRedRoot was developed (Fig. 1A). The pRedRoot vector provides the possiblity to select transgenic roots based on fluorescence since it contains the gene encoding for the red fluorescent protein, *DsRED1* (*24*), under control of the constitutively expressed *UBQ10* promoter of Arabidopsis (*25*). In addition to nondestructive identification of co-transformed roots this vector also allows the detection of chimaeric roots.

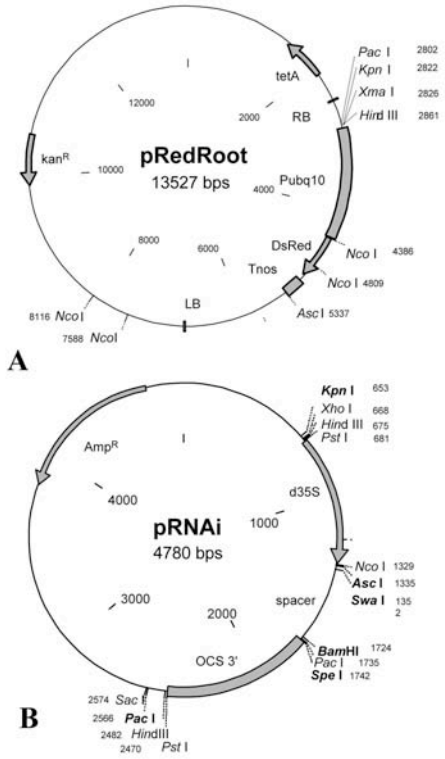

Figure 1. Plasmids used for introduction of RNAi constructs into plants via *A. rhizogenes* mediated root transformation. (A) pRedRoot binary vector, containing *DsRED1* under the control of the *AtUBQ10* promoter within the T-DNA borders. (B) pRNAi vector used to generate hairpin constructs.

To test the pRedRoot vector Medicago accessions A17 and R108 as well as Arabidopsis accessions Landsberg *erecta*, Columbia and Wassilewskija, were transformed by inoculating freshly cut hypocotyls with the *A. rhizogenes* strain MSU440 (harboring pRiA4) containing pRedRoot. The first red fluorescent Medicago roots could be observed approximately three

weeks after inoculation, whereas in Arabidopsis red fluorescent roots were already formed within 8 to 10 days. In Figure 2A a time-laps experiment is shown, following the accumulation of *Ds*RED1 in Arabidopsis at one-day intervals. Newly formed roots are visible 4 days after inoculation with *A. rhizogenes*. However, these roots do not originate from cells expressing *DsRED1* and so are not co-transformed. The *A. rhizogenes* transformed cells form a callus-like structure from which new adventitious roots are induced. To determine whether the observed red fluorescence was the result of *DsRED1* expression, a spectral image of a red fluorescent root versus a control root of Medicago was made using fluorescence spectral imaging microscopy (FSPIM). This showed that the spectrum of *Ds*RED1, with an emission peak at 583 nm, could be clearly distinguished from auto-fluorescence present in Medicago roots (Fig. 3).

The *A. rhizogenes* transformed roots of both Medicago and Arabidopsis have a similar morphology as normal roots. In the case of Medicago, they can be nodulated by the symbiotic partner *Sinorhizobium meliloti* (Fig. 2B,C). Co-transformation efficiencies varied between experiments, but on average ~30% of the newly formed roots in Medicago were co-transformed (ranging from 1 to 3 co-transformed roots per inoculated seedling), whereas in Arabidopsis efficiencies up to 20% were reached. *A. rhizogenes* mediated transformation results in the generation of homogeneously co-transformed roots as well as chimaeric roots. In general, chimaeric roots were observed in about 50% of the cases in Medicago, and only infrequently in Arabidopsis (~10%). These results show that pRedRoot is a useful binary vector for *A. rhizogenes* mediated transformation to identify transgenic roots as well as co-transformed segments in chimaeric roots.

Silencing of trans GFP in Arabidopsis and Medicago

To test the effectiveness of RNAi in *A. rhizogenes* transformed Arabidopsis roots, a *GFP* transgene was targeted in order to visualize the silencing effects. Therefore a construct was made containing 584 bp of the coding sequence of *GFP5*, cloned in both the sense and anti-sense direction separated by a 335 bp spacer, under the control of the 35S promoter in pRNAi (Fig. 1B) and subsequently transferred to pRedRoot resulting in the construct pRR-GFPi. RNA transcribed from this construct produces a hairpin structure, resulting in double stranded RNA. The pRedRoot vector enabled the identification of co-transformed roots by red fluorescence of *Ds*RED1, while the efficiency of silencing could be determined by quantification of GFP fluorescence.

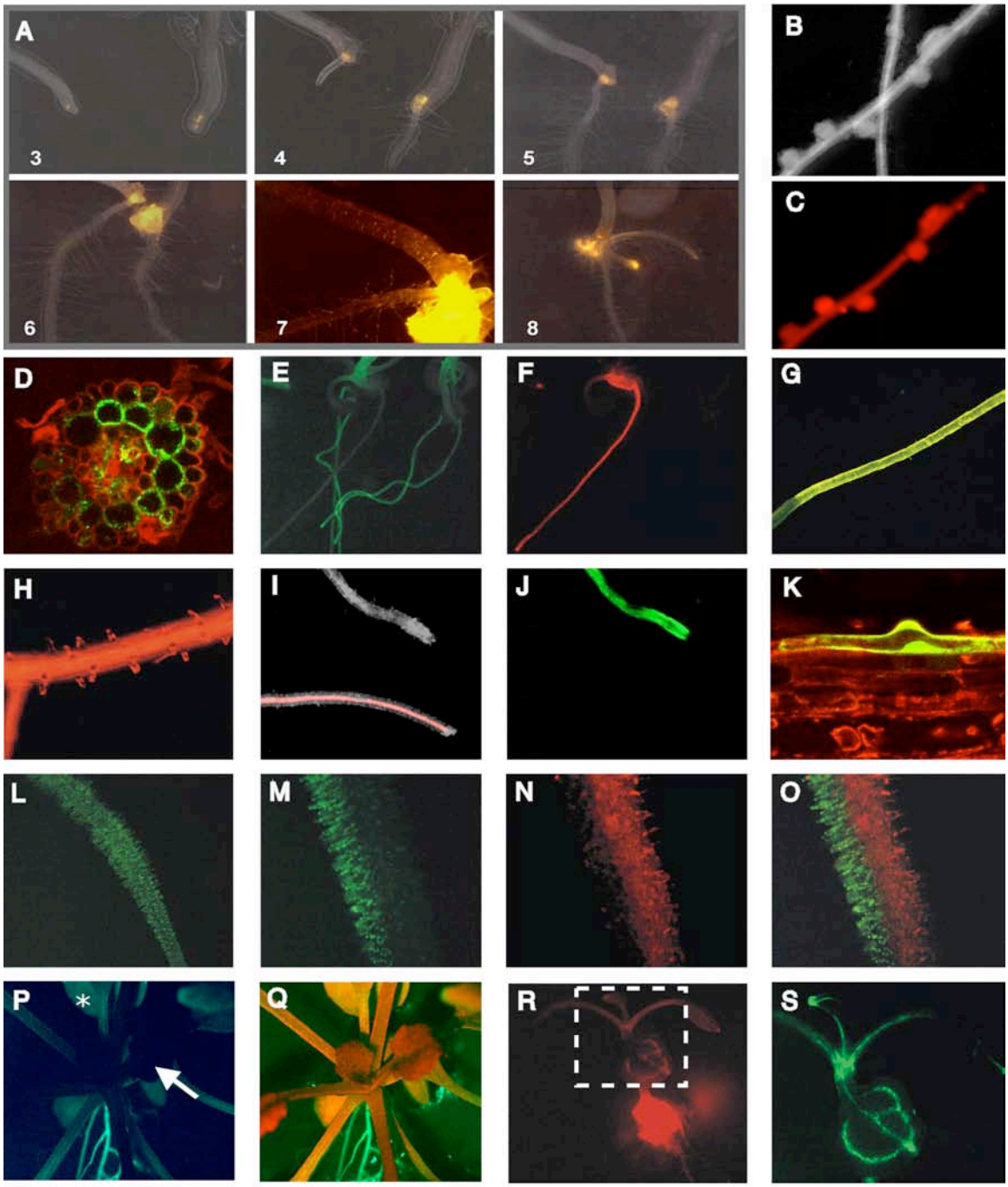

Figure 2. *A. rhizogenes* mediated root transformations in Medicago and Arabidopsis. (A) Time-laps experiment following *DsRED1* expression at one-day intervals in Arabidopsis, 3-8 days after infection with *A. rhizogenes* containing pRedRoot. (B) Brightfield picture of *A. rhizogenes* transformed roots of Medicago, using the pRedRoot binary vector, 14 days after inoculation with *Sinorhizobium meliloti*, resulting in the formation of root nodules. (C) The same roots as shown in (A) using filter settings to visualize *DsRED1* expression (red fluorescence). Only one nodulated root is co-transformed as visualized by red fluorescence. (D) GFP fluorescence in a cross-section of Arabidopsis line J0781, showing strong *GFP* expression in the cortex and stele. Root was counterstained with propidium iodide (0,2 μg/ml). (E) GFP fluorescence in Arabidopsis line J0781 transformed with pRR-GFPi, 14 days after transformation. The left plant contains one co-transformed root as visualized by red fluorescence in (F). Only in this co-transformed root *GFP* is silenced. GFP fluorescence in the non co-transformed roots and the hypocotyl is not affected. (G) Brightfield picture of a 12 day old *A. rhizogenes* transformed root of Arabidopsis, co-transformed with pRR-KJKi showing a hair-less root. (H) Segment of an Arabidopsis root, co-transformed with pRR-KJKi, showing slightly elongated small root hairs.

Figure 2 continued: (I) Chimaeric root on J0781, co-transformed with pRR-GFPi in the stele as judged by red fluorescence. An overlay of the *Ds*RED1 channel with the brightfield image is shown. The upper (non-red) root is a lateral root that formed on this chimaeric root. (J) GFP fluorescence in the chimaeric root shown in (I). No GFP fluorescence is visible in the co-transformed chimaeric root, whereas the (non-red) lateral root has regained GFP fluorescence. (K) Confocal picture showing specific GFP fluorescence in the root epidermis of *A. rhizogenes* transformed Medicago line R108-RH2::GFP. (L) Fluorescence due to expression of *GFP* in the root epidermis of the Medicago line R108-RH2::GFP. (M-O) Chimaeric root on Medicago line R108-*RH2::GFP* 4 weeks after transformation with pRR-GFPi. *GFP* expression (M) and *DsRED1* expression (N) and a merged picture (O) are shown. *GFP* expression is only affected in co-transformed root tissue as visualized by red fluorescence. (P) Partial systemic silencing in Arabidopsis line *35S::GFP* transformed with pRR-GFPi 4 weeks after transformation. Arrow marks a systemically-silenced leaf, asterisk marks a non-silenced leaf. (Q) Brightfield picture (using 525nm long pass filter) of the composite *35S::GFP* plant shown in (P). (R) Arabidopsis line J0661 transformed with pRR-GFPi 14 days after transformation, showing red fluorescence due to *Ds*RED1 in the callus as well as vascular tissue of the shoot. The boxed area is shown in (S) using filter settings to visualize GFP fluorescence.

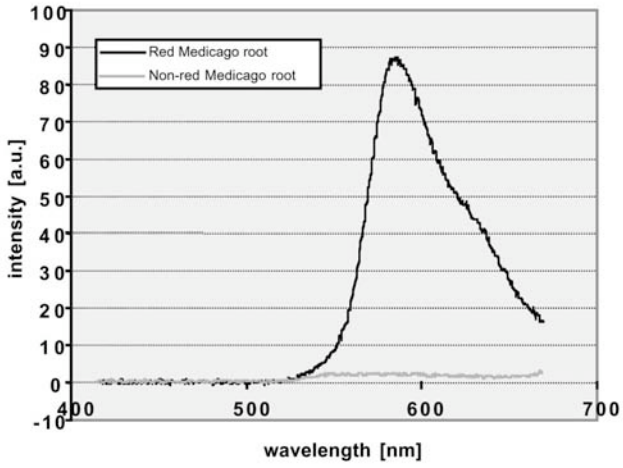

Figure 3. Spectral image of a co-transformed red fluorescent Medicago root and a non co-transformed (non-red) root. The *Ds*RED1 protein has a maximum emission at 583 nm.

In Arabidopsis Gal4 enhancer trap line J0781, expressing*GFP* was used (http://www.plantsci.cam.ac.uk/Haseloff/IndexCatalogue.html). J0781 shows strong *GFP* expression in the root cortex and stele and in the hypocotyl (Fig. 2D,E). Transgenic roots were analyzed twelve days after infection with *A. rhizogenes* carrying pRR-GFPi. In 91% (n=98) of the red fluorescent roots no GFP fluorescence could be detected after co-transformation with pRR-GFPi (Fig. 2E,F), whereas roots (n=63) transformed with the pRedRoot control vector all showed bright GFP fluorescence (Table 1). To verify knock down of *GFP* in the *A. rhizogenes* transformed roots, *GFP* mRNA levels were determined by real-time RT-PCR (qPCR) (Fig. 4A). Since Arabidopsis roots are relatively small, independently transformed roots were clonally propagated in order to isolate sufficient RNA material for the qPCR. The results of the qPCR show that *GFP* mRNA is substantially reduced, at least 10 times, in the pRR-GFPi transformed roots compared to control roots. Since there was still residual *GFP* mRNA present in the *GFP*-silenced roots it was determined whether GFP

protein could still be detected in these roots. Immuno-blotting showed that no GFP protein could be detected in the *GFP*-silenced roots, whereas in the control roots a high level of GFP protein was detected (Fig. 4B). This correlates well with the absence of detectable GFP fluorescence in these roots.

Table 1. Effects of *A. rhizogenes* mediated RNAi in Arabidopsis and Medicago

Construct	Transformed Plant	# Co-Transformed Roots	# Silenced	# Not Silenced
pRedRoot	AtJ0781	63	-	63 (100%)
pRR-GFPi	AtJ0781	98	89 (91%)	9 (9%)
pRedRoot	Mt R108-RH2::GFP	12	-	12 (100%)
pRR-GFPi	Mt R108-RH2::GFP	37	32 (86%)	5 (14%)
pRedRoot	Arabidopsis	40	-	40 (100%)
pRR-KJKi	Arabidopsis	58	53 (91%)	5 (9%)

Similar results were obtained in Medicago, where a stable transformed line R108-*RH2::GFP* was used, which contains the 1.1 kb promoter region of the pea *RH2* gene in front of *GFP* (*26*). The *RH2* promoter is active in root epidermal cells in the zone of the root starting immediately above the root apical meristem and extending into the region containing mature root hairs (*27*). In line R108-*RH2::GFP* GFP fluorescence can be detected in the epidermis of young developing roots (*26*), which was preserved in *A. rhizogenes* transformed roots (Fig. 2K,L). Four weeks after transformation with pRR-GFPi co-transformed roots were analyzed. In 86% (n=37) of homogeneously transformed roots no GFP fluorescence could be detected (Table 1). In control plants, transformed with the pRedRoot vector, all transgenic roots (n=12) showed clear GFP fluorescence.

Silencing endogenous genes in Arabidopsis roots

The potential of *A. rhizogenes* mediated RNAi with respect to silencing of endogenous genes in Arabidopsis was also investigated. For this purpose the gene *KOJAK (KJK/CSLD3)* was selected (*21,22*). *KJK* encodes a cellulose synthase-like protein, which is preferentially expressed in trichoblasts (*21*). Root hair formation is initiated in *kjk* mutants at the correct position but in general stops at the bulge stage, resulting in hair-less roots. A silencing construct for *KJK* was made in the pRedRoot vector and pRR-KJKi was transformed by *A. rhizogenes* mediated transformation to both Arabidopsis accessions Landsberg *erecta* and Wassilewskija. Results are summarized in Table 1. Ninety-one percent (n=58) of the homogeneously transformed roots, as judged by red fluorescence, showed a root hair phenotype. In most roots (62%) root hairs were initiated but failed to elongate resulting in hair-less roots containing small bulges (Fig. 2G). But in some roots (29%), root hair cells developed more than a bulge and showed some elongation resulting in small root hairs (Fig.

2H). Roots transformed with the pRedRoot control vector all contained normal root hairs. To verify knock down of *KJK* in the *A. rhizogenes* transformed roots, the amount of *KJK* mRNA was quantified after clonally propagating the co-transformed roots. qPCR showed that *KJK* mRNA was substantially reduced, at least 8 times, in the pRR-KJKi transformed roots compared to control roots (Fig. 4C). These results show that *A. rhizogenes* mediated RNAi is an effective and very fast method to silence endogenous genes in the roots of Arabidopsis. Furthermore, a spectrum of phenotypes can be obtained from RNAi.

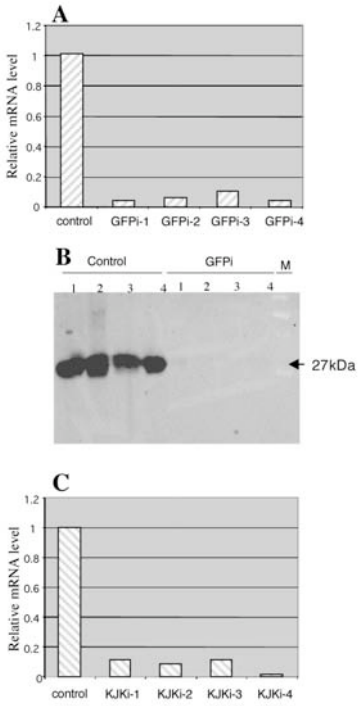

Figure 4. Quantification of mRNA and protein levels in *A. rhizogenes* transformed roots. (a) *GFP* transcript levels of Arabidopsis line J0781 co-transformed with pRR-GFPi. RNA was isolated from four 4-week-old independently co-transformed root cultures, and relative transcript levels were determined by qPCR using *ACTIN* as reference. The average of three independent control roots co-transformed with the empty pRedRoot vector is shown. (b) Immunodetection of GFP protein in five 4-week-old independently co-transformed root cultures of Arabidopsis line J0781. Control roots are co-transformed with the empty pRedRoot vector. (c) *KJK* transcript levels in four 4-week-old Arabidopsis root cultures independently co-transformed with pRR-KJKi. The average of three independent control roots co-transformed with the empty pRedRoot vector is shown.

Systemic spreading of the silencing signal in roots of Arabidopsis and Medicago

In several plant species it was shown that the induction of RNAi results in systemic spread of the silencing signal (*28*). *A. rhizogenes* mediated root transformation makes it possible to determine whether the interference signal is systemically transported to non-transformed roots or the non-transgenic shoot of the composite plant. To examine the extent of systemic spread of the silencing signal in *A. rhizogenes* transformed roots the stable *GFP* expressing Medicago (R108-*RH2::GFP*) and Arabidopsis (J0781) lines were used. As mentioned above, transformation of these lines with pRR-GFPi efficiently knocked down *GFP* expression. However, no reduction in GFP fluorescence was detected in non co-transformed roots on composite plants that also contained silenced roots (Fig. 2E,F).

The use of *DsRED1* as selectable marker enables the identification of chimaeric roots. This provided the possibility to determine the extent of systemic spread of the silencing signal from

co-transformed root tissue to non co-transformed root tissue. Chimaeric roots on Arabidopsis J0781 co-transformed with pRR-GFPi showed knock down of *GFP* expression in the entire cortex and stele of those particular roots. Figure 2I shows a chimaeric pRR-GFPi transformed J0781 root that appears to be co-transformed only in (part of) the stele as judged by red fluorescence. However, no GFP fluorescence was detected in both the cortex and the stele of this chimaeric root (Fig. 2J). When such chimaeric pRR-GFPi transformed J0781 roots were clonally propagated, new lateral roots emerged that did not show any *Ds*RED1 fluorescence and regained GFP fluorescence (Fig. 2I,J). This indicates that systemic spread of the silencing signal does take place within the cortex and stele of a single chimaeric *A. rhizogenes* transformed root, but not to non co-transformed lateral roots. Further, the extent of systemic spread of the silencing signal to the epidermis of the root was investigated. Therefore the Medicago R108-*RH2::GFP* line was used that expresses *GFP* exclusively in the epidermis (Fig. 2K,L). Upon transformation with pRR-GFPi chimaeric roots were searched for that contained transformed epidermal cell files. Figure 2M,N,O shows such a chimaeric root transformed with pRR-GFPi. Approximately half of the epidermal cell files are co-transformed as visualized by red fluorescence. Strikingly, silencing of *GFP* occurs only in the co-transformed cell files, whereas, in the epidermal cell files lacking *DsRED1* expression, GFP fluorescence intensity is as high as in control roots. Even 6 weeks after transformation, the fluorescence in the non-transformed epidermal cell files was as strong as in control roots, indicating that RNAi is cell autonomous in the root epidermis.

Systemic spreading of the silencing signal to the shoot

RNAi of a trans *35S::gusA* gene in *Lotus japonicus* indicated some systemic spreading of the silencing signal to the non-transgenic shoots of *A. rhizogenes* transformed plants (*18*). To investigate the level of systemic spreading of the silencing signal to the shoot two additional transgenic Arabidopsis lines were used; one carrying *35S::GFP* and a second Gal4 enhancer trap line, J0661, which shows strong GFP fluorescence in root vascular tissue and in the vascular tissue of the cotyledons and leafs. *A. rhizogenes* mediated RNAi of *GFP* in the *35S::GFP* transgenic line resulted in 20% of the *A. rhizogenes* transformed plants (n=40) showing no, or very low levels, of GFP fluorescence in the shoots four weeks after transformation. In 60% of the plants bright GFP fluorescence was visible in some leafs whereas other leafs on the same composite plant lacked GFP fluorescence (Fig. 2P,Q), and even variation within one leaf was observed. Twenty percent of the composite plants did not show any sign of silencing in the shoot, while *GFP* expression in the co-transformed roots of these composite plants was efficiently knocked down. In contrast to systemic spreading, albeit inefficiently, in the *35S::GFP* line, no visible reduction of *GFP* expression in the vascular tissue of the leaves of enhancer trap line J0661 was observed 4 weeks after transformation (Fig. 2R,S). Red fluorescence due to the *Ds*RED1 protein could occasionally be observed in the

vascular tissue of the shoot (Fig. 2R). Also in the hypocotyl of *A. rhizogenes* transformed enhancer trap line J0781 GFP fluorescence was not reduced (Fig. 2E).

Discussion

Here it is shown, by targeting *KJK/CSLD3*, that endogenous genes can efficiently be silenced in roots of Arabidopsis via RNAi by using *Agrobacterium rhizogenes* mediated transformation. A high percentage (91% in the case of *KJK*) of the homogeneously transformed roots showed phenotypes identical to the described mutant (*22*). Quantification of mRNA levels by qPCR confirmed the knock down of the corresponding gene. However, residual mRNA could still be detected and also some variation in the level of expression was detected between independently transformed roots. This variation in mRNA levels could be an explanation for the observed variation in phenotypes. In these plants 62% of the homogeneously transformed roots initiated root hairs that stopped at the bulge stage without further elongation, but in 29% of the cases some elongation took place resulting in small root hairs. A similar plasticity in phenotypes has been observed for the *csld3-1* mutant and is thought to be the result of a reduction in the amount of correctly targeted protein to the membrane, resulting in a reduction of delivery of cellulose polymers to the primary cell wall (*22*). The occurrence of intermediate phenotypes as a result of RNAi has also been reported for stable transformed Arabidopsis plants (*13*) and can be an additional tool to gain insight into the function of a gene.

Generally it is thought that a specific mobile silencing signal exists that can travel between cells via plasmodesmata and long distances via the phloem (*29-32*). For example, in Arabidopsis, biolistic delivery of dsRNA into leaf cells triggered silencing capable of spreading locally and systemically. It was reported that systemic spreading of the silencing signal could be detected two weeks after biolistic delivery starting in the veins of non-bombarded leaves and was clearly evident in non-vascular tissues one month after bombardment (*33*). Strikingly, *A. rhizogenes* mediated RNAi of trans *GFP* in Arabidopsis or Medicago roots showed that systemic transport of the silencing signal does not occur to non co-transformed roots. Targeting *GFP* in the Gal4 enhancer trap lines J0661 and J0781 also did not show any systemic spread to the non-transgenic shoot. However, targeting of *GFP* in a *35S::GFP* transgenic line did result in systemic transport of the silencing signal, but the extent of silencing was more limited and greatly variable. Similar results are reported in *Lotus japonicus* where *A. rhizogenes* mediated silencing of a *35S::gusA* transgene did not spread to non co-transformed roots and was limited and variable in the shoots (*18*). The lack of systemic spread of the silencing signal to non co-transformed roots is in agreement with grafting experiments performed in tobacco, which suggested that silencing is unidirectional from the base to the top of the plant (*29,34*). The observed variation in spatial patterns of silencing in the shoot of the *35S::GFP* line has also been observed in different plant species and for different transgenes under the control of the 35S promoter (*34-37*). The extent of systemic silencing in the shoot

could depend on the regulation of the transgene, since no systemic silencing was observed in the shoot of transformed enhancer trap line J0661 and J0781, which express *GFP* under the control of an endogenous enhancer element.

The use of *DsRED1* as selection marker enabled the selection of chimaeric roots to examine the extent of systemic spread of the silencing signal within root tissue. Arabidopsis line J0781 shows strong *GFP* expression in the cortex and stele of the root. Chimaeric J0781 roots partly transformed with pRR-GFPi showed silencing of *GFP* in the entire cortex and vasculatur tissue, indicating that the silencing signal is able to spread systemically in the cortex and stele. Strikingly, lateral roots that formed on these chimaeric roots and were most likely not co-transformed, regained *GFP* expression. This suggests that within one root system, the silencing signal does not spread to non co-transformed lateral roots. Formally it cannot be ruled out that co-suppression of the newly introduced transgene is the cause of the chimaeric nature of these roots. However, this seems less likely since it would imply that the hairpin construct is transcriptionally silenced in a cell autonomous way. The absence of systemic spread to the lateral roots is most likely a result of the unidirectional movement of the silencing signal. In contrast to systemic spread in the cortex and vascular tissue in Arabidopsis, no cell-to-cell movement of the silencing signal was observed in the epidermis of Medicago, demonstrating that silencing in the root epidermis is cell autonomous. One explanation for the fact that spreading of the silencing signal is not observed in the epidermis of *A. rhizogenes* mediated roots, could be that epidermal cells become symplastically isolated. By dye-coupling experiments in Arabidopsis roots it was shown that cells in the meristem and epidermal cells in the elongation zone are symplastically connected through plasmodesmata, but gradually become symplastically isolated as the epidermal cells differentiate. By the time root hair outgrowth is visible the epidermal cells are symplastically isolated (*38*). Similarly, it was shown that symplastically isolated stomatal guard cells do not silence systemically (*30*). So, the symplastic isolation of cells could cause the immobility of the silencing signal.

RNAi via *A. rhizogenes* mediated root transformation is a valuable tool to study genes involved in root development and root-microbe interactions. It is a very fast and efficient system to silence genes in roots. In Arabidopsis, silenced *A. rhizogenes* transformed roots can already be obtained within ten days. Especially for plant species with very time consuming regeneration times this methods offers a big advantage. The fact that silencing is triggered cell autonomously in the root epidermis provides the possibility to use inducible and tissue-specific promoters to more specifically regulate RNAi. At the same time it requires a thorough inspection of the chimaeric nature of *A. rhizogenes* transformed roots in order to correctly interpret the observed phenotypes. The pRedRoot vector provides this possibility.

Materials and methods

Plasmids and vectors

To create pRedRoot the *nptII* gene and NOS terminator of pBINPLUS (*39*) were removed by a Bsu36*I* and Bst98*I* digestion, Klenow treatment and re-ligation. The created plasmid was named pBASIS. The Arabidopsis UBQ10 promoter was PCR amplified using genomic DNA of the accession Columbia as template (used primers: 5'AAGCTTTGTCCCGACGGTGTTGT3' and 5'CCATGGCAAAGATCTGCATCTGTTA3') and subsequently cloned in frame with the ATG startcodon of *DsRED1* (Clontech) in a pGEM-T (Promega) derived vector that contained a NOS terminator. A 2.5 kb Hind*III*-Asc*I* fragment containing UBQ10::*DsRED1*-NOS terminator was cloned into pBASIS resulting in pRedRoot (Fig. 1A).

In order to create inverted repeat constructs a 1.3 kb fragment of vector pFGC1008 (described at http://ag.arizona.edu/chromatin/fgc1008.html) containing Sac*I* 2927 bp – Hind*III* 4150 bp (the RNAi box) was PCR amplified and cloned into pBluescriptIISK+ (Stratagene) (primers: 5'CACTGACGTAAGGGATGA3' and 5'ATGAGCTCTTAATTAAGGATGTGCTGCAAGGCGA3'). A double *CaMV* 35S promoter was PCR amplified from vector pMON999 (primers: 5'TGATCTCGAGCAAGCTTCTGCAGGTCCAT3' and 5'CATGCCATGGAGATCTGCTAGAGTCAGC3') and cloned Xho*I*-Nco*I* in front of this RNAi box to result in the pRNAi vector (Fig. 1B). Inverted repeats were created in pRNAi by two sequential cloning steps. Target regions are first PCR amplified, and subsequently cloned Asc*I*-Swa*I* and BamH*I*-Spe*I* into the created pRNAi derivative. The resulting inverted repeat construct was inserted Kpn*I*–Pac*I* into the pRedRoot binary vector. Target regions were amplified using the following primer combinations:

GFP5 (584 bp)	5'ATACTAGTGGCGCGCCTTGTTGAATTTAGATGGTGATG3'
	5'ATGGATCCATTTAAATTTCGAAAGGGCAGATTG3'
KJK (461 bp)	5'ATACTAGTGGCGCGCCGTGTGCCAGAAGAAAACC3'
	5'ATGGATCCATTTAAATGCCAGTAGCCCATCGGAGAAC3'

The Spe*I*-Asc*I* and BamH*I*-Swa*I* restriction sites that are included within the primers have been underlined.

Bacterial strains

Agrobacterium strain MSU440 containing the pRi plasmid pRiA4 (*40*) was used to transform Medicago and Arabidopsis. The binary vectors were introduced into MSU440 by electrotransformation and grown for two days at 28°C under kanamycin selection (50 µg/ml). Integrity of inverted repeat constructs was checked by mini-prepping and restriction-digestion with Hind*III*.

Plant material

For Medicago the accession Jemalong A17 and the transgenic line R108-*RH2::GFP* were used (*26,41,42*). R108-*RH2::GFP* carries the 1.1 kbp promoter region of the pea *RH2/DRRG* gene (Genbank J03680, *43*) in front of *GFP5* (*26*). For Arabidopsis the accessions Landsberg *erecta*, Columbia and Wassilewskija were used. The Gal4 enhancer trap lines J0661 and J0781 are described at http://www.plantsci.cam.ac.uk/Haseloff/IndexCatalogue.html.

Agrobacterium rhizogenes mediated transformation

Medicago seeds were surface sterilized by incubating for 10 min. in concentrated Sulfuric acid, 6x washing in sterile water, 10 min 4% hyper chlorite (commercial bleach) and 7x washing in sterile water and subsequently plated on Färhaeus medium (1 mM $MgSO_4.7H_2O$, 0.75 mM KH_2PO_4, 1 mM Na_2HPO_4, 15 µM Fe-Citrate, 0.75 mM $Ca(NO3)_2$, 0.7 mM $CaCl_2$ 0.35 µM $CuSO_4.5H_2O$, 4.69 µM MnSO4.$7H_2O$, 8.46 µM $ZnSO_4.7H_2O$, 51.3 µM H_3BO_3, 4.11 µM $Na_2MoO_4.2H_2O$, 0.9 % Daichin agar(Brunschwig)) containing a filter paper. Seeds were vernalized for 1 day at 4°C and germinated at 25°C for 24 hours in darkness (plates upside down). One day old seedlings were transferred to new 9 cm petridishes containing Färhaeus medium and a half-round filter paper (5 seedlings per plate), and grown at

21°C (16h light-8h darkness) after removal of the seed coat. The petridishes were not completely closed by parafilm to enable aeration. The roots of 5 day old seedlings were removed at the hypocotyl and the wound surface was inoculated with *Agrobacterium* MSU440 containing the appropriate binary plasmid. The seedlings are co-cultivated with *Agrobacterium* for 5 days at 21°C (16h light-8 h darkness) and subsequently transferred to Emergence medium (3 mM MES pH 5.8 containing 2,5 g/L KNO_3, 0.4 g/L $MgSO_4.7H_2O$, 0.3 g/L $NH_4H_2PO_4$, 0.2 g/L $CaCL_2.2H_2O$, 10 mg/L $MnSO_4.4H_2O$, 5 mg/L H_3BO_3, 1 mg/L $ZnSO_4.7H_2O$, 1 mg/L KI, 0.2 mg/L $CuSO_4.5H_2O$, 0.1 mg/L $NaMoO_4.2H_2O$, 0.1 mg/L $CoCL_2.6H_2O$, 15 mg/L $FeSO_4.7H_2O$, 20 mg/L Na_2EDTA, 100 mg/L Myoinositol, 5 mg/L Nicotinic acid, 10 mg/L Pyriodoxine HCl, 10 mg/L Thiamine HCl, 2 mg/L Glycine, 1% sucrose, 0.9% Daichin agar containing 300 µg/ml Cefotaxime (Duchefa)) and covered by a (half-) filter paper. Plants were grown for 6-18 days on Emergence medium. In this period new roots are formed that are potentially co-transformed with the T-DNA of the binary vector.

Transformation of Arabidopsis is done in a similar way with the following differences: Seeds were surface sterilized by incubating for 5 min. in 2% hyper chlorite (commercial bleach), 5x washing in sterile water and vernalized at 4°C for 3 days. Two day old seedlings were used for co-cultivation with the appropriate *Agrobacterium* MSU440 strain (20 plants per plate). Plants are grown on plates with a filter paper, containing 0.5x Murashige and Skoog (MS) salts (Duchefa), 1% sucrose and 0,8% (w/v) Daichin agar, for 3 days (21°C; 16h light-8h darkness) and subsequently transferred to 0,5x MS plates containing 300 µg/ml Cefotaxime (Duchefa).

Nodulation of A. rhizogenes transformed roots

Three weeks after transformation composite Medicago plants are starved for nitrate for 3 days (21°C; 16h light-8h darkness) on Färhaeus medium (without $Ca(NO3)_2$.). Then plants are transferred to agra-perlite (Maasmond-Westland, The Netherlands) saturated with Färhaeus medium (without $Ca(NO3)_2$) and inoculated with 1 ml culture of *S. meliloti* 2011.pHC60 (OD_{600} 0.1) per plant and grown for two weeks (21°C; 16h light-8h darkness).

Clonally propagating A. rhizogenes transformed roots

A. rhizogenes transformed Arabidopsis roots were excised (~ 1 cm above the tip) and transferred to 25 ml ARC medium (*44*) containing 0.05 mg/l IAA. After three days, the root pieces were transferred to new 25 ml ARC medium without IAA and cultured in the dark at 25°C for 4 weeks with gentle shaking (100 revolutions/min).

Microscopy

Imaging of *Ds*RED1 or GFP was done using the Leica MZIII fluorescence stereomicroscope with the appropriate filter settings. Images where processed electronically using Adobe Photoshop 5.5. Spectral imaging of *Ds*RED1 was done according to Gadella *et al.,* (*45*). The slit width of the imaging spectograph was 200 µm and the central wavelength was 550 nm. A 525 nm longpass emission filter was used. Imaging of GFP fluorescence in Medicago line R108-*RH2::GFP* and in the Arabidopsis J0781 cross-section was performed on a Zeiss LSM 510 confocal laser scanning microsope (Carl-Zeiss); excitation 488 (GFP), 543 nm (propidium iodide/DsRED1); GFP emission was selectively detected by using a 505-530 nm bandpass filter, propidium iodide/*Ds*RED1 emission was detected in another channel using a 560-615 nm bandpass. The root was counter-stained with 0.2 µg/ml propidium iodide.

qPCR

Total RNA was extracted from 4-week-old Arabidopsis root cultures according to Pawlowski *et al.,* (*46*) followed by DNAseI (Promega) treatment. cDNA was made from 1 µg total RNA using the Taqman Gold RT-PCR kit (Perkin-Elmer Applied Biosystems) in a total volume of 50 µl using the supplied hexamer primers. qPCR reactions were performed in triplo on 6,5 µl cDNA using the SYBR-Green^R PCR Master kit (Perkin-Elmer Applied Biosystems) (40 cycles of 95°C for 10 s, 60°C for 1 min) and real-time detection was performed on the ABI 7700 and analyzed using the GeneAmp 5700 SDS software (Perkin-Elmer Applied Biosystems). Optimal amplification efficiencies for the

different primer sets were determined by performing qPCR with a concentration range of primers, cDNA and control plasmids. The specificity of the PCR amplification procedures was checked with a heat dissociation step (from 65°C-95°C) at the end of the run and by agarose gel electrophoresis. Results were standardized to the ACTIN2/8 expression levels. Primer combinations used in the qPCR were chosen outside of the regions targeted by the RNAi constructs.

Primers used:

AtAct2/8-F:	5' GGTAACATTGTGCTCAGTGGTGG 3'
AtAct2/8-R:	5' AACGACCTTAATCTTCATGCTGC 3'
AtKJK-F:	5' TGAGAGCTCTTGATGGGTTGATGG 3'
AtKJK-R:	5' TCGGTTTTCTTCTGGCACACGG 3'
GFP4-F:	5' CTGTCCTTTTACCAGACAACCATTACC 3'
GFP4-R:	5' CCAGCAGCTGTTACAAACTCAAGAAG 3'

Immuno-blotting

Proteins were isolated from 4-week-old Arabidopsis J0781 root cultures by grinding 1 gram of root tissue in liquid nitrogen and resuspension in extraction buffer (50 mM Tris-acetate, pH 7.4, 10 mM potassium-acetate, 1 mM EDTA, 5 mM DTT, 0.5 mM PMSF) followed by two subsequent centrifugation steps: 1000 rpm 15 min and 15000 rpm 30 min. The supernatant was used for analysis. Protein concentrations were determined using the Bio-Rad Protein Assay (Bio-Rad). 20 μg protein was separated on a 12,5% SDS-PAGE gel. After electrophoresis, proteins were blotted onto nitrocellulose paper (Schleicher and Schull) and immunostained with 1:1000 diluted rabbit anti-GFP (Molecular Probes) followed by 1:5000 diluted anti-rabbit-HRP and detected using the ECL Plus™ Western Blotting Detection Kit for HRP (Amersham Biosciences) on a Storm 840 (Molecular Dynamics). The blot was stained for total protein using Ponceaux S (Sigma Diagnostics).

Acknowledgements

The authors thank Mark Kwaaitaal (Biochemistry, Wageningen University) and Jeroen Pouwels (Molecular Biology, Wageningen University) for their help with the immuno-blotting. Toolbox 21 for their work on Arabidopsis line *35S::GFP.* Oscar Vorst and Jos Molthoff (Plant Research International, Wageningen) for their assistance with the qPCR. Jan-Willem Borst (Biochemistry, Wageningen University) for assistance with the FSPIM. Arabidopsis line *35S::GFP* was kindly provided by Renze Heidstra (Molecular Cell Biology, Utrecht University). E.L., T.B. and R.G. is supported by The Netherlands Organization of Scientific Research (NWO), and the E.U. FP5 program QLG-CT2000-00676.

References

1 Fire A, Xu S, Montgomery MK, Kostas SA, Driver SE, Mello CC: **Potent and specific genetic interference by double-stranded RNA in *Caenorhabditis elegans.*** *Nature* 1998, **391**: 806-811.

2 Tavernarakis N, Wang SL, Dorovkov M, Ryazanov A, Driscoll M: **Heritable and inducible genetic interference by double-stranded RNA encoded by transgenes.** *Nature Genet* 2000, **24**: 180-183.

3 Elbashir SM, Harborth J, Lendeckel W, Yalcin A, Weber K, Tuschl T: **Duplexes of 21-nucleotide RNAs mediate RNA interference in cultured mammalian cells**. *Nature* 2001, **411**: 494-498.

4 Van der Krol AR, Mur LA, Beld M, Mol JN, Stuitje AR: **Flavonoid genes in petunia: addition of a limited number of gene copies may lead to a suppression of gene expression.** *Plant Cell* 1990, **2**: 291-299.

5 Ratcliff F, Martin-Hernandez AM, Baulcombe DC: **Tobacco rattle virus as a vector for analysis of gene function by silencing.** *Plant J* 2001, **25**: 237-245.

6 Sharp PA: **RNA interference-2001.** *Genes Dev* 2001, **15**: 485-490.

7 Hammond SM, Caudy AA, Hannon GJ: **Post-transcriptional gene silencing by double-stranded RNA**. *Nature Rev Genet* 2001, **2**: 110-119.

8 Hannon GJ: **RNA interference.** *Nature* 2002, **418**: 244-251.

9 Fraser AG, Kamath RS, Zipperlen P, Martinez-Campos M, Sohrmann M, Ahringer J: **Functional genomic analysis of *C. elegans* chromosome I by systematic RNA interference.** *Nature* 2000, **408**: 325-330.

10 Gönczy P, Echeverri C, Oegema K, Coulson A, Jones SJ, Copley RR, Duperon J, Oegema J, Brehm M, Cassin E, Hannak E, Kirkham M, Pichler S, Flohrs K, Goessen A, Leidel S, Alleaume AM, Martin C, Ozlu N, Bork P, Hyman AA: **Functional genomic analysis of cell division in *C. elegans* using RNAi of genes on chromosome III.** *Nature* 2000, **408**: 331-336.

11 Maeda I, Kohara Y, Yamamoto M, Sugimoto A: **Large-scale analysis of gene function in *Caenorhabditis elegans* by high-throughput RNAi.** *Curr Biol* 2001, **11:** 171-176.

12 Waterhouse PM, Graham MW, Wang MB: **Virus resistance and gene silencing in plants can be induced by simultaneous expression of sense and antisense RNA.** *Proc Natl Acad Sci USA* 1998, **95**: 13959-13964.

13 Chuang C, Meyerowitz M: **Specific and heritable genetic interference by double-stranded RNA in *Arabidopsis thaliana.*** *Proc Natl Acad Sci USA* 2000, **97**: 4985-4990.

14 Wesley SV, Helliwell CA, Smith NA, Wang MB, Rouse DT, Liu Q, Gooding PS, Singh SP, Abbott D, Stoutjesdijk PA, Robinson SP, Gleave AP, Green AG, Waterhouse PM: **Construct design for efficient, effective and high-throughput gene silencing in plants.** *Plant J* 2001, **27**: 581-590.

15 Johansen LK, Carrington JC: **Silencing on the spot. Induction and suppression of RNA silencing in the *Agrobacterium*-mediated transient expression system.** *Plant Physiol* 2001, **126**: 930-938.

16 Schweizer P, Pokorny J, Schulze-Lefert P, Dudler R: **Double-stranded RNA interferes with gene function at the single-cell level in cereals.** *Plant J* 2000, **24**: 895-903.

17 Limpens E, Franken C, Smit P, Willemse J, Bisseling T, Geurts R: **LysM domain receptor kinases regulating rhizobial Nod factor-induced infection.** *Science* 2003, **302**: 630-633.

18 Kumagai H, Kouchi H: **Gene silencing by expression of hairpin RNA in Lotus *japonicus* roots and root nodules.** *Mol Plant-Microbe Interact* 2003, **8**: 663-668.

19 Chilton MD, Tepfer DA, Petit A, David C, Casse-Delbart F, Tempé J: ***Agrobacterium rhizogenes* inserts T-DNA into the genome of the host plant root cells.** *Nature* 1982, **295**: 432-434.

20 Nilsson O, Olsson O: **Getting to the root: The role of *Agrobacterium rhizogenes rol* genes in the formation of hairy roots.** *Physiol Plant* 1997, **100**: 463-473.

21 Favery B, Ryan E, Foreman J, Linstead P, Boudonck K, Steer M, Shaw P, Dolan L: ***KOJAK* encodes a cellulose synthase-like protein required for root hair cell morphogenesis in Arabidopsis.** *Genes Dev* 2001, **15**: 79-89.

22 Wang X, Cnops G, Vanderhaegen R, De Block S, Van Montagu M, Van Lijsebettens M: ***AtCSLD3*, a cellulose synthase-like gene important for root hair growth in Arabidopsis.** *Plant Physiol* 2001, **126**: 575-586.

23 Boisson-Dernier A, Chabaud M, Garcia F, Bécard G, Rosenberg C, Barker DG: ***Agrobacterium rhizogenes*-transformed roots of *Medicago truncatula* for the study of nitrogen-fixing and endomycorrhizal symbiotic associations.** *Mol Plant-Microbe Interact* 2001, **14**: 695-700.

24 Matz MV, Fradkov AF, Labas YA, Savitsky AP, Zaraisky AG, Markelov ML, Lukyanov SA: **Fluorescent proteins from nonbioluminescent *Anthozoa* species.** *Nature Biotechnol* 1999, **17**: 969-973.

25 Norris SR, Meyer SE, Callis J: **The intron of *Arabidopsis thaliana* polyubiquitin genes is conserved in location and is a quantitative determinant of chimeric gene expression.** *Plant Mol Biol* 1993, **21**: 895-906.

26 Ramos J, Bisseling T: **A method for the isolation of root hairs from the model legume *Medicago truncatula*.** *J Exp Bot* 2003, **54**: 2245-2250.

27 Mylona P, Moerman M, Yang WC, Gloudemans T, Van de Kerckhove J, van Kammen A, Bisseling T, Franssen HJ: **The root epidermis-specific pea gene *RH2* is homologous to a pathogenesis-related gene.** *Plant Mol Biol* 1994, **26**: 39-50.

28 Hamilton A, Voinet O, Chappell L, Baulcombe D: **Two classes of short interfering RNA in RNA silencing.** *EMBO J* 2002, **21**: 4671-4679.

29 Palauqui J-C, Elmayan T, Pollien JM, Vaucheret H: **Systemic acquired silencing: Transgene-specific post-transcriptional silencing is transmitted by grafting from silenced stocks to non-silenced scions.** *EMBO J* 1997, **16**: 4738-4745.

30 Voinnet O, Vain P, Angell S, Baulcombe DC: **Systemic spread of sequence-specific transgene RNA degradation in plants is initiated by localized introduction of ectopic promoter-less DNA.** *Cell* 1998, **103**: 157-167.

31 Jorgensen RA: **RNA traffics information systemically in plants.** *Proc Natl Acad Sci USA* 2002, **99**: 11561-11563.

32 Mlotshwa S, Voinnet O, Mette MF, Matzke M, Vaucheret H, Wei Ding S, Pruss G, Vance VB: **RNA silencing and the mobile silencing signal.** *Plant Cell* 2002, **14**: Suppl, S289-301.

33 Klahre U, Crété P, Leuenberger SA, Iglesias VA, Meins F Jr: **High molecular weight RNAs and small interfering RNAs induce systemic posttranscriptional gene silencing in plants.** *Proc Natl Acad Sci USA* 2002, **99**: 11981-11986.

34 Palauqui J-C, Elmayan T, Dorlhac de Borne F, Crété P, Carles C, Vaucheret H: **Frequencies, timing and spatial patterns of co-suppression of nitrate reductase and nitrite reductase in transgenic tobacco plants.** *Plant Physiol* 1996, **112**: 1447-1456.

35 Boerjan W, Bauw G, Van Montagu M, Inze D: **Distinct phenotypes generated by overexpression and suppression of S-adenosyl-L-methionine synthetase reveal developmental patterns of gene silencing in tobacco.** *Plant Cell* 1994, **6**: 1401-1414.

36 Jorgensen RA, Cluster PD, English JJ, Que Q, Napoli CA: **Chalcone synthase cosuppression phenotypes in petunia flowers: comparison of sense vs. antisence constructs and single-copy vs. complex T-DNA sequences.** *Plant Mol Biol* 1996, **31**: 957-973.

37 Kunz C, Schöb H, Stam M, Kooter JM, Meins F: **Developmentally regulated silencing and reactivation of tobacco chitinase transgene expression.** *Plant J* 1996, **10**: 437-450.

38 Duckett CM, Oparka KJ. Prior DAM, Dolan L, Roberts K: **Dye-coupling in the root epidermis of *Arabidopsis* is progressively reduced during development.** *Development* 1994, **120**: 3247-3255.

39 Van Engelen FA, Molthoff JW, Conner AJ, Nap J-P, Pereira A, Stiekema, WJ: **pBINPLUS: an important improved plant transformation vector based on pBIN19.** *Transgen Res* 1995, **4**: 288-290.

40 Sonti RV, Chiurazzi M, Wong D, Davies CS, Harlow GR, Mount DW, Signer ER: **Arabidopsis mutants deficient in T-DNA integration.** *Proc Natl Acad Sci USA* 1995, **92**: 11786-11790.

41 Hoffmann B, Trinh TH, Leung J, Kondorosi A, Kondorosi E: **A new *Medicago truncatula* line with superior in vitro regeneration, transformation, and symbiotic properties isolated through cell culture selection.** *Mol Plant-Microbe Interact* 1997, **10**: 307-315.

42 Penmetsa RV, Cook DR: **A legume ethylene-insensitive mutant hyperinfected by its rhizobial symbiont.** *Science* 1997, **275**: 527-530.

43 Chiang CC, Hadwiger LA. **Cloning and characterization of a disease resistance response gene in pea inducible by *Fusarium solani*.** *Mol Plant-Microbe Interact* 1990, **3**: 78-85.

44 Czakó M, Wilson J, Yu X, Márton L: **Sustained root culture for generation and vegetative propagation of transgenic *Arabidopsis thaliana*.** *Plant Cell Report* 1993, **12**: 603-606.

45 Gadella TW Jr, Vereb G Jr, Hadri AE, Rohrig H, Schmidt J, John M, Schell J, Bisseling T: **Microspectroscopic imaging of nodulation factor-binding sites on living *Vicia sativa* roots using a novel bioactive fluorescent nodulation factor.** *Biophys J* 1997, **72**: 1986-1996.

46 Pawlowski K, Kunze R, de Vries S, Bisseling T: **Isolation of total, poly(A) and polysomal RNA from plant tissues.** In: Gelvin, SB Schilperoort RA (eds) *Plant Molecular Biology Manual*. Kluwer Academic Publishers. Dordrecht 1994, pp D5 1-13.

Chapter 4

LysM domain receptor kinases regulating rhizobial Nod factor induced infection

---

Erik Limpens, Carolien Franken, Patrick Smit, Joost Willemse, Ton Bisseling and René Geurts

Science 2004, **302**: 630-633

The rhizobial infection of legumes has the most stringent demand towards Nod factor structure of all host responses and therefore a specific Nod factor entry receptor has been proposed. The *SYM2* gene identified in certain ecotypes of pea (*Pisum sativum*) is a good candidate for such an entry receptor. We exploited the close phylogenetic relationship of pea and the model legume *Medicago truncatula* to identify genes specifically involved in the rhizobial infection process. The *SYM2* orthologous region of *M. truncatula* contains 15 putative receptor–like genes of which 7 are LysM domain containing receptor-like kinases (LYKs). Using reverse genetics in *M. truncatula,* we show that two *LYK* genes are specifically involved in infection thread formation. This as well as the properties of LysM domains strongly suggests that they are Nod factor entry receptors.

The establishment of a nitrogen-fixing nodule symbiosis by rhizobial bacteria on the roots of legumes requires that the bacteria enter the root in a host-controlled manner. In most legumes this infection starts with curling of root hairs. A bacterium becomes entrapped in a cavity formed by the curl where it forms a micro-colony (*1*, Fig. 1A). Infection thread formation is initiated within such cavity by invagination of the root hair plasma membrane. In this way a tube-like structure is formed by which the bacteria enter the plant and reach the base of the root hair (Fig. 1B). Ultimately, the infection thread reaches a nodule primordium that is formed in the root cortex and develops into a nitrogen-fixing nodule upon release of bacteria. Rhizobia secrete specific lipo-chitooligosaccharides, the so-called Nod factors, when they colonize the roots of their legume host. Nod factors consist of a β-1,4-linked *N*-acetyl-*D*-glucosamine backbone of 4 or 5 residues of which the non-reducing terminal residue is substituted at the C2 position with an acyl chain (*2*). Depending on the rhizobial species, the structure of the acyl chain can vary and substitutions at the reducing and non-reducing terminal glucosamine residues can be present (*3*). Nod factors are involved in induction of early steps of nodulation and are also a major determinant of host specificity of this interaction. Since responses are induced in the plant by Nod factor concentrations in a nano- to picomolar range it seems probable that Nod factors are recognized by specific receptors (3-*7*). Infection thread formation shows the highest demand towards Nod factor structure of all *Rhizobium* induced responses (*7-10*). This has been studied in detail in the interaction of *Sinorhizobium meliloti (Sm)* and the model legume *Medicago truncatula* (*7,8*). A *nodFnodL* mutant of *Sm* produces Nod factors that in comparison to those secreted by wild type bacteria, lack an acetate substitution at the non-reducing terminal glucosamine residue and the specific acyl chain of 16 C-atoms containing 2 double bonds (C16:2) is replaced by vaccenic acid (C18:1). This *nodFnodL* mutant is able to induce most steps of the nodulation process, e.g. formation of root hair curls in which bacteria form a micro-colony and cortical cell activation, but the entrapped bacteria are unable to induce infection thread formation.

Therefore it was proposed that the induction of infection thread formation requires a highly specific Nod factor receptor, which was named the entry receptor (*7,8*).

The stage at which infection thread formation is blocked when *M. truncatula* is inoculated with a *nodFnodL* mutant (*Sm* 2011*ΔnodF/nodL::*Tn5-*GFP*) was analyzed in more detail with confocal laser scanning microscopy (CLSM). Most (~80%) of the infections are blocked at the initiation of infection thread formation, as only micro-colonies are formed. However, in about 20% of the cases infection thread like structures are initiated, but instead of a continuous tube a structure composed of tube- and sac-like structures is formed, the growth of which is aborted very early in the hair (Fig. 1C). Most likely, this means that during infection thread formation the polar mode of growth is lost and regained. These data suggest that the recognition of a Nod factor with a specific structure is required for the initiation of infection thread formation (= entry) as well as for maintenance of infection thread growth.

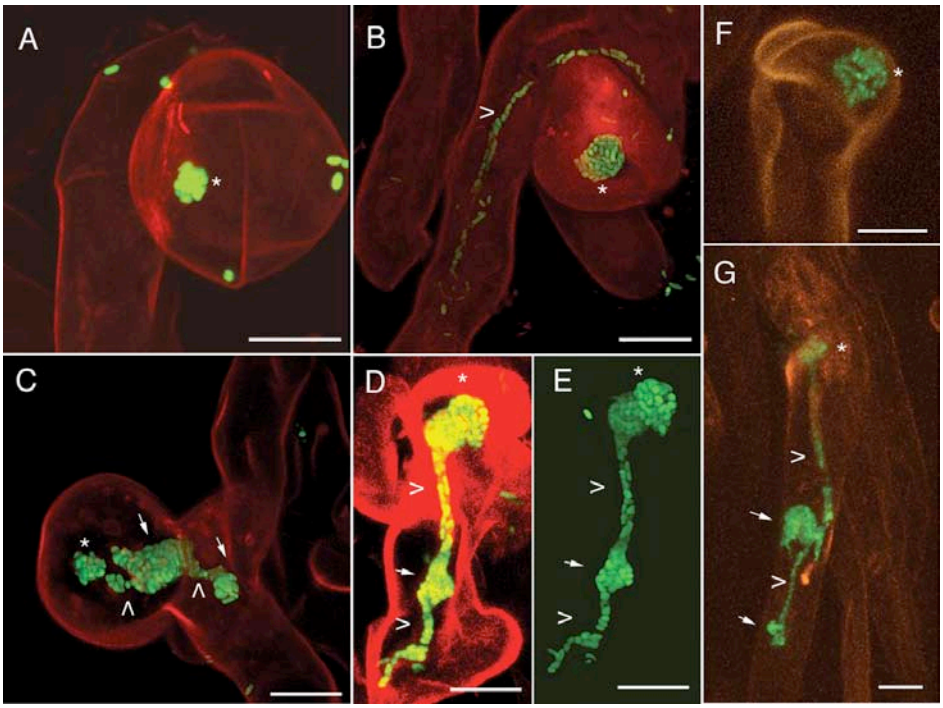

Fig 1: CLSM 3D reconstruction analysis of *Sinorhizobium meliloti* (*Sm*) infection of *M. truncatula* root hairs. The root hairs in A-D are counterstained with propidium iodide (0,2 µg/ml). (A) A curled root hair 4 days post inoculation (dpi) with a wild type *Sm* 2011-*GFP* micro-colony. (B) A micro-colony and infection thread (tube) formed by wild type *Sm* 2011-*GFP*, 7 dpi. (C) Infection structure formed by *Sm* 2011Δ*nodFnodL*::Tn5-*GFP*, consisting of tube- and sac-like structures (7 dpi). (D,E) Infection thread formed by *Sm* 2011*nodL*::Tn5-*GFP* (7dpi). These infection threads can successfully infect nodule primordia, although sac-like structures are present. (F,G) *LYK3* knock down root inoculated with *Sm* 2011Δn*odFE-GFP* (14 dpi). Red-orange colouring is the result of *Ds*RED1 fluorescence, which is used as selection marker for transgenic roots. (*F*) Infection event arrested at the micro-colony stage. (*G*) Infection thread consisting of tube- and sac-like structures. Bars in figures = 10 µm. All *Sm* strains used carry the plasmid pHC60 containing *GFP* under the control of a constitutive promoter (*23*). Micro-colonies, infection threads (tube) and sac-like structures are marked with an asterisk, arrowhead and arrow respectively.

A single *nodL* mutation (*Sm* 2011*nodL::*Tn*5-GFP*), resulting in Nod factors lacking the acetate substitution at the non-reducing terminal glucosamine, causes a comparable but weaker infection phenotype resulting in infection threads with sac-like structures (Fig. 1D,E). A *nodL* mutant is still able to infect nodule primordia. In contrast, inoculation with a *nodFE* mutant (*Sm* 2011*ΔnodFE-GFP*) that produces Nod factors containing a C18:1 acyl chain, results in the formation of infection threads that by number and morphology are indistinguishable from those formed by wild type bacteria. This shows that *nodL* and *nodFE* mutations have a synergistic effect.

Mutations causing a specific block of the formation of infection threads in a Nod factor structure-dependent manner have not been identified in *M. truncatula* or *Lotus japonicus*, two legume species that are amenable to positional cloning. However, a good candidate gene has been described in pea, namely *SYM2*. *SYM2* has been identified in several pea ecotypes and the allele of the ecotype Afghanistan has been best characterized (*10,11*). Pea lines with an introgressed *SYM2* allele from Afghanistan pea ($SYM2^A$) have a high demand on Nod factor structure with respect to infection thread formation. They efficiently form infected nitrogen fixing nodules when inoculated with *Rhizobium leguminosarum* biovar *viciae* (*Rlv*) strains that contain the *nodX* gene. *nodX* encodes an acetyl transferase that can acetylate the reducing *N*-acetyl-glucosamine residue of *Rlv* Nod factors (*12*). This NodX modification is not required for efficient infection of regular peas. Pea $SYM2^A$ introgression lines that are inoculated with incompatible *Rlv* strains, lacking *nodX*, have a strongly reduced nodulation efficiency (*10*). However, a complete block of nodulation is obtained when in addition to the absence of *nodX, nodE* is mutated, by which the specific C18:4 acyl chain is replaced by vaccenic acid (data not shown). The incompatible bacteria are able to induce responses like root hair curling and nodule primordium formation, but are specifically blocked in the formation and growth of infection threads. Most infections get arrested at the micro-colony stage, whereas some infection thread like structures are formed that abort in the root hair (*10*). This phenotype is similar to that of the interaction of an *Sm nodFnodL* mutant on *M. truncatula* and therefore *SYM2* is a good candidate to be a Nod factor entry receptor.

Pea is not amenable to positional cloning due to its large genome and the lack of efficient transformation methods. Since *M. truncatula* and pea are phylogenetically closely related and therefore highly syntenic (*13,14*), we decided to characterize the *SYM2* orthologous region in *M. truncatula* and test whether it contains genes specifically required for the rhizobial infection process. The identification of a 300 kb orthologous region in *M. truncatula* delineated by markers that flank *SYM2* has been described previously (*14*). As a first step to characterize the gene content within this region we survey sequenced four BAC clones representing a minimum tiling path spanning this region (*15*). A total of 21 putative genes were identified and annotated based on sequence homologies and EST data (Fig. 2). Interestingly, BLAST searches revealed 15 putative genes encoding receptor-like proteins; a gene homologous to

TMV-resistance gene *N* of tobacco (*MtHTR*) (belonging to the TIR-NB-LRR class of resistance genes), 7 genes homologous to *Cladosporium fulvum (Cf)* resistance genes (*MtHCR1-7)* (consisting of 18-20 extracellular LRR domains) and 7 receptor-like kinases, predicted to contain one or two extracellular domains with homology to lysin motives (LysM) (*LYK1-7*). The remaining putative genes were named A-F (Fig. 2). Cross-hybridization and RFLP analyses showed that homologous sequences are present in the pea *SYM2* region, confirming the microsynteny between these two legumes (data not shown).

To identify candidate genes involved in the rhizobial infection process, we first selected the genes that are expressed in roots. Therefore RT-PCR was performed on RNA isolated from nodules, leaves and roots to determine the expression pattern of the identified genes. *MtHTR, MtHCR4, MtHCR5, MtHCR6, LYK3, LYK6, LYK7* and genes with unknown function B, C, E and F could be detected in roots (Fig. 2).

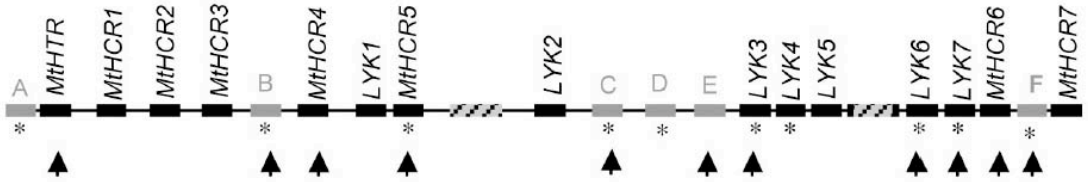

Fig. 2: Gene content of the *SYM2* orthologous region of *M. truncatula*. Based on different gene annotation programs (http://www.arabidopsis.org/links/gene_id.html) and BLAST analysis 21 putative genes are predicted. Of these 15 encode putative receptor-like proteins; 7 receptor-like kinases containing LysM domains in the putative extracellular part (named *LysM DOMAIN CONTAINING RECEPTOR-LIKE KINASE; LYK1* to *LYK7),* 7 homologs of tomato *Cladosporium fulvum* resistance genes (named *M. truncatula HOMOLOG OF CF RESISTANCE*; *MtHCR1* to *MtHCR7*) and 1 putative receptor of the TIR-NB-LRR type, homologous to the TMV resistance gene *N* of tobacco (named *M. truncatula HOMOLOG OF TMV RESISTANCE; MtHTR*). Furthermore, 4 putative genes of unknown function (marked B, D, E and F), 1 gene encoding a protein highly homologous to a *UBIQUITIN CARBOXYL-TERMINAL HYDROLASE* (marked A), and 1 gene homologous to *UFD1* of Arabidopsis (marked C) are present. Putative retroelements are shown as a shaded box. *LYK3*, *LYK4*, *LYK5*, *LYK6* and *LYK7* form a cluster of 46 kb. *LYK5* most likely is a pseudogene since it contains a mutation in the conserved donor splice-site of intron 8. Further, a retroelement-like insertion is present in a *LYK* pseudo gene that is located between *LYK5* and *LYK6*. For 10 putative genes (marked with an asterisk) it is shown by EST data or root cDNA library screenings that they are expressed. Genes that are expressed in roots are marked with an arrow.

To determine whether these candidate genes are involved in the infection process, we decided to knock down gene expression by RNA interference (RNAi) using *Agrobacterium rhizogenes* mediated root transformation (*16,17*). *A. rhizogenes* mediated root transformation results in co-transformation of ~30% of the roots formed. Each root is the result of an independent transformation event. Some of these roots are chimaeric. Selection of homogeneously co-transformed roots was facilitated using a binary vector that carries *DsRED1* as fluorescent selection marker. Co-transformed roots expressing *DsRED1* can be efficiently nodulated by compatible *Sm* strains (including *Sm* 2011-*GFP* and *Sm* 2011*ΔnodFE-GFP*) and infection threads are similar to those of wild type roots. To trigger

RNAi, hairpin constructs were used containing ~500 bp regions of the target gene under control of the CaMV 35S promoter (17,*18*). We first tested the effectiveness of *A. rhizogenes* mediated RNAi in the roots of *M. truncatula* by targeting the *DMI2* gene. *DMI2* encodes an LRR-domain containing receptor kinase that is an essential element of Nod factor induced signaling (*19*). Targeting *DMI2* resulted in 75% of the transgenic roots (as judged by red fluorescence) in a completely Nod-minus phenotype and no infections or curled root hairs occurred on these roots. In contrast 80-100% of the control roots were efficiently nodulated (on average 11 nodules / root). This shows that *A. rhizogenes* mediated RNAi is a fast and efficient tool to knock down genes in roots of *M. truncatula.* To identify genes that are involved in infection thread formation we knocked down, by RNAi, the genes of the *SYM2* orthologous region of *M. truncatula* that are expressed in roots. Plants carrying transgenic roots were inoculated and checked for nodulation efficiency two weeks post inoculation (Table S1). Since pea $SYM2^{A}$ lines are completely blocked in nodulation when inoculated with *Rlv* strains lacking *nodX* and *nodE* we inoculated the *M. truncatula* knock down plants with wild-type *Sm* 2011-*GFP* or *Sm* 2011Δ*nodFE-GFP*, which have similar efficiencies to infect wild type roots. A marked reduction of nodulation only occurred in *LYK3* knock down roots inoculated with *Sm* 2011Δ*nodFE-GFP*. In this case 60% of the co-transformed roots (n=55) were completely lacking nodules. In contrast, inoculation with wild type *Sm* 2011-*GFP* resulted in only a single Nod-minus root, whereas the remaining roots were Nod-plus (n=13, on average 7 nodules / root). Control roots inoculated with *Sm* 2011-*GFP* or *Sm* 2011Δ*nodFE-GFP* were efficiently nodulated (on average 11 and 9 nodules / root, respectively). To determine the reduction of *LYK3* mRNA levels in the knock down roots, we selected three large roots to isolate RNA. Quantitative RT-PCR showed a ~70 % reduction of *LYK3* mRNA (Fig. S1). We examined the effect of *LYK3* knock down on infection thread morphology by fluorescence microscopy and CLSM. *LYK3* knock down roots that did not contain nodules after inoculation with *Sm* 2011Δ*nodFE-GFP* (n=28) were still able to entrap bacteria within curled root hairs. However, the number of infection threads was markedly reduced. Most infections (78%) were arrested at the micro-colony stage (n=482; on average 17 / root) (Fig. 1F). Furthermore, infection thread-like structures were formed but these aborted in the root hair (n=136; on average 5 / root) and had aberrant morphologies consisting of tube- and sac-like structures (Fig. 1G). In contrast, on control roots (n=19) 81% of the infections resulted in tubular infection threads (on average 22 / root). When *LYK3* knock down roots were inoculated with wild type *Sm* 2011-*GFP* the majority of the infection events resulted in tubular infection threads (n=148; on average 11 / root). In about 20% of the cases tubes containing sac-like structures were observed (n=43; on average 3 / root). Control roots inoculated with either *Sm* 2011–*GFP* or *Sm* 2011Δ*nodFE-GFP* only occasionally showed infection threads with aberrant structures (<5%). To confirm the knock down phenotype a second *LYK3* hairpin construct was made covering a different region of the gene. Targeting *LYK3* with this second construct resulted in 90% of the transformed roots (n=36), inoculated with *Sm* 2011Δ*nodFE*-GFP, in a Nod-minus phenotype. 23 of these roots

were further analyzed for infection events, showing that 91% of all infections (n=172, on average 8 / root) got arrested at the micro-colony stage, whereas the infection thread-like structures (n=18, on average 1 / root) showed aberrant morphologies as described above. These data show that knock down of *LYK3* with two independent hairpin constructs causes a similar phenotype: a block of infection thread initiation and growth in a Nod factor structure dependent manner. This phenotype is similar to that observed with the *Sm* 2011*nodFnodL* mutant on wild type *M. truncatula* plants and incompatible *Rlv* strains on *SYM2*^{A} peas.

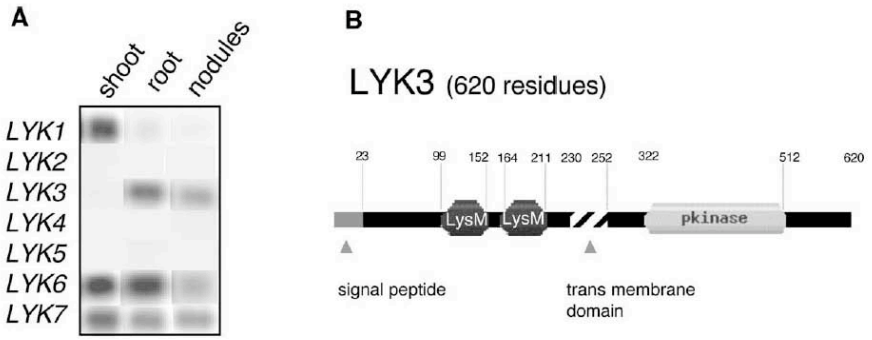

C

```
LysM              YtVkkGDTLssIArrygvsvqe---Lael-NpgLsspniyvGQLk--iP

CL-A          G--CTYTIQPGDTFWAIAQRRGTTVDV---IQSL-NPGVVPTRLQVGQVIN-VPC
              G--CTYTIQPGDTFWAIAQRRGTTVDV---IQSL-NPGVNPARLQVGQVIN-VPC

LYK1     96- GHTFLYEFHPRETYASIAELTFSNLTNKEWMEKV-N-------VPDSVKVN-V   -139
        155- GLFITYPLSSEDTLESIAKHTKVKPELLQKYTPGVN-------FSKGSGLVFIPG -202

LYK2    100- GHVFEYSAKEGDTYDLIANSYYASLTTVELLKKF-NSYDQDHIPAKAKVNVTVNC -153
        165- GLFITYPLRTDDTLQKIANQSNLDEGL---IQSY-NSG---VNFSNGSGIVFIPG -212

LYK3     99- GHVFEYTTKEGDDYDLIANTYYASLTTVELLKKF-NSYDPNHIPVKAKINVTVIC -152
        164- GLFVTYPLRSDDTLAKIATKAGLDEGL---IQNF-N---QDANFSIGSGIVFIPG -211

LYK4     99- GHVFEYTTKEGDDYDLIANTYYASLTTVELLKKF-NSYDPNHIPVKAKINVTVIC -152
        164- GLFVTYPLRSDDTLAKIATKADLDEGL---LQNF-N---QDANFSKGSGIVFIPG -211

LYK6    148- GLFITYPLRSEDTLESIAKGAEIEAEL---LQRY-NPG---VNFSKGSGLVFIPG -195

LYK7     98- GHIFQYQVATKDTYLSVASNNYSNLTTSEWLQNF-NSYPSNDIPDTGTLNVTVNC -151
        163- GLFITYPLRPEDSLELISNKTEIDAEL---LQKY-NPG---VNFSQGSGLVYIPG -210
```

Fig 3: Analysis of the *LYK* genes present in the *SYM2* orthologous region of *M. truncatula*. (A) Reverse transcriptase (RT) PCR analysis of *LYK1 - 7* using RNA isolated from shoots, nitrogen starved roots and nodules as template. PCR was conducted using a concentration range of cDNA, shown are the results obtained with 2 ng of total RNA starting material. (B) The predicted structure of LYK3 based on prediction programs (www.expasy.org). (C) Alignment of the LysM domains of 6 LYK proteins to the LysM domains of *Volvox carteri* f. *naragiensis* chitinase CL-A (19) and the LysM domain consensus sequence (as predicted by Pfam: www.sanger.ac.uk/Software/Pfam/search.shtml). Highly conserved amino acids are shown in bold.

LYK3 is highly homologous to *LYK4*, especially in the extracellular domain (Fig. S2). The first *LYK3* hairpin construct targeted a region of this extracellular domain, by which it is possible that also *LYK4* was knocked down. Although we did not detect *LYK4* expression in roots by RT-PCR, we identified a single EST from a root cDNA library. Therefore also a *LYK4* hairpin

construct was made from a region that shows <20% homology to *LYK3*. *LYK4* knock down roots (n=10) inoculated with *Sm* 2011Δ*nodFE-GFP* did not show a clear effect on nodulation (5 nodules / root), but did affect infection thread morphology. 70% of the tubular infection threads contained sac-like structures (on average: 11 / root) along its length, similar to what was observed for the *Sm* 2011*nodL* mutant. These data indicate that also *LYK4* plays a role in infection thread formation. However, knock-out mutants, for example obtained by TILLING (*20*), are needed to elucidate the contribution of the individual genes.

Expression analysis by RT-PCR and electronic northerns based on EST data revealed that *LYK3* is exclusively expressed in root tissue (Fig. 2, Fig. 3A). *LYK1* is specifically active in shoots, whereas *LYK6* and *LYK7* are expressed in both roots and shoots. In addition, screening of available EST sequences revealed 4 additional LysM domain containing receptor-like kinases, indicating the existence of a rather large gene family. Some members of this family (*LYK3/4*) have a specific function in symbiosis. However other, e.g. those expressed in shoots and those of which RNAi did not lead to an infection phenotype, most likely have a non-symbiotic function. The involvement of certain *LYK* genes in non-symbiotic processes is further supported by the fact that LysM domain containing receptor-like kinases are also present in non-legume species e.g. Arabidopsis, which contains 5 such genes of which At3g21630 is most homologous to the *LYK* genes.

Two models for Nod factor perception have been proposed. One model includes a two-receptor mechanism with a Nod factor signaling receptor that triggers all responses and an entry receptor that controls infection (*7*). Alternatively, a single Nod factor receptor has been proposed, which has different affinities for Nod factors depending on their structure (*4*). The observed infection phenotype does not exclude the single Nod factor receptor model, since we did not check for the presence of residual LYK3/4 protein that might be sufficient to trigger root hair curling in the *LYK3/4* knock down roots. However, our experiments show that *LYK3/4* knock down specifically affects infection thread formation, whereas root hair curling and the formation of micro-colonies are not influenced. This specific block of infection fits best with a two-Nod-factor receptor model in which LYK3/4 specifically controls bacterial entry. The involvement of multiple Nod factor receptors is further supported by the phenotype of the *M. truncatula* Nod factor perception mutant (*nfp)*, which strongly suggests that NFP represents a Nod factor signaling receptor (*6*).

Here we show that knock down of *LYK3/4* causes an almost complete block of infection thread formation when plants are inoculated with an *Sm* 2011Δ*nodFE* mutant. The interaction with wild type *Sm* leads to the formation of infection threads but these frequently loose their polar mode of growth. This suggests that other *LYK* genes might also encode Nod factor receptors and these might more efficiently recognize wild type C16:2 acyl chain containing Nod factors. Alternatively, LYK3/4 might have a lower affinity for C18:1 Nod factors (*nodFE*

mutant) by which residual protein in the knock down lines still allows infection thread formation by wild type bacteria but not by *Sm* 2011*ΔnodFE.* The hypothesis that LYK3/4 is a Nod factor receptor implicates that the extracellular domain of LYK3/4, containing two LysM domains (Fig. 3B), can directly interact with Nod factors. LysM domains are proposed to have a general peptidoglycan binding function (*21*). The LysM domains of the LYK3/4 proteins show the highest homology to the LysM domains present in a chitinase from *Volvox carteri* f. *nagariensis* (*CL-A*) (Fig. 3C) (*22*). The structural homology between chitin, peptidoglycan subunits and the *N*-acetylglucosamine backbone of the Nod factor supports the hypothesis that Nod factors are ligands of LYK3/4.

Acknowledgements

E.L., P.S., T.B. and R.G. are funded by The Netherlands Organization of Scientific Research (NWO), the E.U. FP5 program QLG-CT2000-00676 and the graduate school Experimental Plant Sciences. We thank Greenomics (PRI, Wageningen) for sequencing the BAC clones and M. Reijns, J. Zhao, M. Haring, X. Zhang, R. Siddappa, P. Twumasi and I. Melis who participated as undergraduate students in this project.

References

1 Gage DJ: **Analysis of infection thread development using Gfp- and DsRed-expressing *Sinorhizobium meliloti.*** *J Bacteriol* 2002, **184**: 7042-7046.

2 Lerouge P, Roche P, Faucher C, Maillet F, Truchet G, Promé JC, Dénarié J: **Symbiotic host-specificity of *Rhizobium meliloti* is determined by a sulphated and acylated glucosamine oligosaccharide signal.** *Nature* 1990, **344**: 781-784.

3 Cullimore JV, Ranjeva R, Bono JJ: **Perception of lipo-chitooligosaccharidic Nod factors in legumes.** *Trends Plant Sci* 2001, **6**: 24-30.

4 Oldroyd GE, Mitra RM, Wais RJ, Long SR: **Evidence for structurally specific negative feedback in the Nod factor signal transduction pathway.** *Plant J* 2001, **28**: 191-199.

5 Geurts R, Bisseling T: ***Rhizobium* Nod factor perception and signalling.** *Plant Cell* 2002, supplement: S239-S249.

6 Amor BB, Shaw SL, Oldroyd GE, Maillet F, Penmetsa RV, Cook D, Long SR, Dénarié J, Gough C: **The *NFP* locus of *Medicago truncatula* controls an early step of Nod factor signal transduction upstream of a rapid calcium flux and root hair deformation.** *Plant J* 2003, **34**: 495-506.

7 Ardourel M, Demont N, Debellé F, Maillet G, De Billy F, Promé JC, Dénarié J, Truchet G: ***Rhizobium meliloti* lipoligosaccharide nodulation factors: different structural requirements for bacterial entry into target root hair cells and induction of plant symbiotic developmental responses.** *Plant Cell* 1994, **6**: 1357-1347.

8 Catoira R, Timmers AC, Maillet F, Galera C, Penmetsa RV, Cook D, Denarie J, Gough C: **The *HCL* gene of *Medicago truncatula* controls *Rhizobium*-induced root hair curling.** *Development* 2001, **128**: 1507-1518.

9 Walker SA, Downie JA: **Entry of *Rhizobium leguminosarum bv.viciae* into root hairs requires minimal Nod factor specificity, but subsequent infection thread growth requires *nodO* or *nodE*.** *Mol Plant Microbe Interact* 2000, **13**: 754-762.

10 Geurts R, Heidstra R, Hadri AE, Downie A, Franssen H, Van Kammen A, Bisseling T: **Sym2 of *Pisum sativum* is involved in a Nod factor perception mechanism that controls the infection process in the epidermis.** *Plant Physiol* 1997, **115**: 351-359.

11 Lie TA: **Host genes in Pisum sativum L. conferring resistance to European *Rhizobium leguminosarum* strains.** *Plant Soil* 1984, **82**: 462-465.

12 Firmin JL, Wilson KE, Carlson RW, Davies AE, Downie J: **Resistance to nodulation of c.v. Afghanistan peas is overcome by *nodX*, which mediates an *O*-acetylation of the *Rhizobium leguminosarum* lipo-oligosaccharide nodulation factor.** *Mol Microbiol* 1993, **10**: 351-360.

13 Young ND, Mudge J, Ellis TH: **Legume genomes: more than peas in a pod.** *Curr Opin Plant Biol* 2003, **6**: 199-204.

14 Gualtieri G, Kulikova O, Limpens E, Kim DJ, Cook DR, Bisselin T, Geurts R: **Microsynteny between pea and *Medicago truncatula* in the *SYM2* region.** *Plant Mol Biol* 2002, **50**: 225-235.

15 BAC clones MtH1-015B03, MtH1-041N12, MtH1-003I09 and MtH1-052O10 were shotgun sequenced with an 8x coverage. The sequence between MtH1-015B03 and MtH1-041N12 was determined by a PCR based strategy using MtH2-022J24. BAC clones MtH1-003I09 and MtH1-052O10 showed to form a contig with BAC MtH2-033L22 (AC123570) that was sequenced at Oklahoma University.

16 Boisson-Dernier A, Chabaud M, Garcia F, Bécard G, Rosenberg C, Barker DG: ***Agrobacterium rhizogenes*-transformed roots of *Medicago truncatula* for the study of nitrogen-fixing and endomycorrhizal symbiotic associations.** *Mol Plant-Microbe Interact* 2001, **14**: 695-700.

17 E. Limpens, R. Geurts, unpublished data.

18 Chuang C, Meyerowitz M: **Specific and heritable genetic interference by double-stranded RNA in *Arabidopsis thaliana.*** *Proc Natl Acad Sci USA* 2000, **97**: 4985-4990.

19 Endre G, Kereszt A, Kevei Z, Mihacea S, Kaló P, Kiss GB: **Cloning of a receptor kinase gene regulating symbiotic nodule development.** *Nature* 2002, **417**: 962-966.

20 McCallum CM, Comai L, Greene EA, Henikoff S: **Targeting induced local lesions IN genomes (TILLING) for plant functional genomics.** *Plant Physiol* 2000, **123**: 439-442.

21 Bateman A, Bycroft M: **The structure of a LysM domain from *E. coli* membrane-bound lytic murein transglycosylase D (MltD).** *J Mol Biol* 2000, **299**: 1113-1119.

22 Amon P, Haas E, Sumper M: **The sex-inducing pheromone and wounding trigger the same set of genes in the multicellular green alga *Volvox*.** *Plant Cell* 1998, **10**: 781-789.

23 Cheng HP, Walker GC: **Succinoglycan is required for initiation and elongation of infection threads during nodulation of alfalfa by *Rhizobium meliloti*.** *J Bacteriol* 1998, **180**: 5183-5191.

Supporting Material

Materials and methods

Bacterial strains

Rlv 248 (*S1*)
Rlv 248*nodX* (*S1*)
Rlv 248*nodE::*Tn5 = RBL1401 (provided by H.P. Spaink, Leiden University).

Sm 2011-*GFP*:	*Sinorhizobium meliloti* strain 2011 carrying pHC60 (*S2,S3*).
Sm 2011Δ*nodFE –GFP:*	*S. meliloti* strain GMI5622 carrying pHC60 (*S2,S3*).
Sm 2011Δ*nodL*::Tn5 *–GFP:*	*S. meliloti* strain GMI6436 carrying pHC60 (*S2,S3*).
*Sm 2011*Δ*nodFnodL*:: Tn5-*GFP:*	*S. meliloti* strain GMI6628 carrying pHC60 (*S2,S3*).

pHC60 (*S3*) was introduced into *Sm* strains by triparental mating using the helper plasmid pRK2013 and GMI3540 as donor strain (*S1, S2*). Counter-selection was conducted on V-medium (per liter): 1 g KH_2PO_4, 1 g K_2HPO_4, 0.25 g $MgSO_4.7H_2O$, 0.2 g sucrose, 0.6 gram KNO_3, 350 µl of a 0.1 M $FeCl_3$ stock, 280 µl of a 1 M $CaCl_2$ stock (after autoclaving) and 500 µl of a 10 mg/ml d-Biotin stock (after autoclaving).

Plant material

For *Medicago truncatula* we used accession Jemalong A17 and for pea the cultivar Rondo and the *SYM2*^{A} intogression line A541 was used (*S1*).

RT-PCR protocol and primers

Total RNA was extracted from nitrogen-starved roots, leaves and nodules, followed by DNAseI (Promega) treatment (*S4*). cDNA was made from 1 µg total RNA in a volume of 20 µl using 200 U M-MuLV (Invitrogen) and subsequently diluted to 100 µl. The PCR reactions were performed on 1 µl, 0.2 µl, 0.04 µl, 0.008 µl of cDNA using a fixed number of 30 PCR cycles with specific primers for the different genes. Products were separated on a 1% aragose gel, blotted to a nylon membrane and hybridized to a ^{32}P-labelled probe.

Primers:

MtHCR1:	5' CAAAGCGGTGGGAATCTC 3'	and	5' GCCGACAACATGCATCAGGAAT 3'
MtHCR2:	5' TTAGGCTAGGAGAAATTGGGTTGC 3'	and	5' AGGTTGGGTAGATGAAAAAGTGATGAT 3'
MtHCR3:	5' TTCATACTCTGGTCCTAGTTG 3'	and	5' CAAGTTCGACAAAGTTAAAGC 3'
MtHCR4:	5' TTCTTTTGCCTTGTTTTGCCC 3'	and	5' GAGTTCCAAAGAATCATAATTGTT 3'
MtHCR5:	5' CCGATATCATTTTTGGCCTAGATGT 3'	and	5' CATATGCCAATCATAATAACTGC 3'
MtHCR6:	5' GCCTTCCGCTTAGTCTTTGC 3'	and	5' AGATCAGCATTCCCTTCATAACT 3'
LYK1:	5' TTACTTATGTTGCTGGCCTCCTCTA 3'	and	5' CAACTCAGGCTTAACTTTTGTATGC 3'
LYK2:	5' AGATTGCAAACCAATCTAA 3'	and	5' ATAATGCCTGTAAATACAGTA 3'
LYK3:	5' GTGGGCATGCTACTGGT 3'	and	5' CACAATTCAATTTGTCACAC 3'
LYK4:	5' GAGGACTTATACAAATTTGACT 3'	and	5' ACATCATCAAGAACAAATATTCAA 3'
LYK5:	5' GAGATCCTATAGAAGGTCT 3'	and	5' TAGAAATTAGTTTCATAAGAGA 3'
LYK6:	5' AGTCTAGCTCTAGCGTCATACACCTTA 3'	and	5' TCTGCACCCTTAGCAATAGACTCC 3'
LYK7:	5' TTTAGTCAAGGGAGTGGTT 3'	and	5' TTGGTTAATCCGAAGTCTG 3'
MtHTR:	5' GCGGAATGGGAAAGACAAC 3'	and	5' GCCCCCTGCATAAGTGATT 3'
B:	5' GCGACTGGCGTTTTGTTTG 3'	and	5' TGGTTTGGCATATCTTGTCTA 3'
C:	5' AGTCCGCTATGTTTGGCTTCC 3'	and	5' CAATGCTGTAAGTCCCCGAACC 3'
D:	5' TTTGAATGAATTTTGATGTGTC 3'	and	5' AATGAGGAGATCGAGAACAA 3'
E:	5' ATCTGAAATTCTGGTTGACTATG 3'	and	5' GGCTTGCGTTTTCTTGTATCAT 3'
F:	5' TAGCGGGAAGGTTAGCAGGAAAAG 3'	and	5' GACATATTCTCAGCCCATACTTTCAT 3'
MtACTIN5:	5' ACAATGGAACTGGAATGG 3'	and	5' CCTCCAATCCAGACACT3'

Agrobacterium rhizogenes mediated transformation

The roots of 5 day-old *M. truncatula* seedlings are removed at the hypocotyl and the wound surface inoculated with *Agrobacterium* MSU440 (*S5*) containing the appropriate binary plasmid. The seedlings are co-cultivated with *Agrobacterium* for 5 days at 21°C (16h light-8 h darkness) and subsequently transferred to Emergence medium (3 mM MES pH 5.8 containing 2,5 g/L KNO_3, 0.4 g/L $MgSO_4.7H_2O$, 0.3 g/L $NH_4H_2PO_4$, 0.2 g/L $CaCL_2.2H_2O$, 10 mg/L $MnSO_4.4H_2O$, 5 mg/L H_3BO_3, 1 mg/L $ZnSO_4.7H_2O$, 1 mg/L KI, 0.2 mg/L $CuSO_4.5H_2O$, 0.1 mg/L $NaMoO_4.2H_2O$, 0.1 mg/L $CoCL_2.6H_2O$, 15 mg/L $FeSO_4.7H_2O$, 20 mg/L Na_2EDTA, 100 mg/L Myoinositol, 5 mg/L Nicotinic acid, 10 mg/L Pyriodoxine HCl, 10 mg/L Thiamine HCl, 2 mg/L Glycine, 1% sucrose, 0.9% Daichin agar containing 300 µg/ml Cefotaxime (Duchefa)). Plants are grown for 6-18 days on Emergence medium. In this period new roots form that are potentially co-transformed with the T-DNA of the binary vector (*S6*).

Nodulation of A. rhizogenes transformed roots

Three weeks after transformation transgenic plants are starved for nitrate for 3 days (21°C; 16h light-8h darkness). Plants are transferred to agra-perlite (Maasmond-Westland, The Netherlands) saturated with Färhaeus medium (without $Ca(NO3)_2$) and inoculated with ~10^8 bacteria per plant and grown for two weeks (21°C; 16h light-8h darkness) (*S6*).

RNAi constructs

A binary vector (pBINPLUS (*S7*) derivative, not containing the *nptII* gene) was constructed containing *DsRED1* under the control of the *AtUBQ10* promoter. This vector was named pRedRoot (*S6*). Regions of selected genes were PCR-amplified with primers containing added restriction sites (see below) and subsequently cloned as an inverted repeat separated by a 335 bp spacer sequence in a modified pBluescript SK+ vector containing the CaMV 35S promoter (*S6*). The hairpin construct was subsequently cloned in the pRedRoot vector.

Primers (Spe*I*-Asc*I* and BamH*I*-Swa*I* restriction sites included within the primers have been underlined):

DMI2 (555 bp)	5'ATACTAGTGGCGCGCCACCGTCCTCCTTGCTGATA3'	5'ATGGATCCATTTAAATCGGGTTCCCTGAGTTGATG3'
LYK3-1 (512 bp)	5'ATACTAGTGGCGCGCCGTTCATTCTGTTTCTGGATTGTG3'	5'ATGGATCCATTTAAATTTCGCAAGAGTATCATCAGACC3'
LYK3-2 (496 bp)	5'ATACTAGTGGCGCGCCGTGGGCATGCTACTGGT3'	5'ATGGATCCATTTAAATCGCAAATTTTCGTCTATCA3'
LYK4 (329 bp)	5'ATACTAGTGGCGCGCCACTTAGCTAGAAGTTTAGTTG3'	5'ATGGATCCATTTAAATCTTGCCTCCCAGCACTCCA3'
LYK6 (424 bp)	5'ATACTAGTGGCGCGCCTAGCTCTAGCGTCATACACCTTA3'	5'ATGGATCCATTTAAATGCACCCTTAGCAATAGACTCC3'
LYK7 (483 bp)	5'ATGGATCCATTTAAATCACGCGTCAACACCTTCA3'	5'ATACTAGTGGCGCGCCTGGGAAAGACCAAAATCGTA3'
MtHTR (587)	5'ATACTAGTGGCGCGCCTAGAAGGCGTGGTGAGAAAC3'	5'ACGGATCCATTTAAATAACGAAGATGTAAAGCCAAAAG3'
MtHCR4 (737 bp)	5'ATACTAGTGGCGCGCCTTCACTTGTTCTCGTTGTTG3'	5'ATGGATCCATTTAAATGAAGATTAGGTAAAGAGAGG3'
MtHCR5 (400 bp)	5'ATACTAGTGGCGCGCCTTCCCACACTTTCTCATTG3'	5'ATGGATCCATTTAAATACCACCGAGGGAACAG3'
MtHCR6 (541 bp)	5'ATACTCGTGGCGCGCCTTGGGACAGTAAGAGTGAATG3'	5'ATGGATCCATTTAAATGATGGGTTAAAAGAGTGAG3'
B (446 bp)	5'ATACTAGTGGCGCGCCGCGACTGGCGTTTTGTTTG3'	5'ATGGATCCATTTAAATTGGTTTGGCATATCTTGTCTA3'
C (464 bp)	5'ATACTAGTGGCGCGCCCTCTCATATTTCCTACACG3'	5'ATGGATCCATTTAAATCCGCAAGGGCACTGAAG3'
D (499 bp)	5'ATACTAGTGGCGCGCCATCGTGAGTCGTTAAAGGAGA3'	5'ATGGATCCATTTAAATGAGCAGTGTCGATGATGGTG3'
F (420 bp)	5'ATACTAGTGGCGCGCCGGCACGTCGTTCAAGATA3'	5'ATGGATCCATTTAAATGGAGGCCACCATACCAAT3'

Quantification of LYK3 mRNA levels

Total RNA was isolated and DNAse treated using the Plant RNeasy kit (Qiagen; according to the manufacturers instructions) from three independent *LYK3-1* knock down roots inoculated with *Sm* 2011-*GFP* and compared to control roots. cDNA was made as described above. PCR was performed on 1 µl cDNA. Samples were normalized using *MtACTIN5* (*MtACT5*) as reference (for primers see above). *MtACT5* was exponentially amplified between 19 and 24 cycli, and *LYK3* between 24 to 29 cycli. Amplified products were separated on a 1% aragose gel, blotted to a nylon membrane and hybridized to a ^{32}P-labelled probe. mRNA levels were quantified using ImageQuant V.1.2 software (Molecular Dynamics).

Fluorescence and Confocal microscopy

Imaging of DsRED1 and GFP fluorescence was done using a Leica MZIII fluorescence stereomicroscope and a Nikon Optiphot-2 coupled to a mercury-lamp. Confocal images were taken on a Zeiss LSM 510 confocal laser scanning microsope (Carl-Zeiss); excitation 488 (GFP), 543 nm (DsRED1/propidium iodide); GFP emission was selectively detected by using a 505-530 nm bandpass filter; DsRED1/propidium iodide emission was detected in another channel using a 560-615 nm bandpass. Root hair cell walls are counter-stained with 0.2 µg/ml propidium iodide. Images are processed with Adobe Photoshop software and Microtome deconvolution software.

Supplementary figures

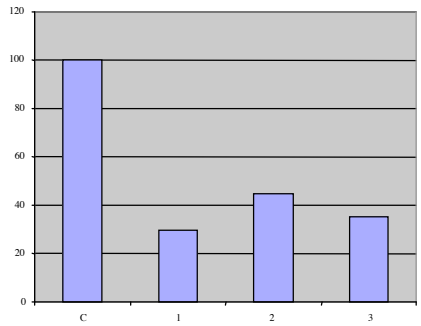

Fig. S1. Quantitative analysis of *LYK3* mRNA levels normalized against *MtACTIN5* as internal reference. C= control roots, 1-3= three independent *LYK3* knock down roots. Control experiments in which a *GFP* transgene was targeted in the roots, showed a similar reduction of mRNA levels, whereas these *GFP* knock down roots lacked any *GFP* fluorescence (*S6*).

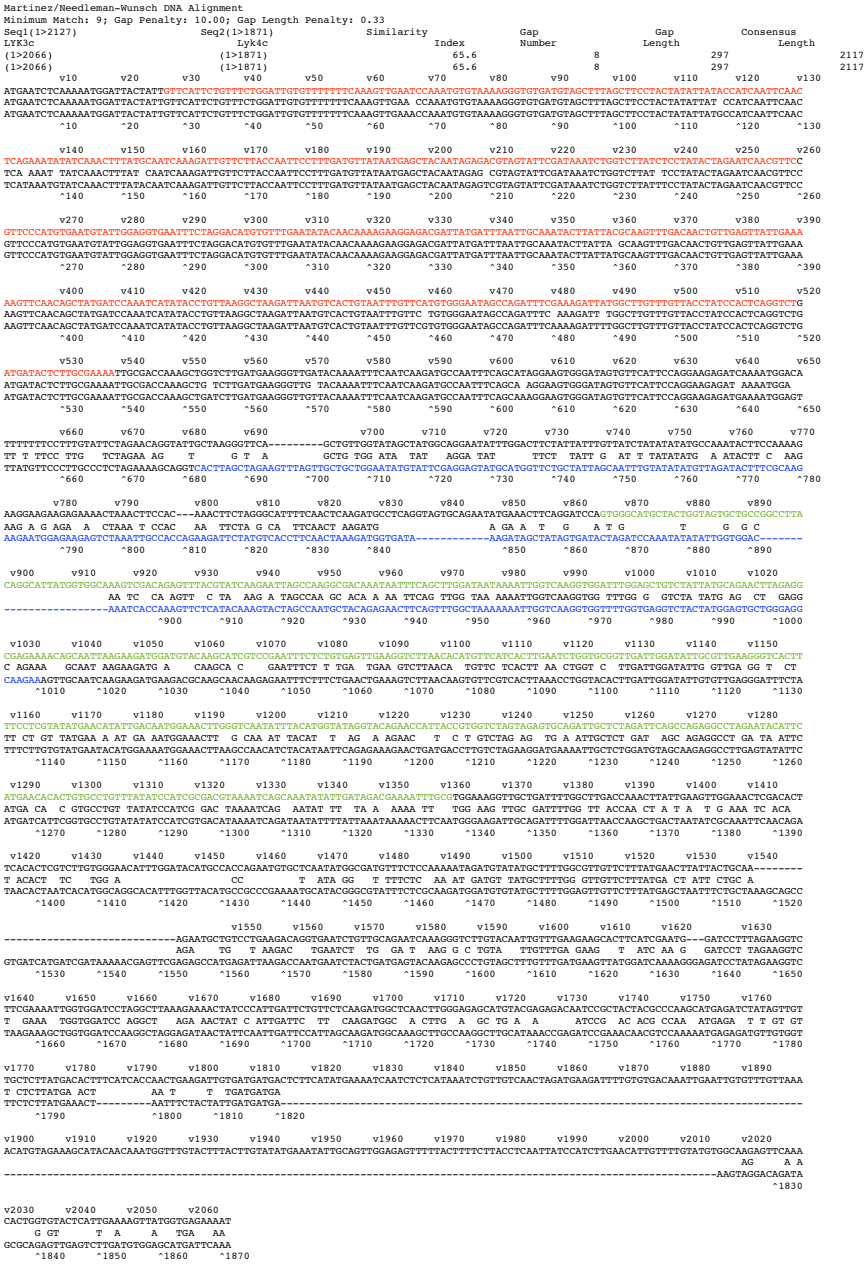

Fig. S2. Alignment of *LYK3* and *LYK4* cDNA sequences. Regions of *LYK3* and *LYK4* used to make hairpin constructs: red *LYK3-1* construct (512 bp), green *LYK3-2* construct (496 bp), blue *LYK4* construct (329 bp).

	average # nodules / root (n)	
	Sm 2011-*GFP*	*Sm* 2011*ΔnodFE-GFP*
control	11 (n=37)	9 (n=19)
MtHTR	8 (n=8)	10 (n=11)
MtHCR4	7 (n=22)	6 (n=10)
MtHCR5	7 (n=10)	6 (n=10)
MtHCR6	7 (n=8)	5 (n=4)
B	6 (n=10)	5 (n=5)
C	7 (n=7)	5 (n=4)
E	6 (n=6)	6 (n=6)
LYK3 (1)	7 (n=13)	0 (n=33) [*1]
LYK3 (2)	*n.d.*	0 (n=32) [*2]
LYK4	*n.d.*	5 (n=10)
LYK6	8 (n=12)	7 (n=15)
LYK7	8 (n=12)	8 (n=15)

Table S1. Effect of *A. rhizogenes* mediated RNAi on nodulation efficiency of both *Sm* 2011-*GFP* and *Sm* 2011*ΔnodFE-GFP*. Average number of nodules per transgenic root (n= number of transgenic roots examined) is given for the different hairpin construct used. Control roots are transformed with empty pRedRoot vector. [*1] 22 additional transgenic roots contained on average 6 nodules / root. [*2] 4 additional transgenic roots contained on average 1 nodule. *n.d.* = not done.

References

S1 Geurts R, Heidstra R, Hadri AE, Downie A, Franssen H, Van Kammen A, Bisseling T: **Sym2 of *Pisum sativum* is involved in a Nod factor perception mechanism that controls the infection process in the epidermis.** *Plant Physiol* 1997, **115**: 351-359.

S2. Ardourel M, Demont N, Debellé F, Maillet G, De Billy F, Promé JC, Dénarié J, Truchet G: ***Rhizobium meliloti* lipoligosaccharide nodulation factors: different structural requirements for bacterial entry into target root hair cells and induction of plant symbiotic developmental responses.** *Plant Cell* 1994, **6**: 1357-1347.

S3 Cheng HP, Walker GC: **Succinoglycan is required for initiation and elongation of infection threads during nodulation of alfalfa by *Rhizobium meliloti*.** *J Bacteriol* 1998, **180**:5183-5191.

S4 Pawlowski K, Kunze R, de Vries S, Bisseling T: **Isolation of total, poly(A) and polysomal RNA from plant tissues.** In: Gelvin, SB Schilperoort RA (eds) *Plant Molecular Biology Manual*. Kluwer Academic Publishers. Dordrecht 1994, pp D5 1-13.

S5 Sonti RV, Chiurazzi M, Wong D, Davies CS, Harlow GR, Mount DW, Signer ER: **Arabidopsis mutants deficient in T-DNA integration.** *Proc Natl Acad Sci USA* 1995, **92**: 11786-11790.

S6 Limpens E, Ramos J, Franken C, Raz V, Compaan B, Franssen H, Bisseling T, Geurts R: **RNA interference in *Agrobacterium rhizogenes* transformed roots of Arabidopsis and *Medicago truncatula***. *J Exp Bot* 2004, **55**: 983-992.

S7 Van Engelen FA, Molthoff JW, Conner AJ, Nap J-P, Pereira A, Stiekema, WJ: **pBINPLUS: an important improved plant transformation vector based in pBIN19.** *Transgen Res* 1995, **4**: 288-290.

Chapter 5

Nod factor signaling inside

Erik Limpens, Carolien Franken, Ton Bisseling and René Geurts

The establishment of a nitrogen-fixing legume root nodule requires the coordination of responses in the epidermis leading to the entry of the bacteria and responses in the cortical cell layers by which a nodule primordium is formed. These spatially separated responses are triggered by bacterial signal-molecules, the Nod factors. We show that the presence of an essential component of the Nod factor-signalling pathway, *NODULATION RECEPTOR KINASE* (*NORK*), exclusively in the epidermis is sufficient to trigger Nod factor responses in the inner cell layers. This shows that cortical cell divisions are induced by Nod factors in a non cell-autonomous manner. Most consistent with this is the hypothesis that a secondary signal generated in the epidermis triggers the formation of a nodule primordium, and this is the molecular mechanism underlying the tight coordination of the two spatially separated responses.

Rhizobial Nod factors are signal molecules that are pivotal in the induction of several steps of the legume nodulation process. The formation of nitrogen fixing nodules requires the formation of a nodule primordium, which develops into a nodule, from root cortical cells. On the other hand, the bacteria enter the host by advanced infection structures, the so-called infection threads, whose formation is initiated in the root hairs (*1)*. So the formation of infection threads and nodule primordia is initiated in different tissues, but the ultimate successful interaction requires that the induction of these two processes, in time and space, is tightly coordinated. The formation of infection threads and nodule primordia are both induced by Nod factors (*2*). The occurrence of tight coordination is best indicated by the phenotypes of symbiotic legume mutants. In all mutants currently characterized the loss of (all) Nod factor responses in the epidermis is always correlated with the loss of the cortical cell division (nodule primordium) response (*3-6*). In other words, none of the legume symbiotic mutants has maintained the ability to induce cortical cell divisions in case it has completely lost the epidermal responses. This strict coupling of cortical cell division and the epidermal responses led to the hypothesis that Nod factor signalling in the epidermis results in the generation of a secondary signal that subsequently triggers cortical cell division (*3*). This would imply that a legume mutant only able to recognize Nod factors in its epidermis is able to respond with cortical cell divisions despite the lack of a functional Nod factor perception and transduction machinery in the cortical cells. Recently, several legume genes that are essential for Nod factor signalling have been cloned. One of these is the *Medicago truncatula* (Medicago) *NODULATION RECEPTOR KINASE (NORK)*, which functions at an early step of Nod factor signalling and is essential for Nod factor responses in the inner cell layers (*7*). The *nork* mutant is completely blocked for Nod factor induced responses such as early nodulin gene expression (e.g. *ENOD11*) and calcium spiking in the epidermis and for the induction of early nodulin gene expression (e.g. *ENOD40*) and cell divisions in the pericycle and cortex (*8,9*).

To test whether Nod factor signalling in the epidermis is sufficient to trigger cortical cell divisions we fused the *NORK* coding sequence to the *Lycopersicon esculentum Extensin1* promoter. This promoter was shown to be exclusively active in growing root hairs of tomato, tobacco and also Medicago (*10,11*). This construct was introduced via *Agrobacterium rhizogenes* mediated root transformation into the *nork* mutant TR25, which contains a transgene composed of the early nodulin *ENOD11* promoter fused to the *uidA* reporter (*GUS*) gene (*8*). The *ENOD11* promoter is induced by Nod factors in the epidermis during infection and pre-infection stages, whereas non-symbiotic expression occurs in root cap cells and lateral root primordia (*12*). First we checked whether *LeExtensin1::NORK* complements for Nod factor induced responses in the epidermis. In the epidermis of *LeExtensin1::NORK* transformed TR25 roots (n=10) *ENOD11::GUS* expression was induced to identical levels as in wild-type roots 6 hours after inoculation with 10^{-9} M *Sinorhizobium meliloti* Nod factors (Fig. 1A). Control TR25-*ENOD11::GUS* roots (n=8) transformed with an empty binary vector only showed non-symbiotic GUS activity in the apex of the root (Fig. 1B). Sixteen hours after Nod factor treatment root hair deformations were observed in *LeExtensin1::NORK* transformed TR25 roots (n=6) similar to those triggered in wild-type roots (Fig. 1C). In control TR25 roots (n=7) only the typical root hair swelling response reported for *nork* mutants was observed (Fig. 1D). These results indicate that the *LeExtensin1::NORK* construct efficiently complements early Nod factor induced responses in the epidermis of the *nork* mutant.

Purified Nod factors can also induce the formation of root nodule primordia when applied externally, as has been shown for a number of legumes (2,13). On wild type Medicago roots external application of 10^{-8} M *S. meliloti* Nod factors resulted in the induction of cell divisions in the cortex (Fig. 1E). Nod factor treatment resulted in 1 – 2 cell divisions per cortical cell after which cell division stopped. The fact that Nod factor induced cortical cell divisions stop at an early stage suggests that infection thread growth through the cortex (and continuous Nod factor signalling) is required to sustain division of cortical cells. Since external application of Nod factors induces cell divisions in the inner cell layers of the root we examined whether the presence of *NORK* exclusively in the epidermis would be sufficient to trigger nodule primordium formation. Four days after spot-inoculation with *S. meliloti* 2011-pHC60, expressing *GFP*, cortical cell divisions could be observed in the *LeExtensin1::NORK* transformed roots (n=6) (Fig. 1F,G). The cortical cell divisions were associated with *ENOD11::GUS* expression in the epidermis and outer cortex and few infections limited to the epidermis were observed. The induced nodule primordia developed similarly as the Nod factor induced primordia and the extent of induced cells divisions in the inner cell layers was more extensive than after treatment of wild-type Medicago roots with Nod factors.

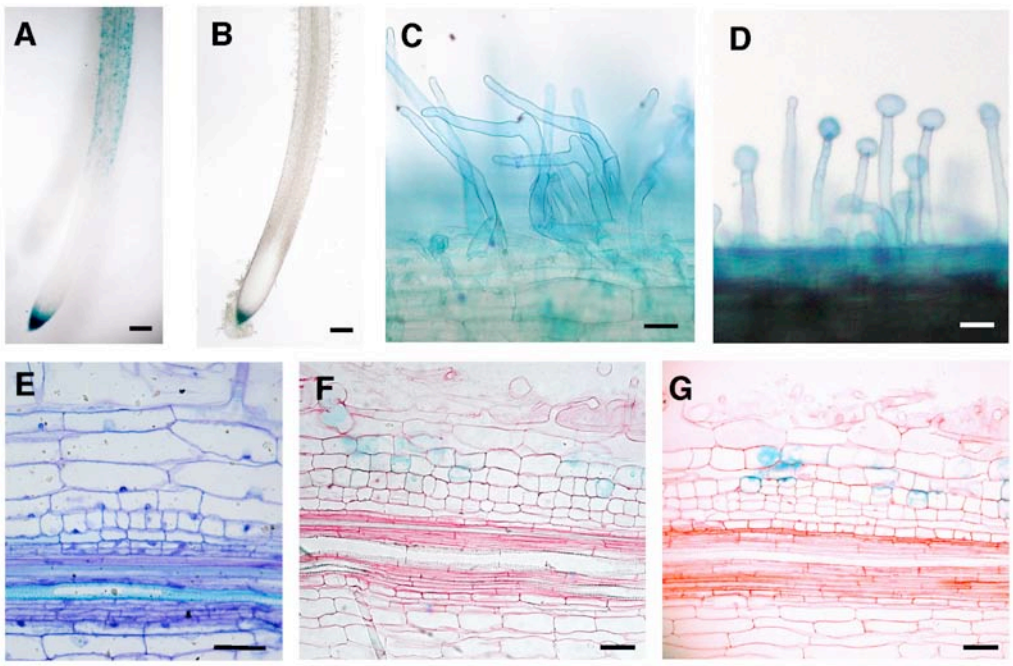

Figure 1. Phenotypes of *LeExtensin1::NORK* transformed TR25 roots compared to control roots. (A) *LeExtensin1::NORK* transformed TR25 roots 6 hours after Nod factor treatment (10^{-9} M) showing *ENOD11-GUS* activity in the region of developing root hairs. Non-symbiotic GUS activity is observed in the root cap cells. (B) TR25 control root 6 hours after Nod factor treatment, showing only non-symbiotic GUS activity in the root cap cells. (C) Root hair deformations observed in the *LeExtensin1::NORK* transformed TR25 16 hours after Nod factor treatment. (D) Typical root hair swelling response observed in the TR25 mutant 16 hours after Nod factor treatment. (E) Cortical cell divisions observed in wild type roots 5 days after Nod factor treatment (10^{-8} M). (F,G) Cortical cell divisions observed in *LeExtensin1::NORK* transformed TR25 roots 4 days after inoculation with *S. meliloti* 2011-pHC60. *ENOD11-GUS* expression can be observed in the epidermis and outer cortex. Bars in (A,B) = 150 μm; Bars in (C,D) = 50 μm; Bars in (E-G) = 100 μm.

These data show that Nod factor signal transduction in the epidermis is sufficient to cause cell divisions in the cortex in a non cell-autonomous manner. Such non cell-autonomous signalling requires intercellular communication, which is a common mechanism used to coordinate developmental processes (*14*). Intercellular communication can be achieved via two ways. One way involves the secretion and recognition of signal molecules, such as small diffusible peptides (for example CLV3 controlling shoot apical meristem organization (*15*) or systemin involved in wound-induced defence signalling (*16*) or phytohormones (*17*). The second way of intercellular communication involves the transport of larger proteins, such as transcription factors (for example KNOTTED (*18,19*) and LEAFY (*20*)) via plasmodesmata, and also RNA can be transported via plasmodesmata to transmit long distance information (*21*). In line with such studies we propose that cortical cell divisions are triggered by "secondary signals" that are generated upon Nod factor perception in the epidermis and this is the molecular mechanism underlying the tight coordination of Nod factor induced responses at spatially separated places. It was observed that Nod factors are immobilized in cells walls, which makes it unlikely that Nod factors produced by bacteria colonizing the root

can efficiently reach the inner cell layers (*22)*. The responses in the inner cell layers are induced within a couple of hours. Therefore, the observed immobilization of Nod factors is consistent with the hypothesis that responses in the inner cell layers are induced by "secondary signals" generated in the epidermis. Which molecules are involved in the epidermis-cortex communication remains unknown.

Material and Methods

Plasmids and vectors

The pBin19-*LeExt1p* construct, containing a 1.1 kb fragment of the *Lycopersicon esculentum Extensin1* promoter fused to *uidA*, is described in (*10*), designated as Δ1.1. The *LeExtensin1* promoter was PCR amplified using pBin19-*LeExt1p* as template with primers containing HindIII and XbaI restriction sites: 5' CTCCACAAGCTTTAAGTATGAAT 3' and 5' GCTCTAGAGGAGAAGAATTGGA 3'. The full length *NORK* coding sequence was PCR amplified from Medicago cDNA using primers containing NheI and SacI restriction-sites: 5' CTAGCTAGCATGATGGAGTTACAAGTTATTAAG 3' and 5' TCCGAGCTCTATAGCTCTGTTGAAGTGTC 3'. The 3103 bp fragment was subsequently cloned into pGEM-t (Promega). After sequence analysis, the full length *NORK* cDNA was cloned NheI-SacI into a modified pBluescriptII SK+ vector, which contains *LeExtensin1* promoter and a NOS-terminator sequence with an introduced PacI restriction-site and subsequently cloned HindIII-PacI into the binary vector pRedRoot (*23*), resulting in *LeExtensin1::NORK*.

Plant material and rhizobial strain

Medicago accession Jemalong A17 and *nork* mutant TR25 containing *MtENOD11::GUS* (*8*) were used for transformations. *Sinorhizobium meliloti* 2011.pHC60 (*23*) was used to inoculate plants.

A. rhizogenes mediated transformation

Agrobacterium strain MSU440 containing the pRi plasmid pRiA4 (*24*) was used to transform Medicago. The binary vectors were introduced into MSU440 by electrotransformation and grown for two days at 28^0C under kanamycin selection (50 µg/ml). *A. rhizogenes* mediated root transformation of 5 day old Medicago seedlings was performed according to (*23*).

Plant assays

Medicago seeds were surface sterilized by incubating for 10 min. in concentrated Sulfuric acid, 6x washing in sterile water, 10 min incubation in 4% hyper chlorite (commercial bleach) and 7x washing in sterile water and subsequently plated on Färhaeus medium (*23*). Seeds were vernalized for 1 day at 4^0C and germinated at 25^0C for 24 hours in darkness. For mass-inoculation with *S. meliloti* 2011.pHC60 composite Medicago plants were starved for nitrate for 3 days (22^0C; 16h light-8h darkness) on agra-perlite (Maasmond-Westland, The Netherlands) saturated with Färhaeus medium (without $Ca(NO3)_2$). Plants were inoculated with 1 ml culture of *S. meliloti* 2011.pHC60 (OD600: 0.1) per plant and grown for two weeks (22^0C; 16h light-8h darkness). Root hair deformation studies were performed with 10^{-9} M *S. meliloti* Nod factors added directly to transformed plants growing on BNM medium (*25*) with 1.2% agar and 0.1 µM AVG. Six hours after treatment with 10^{-9} M *S. meliloti* Nod factors *A. rhizogenes* transformed roots were stained for *ENOD11::GUS* activity. Root hair deformations were checked 16h post inoculation after staining with 0.002% methylene blue. To examine cortical cell divisions *A. rhizogenes* transformed roots were grown on BNM medium and spot inoculated with ~0.3 µl *S. meliloti* 2011.pHC60 (OD600: 0.1) or inoculated with 10^{-9} M *S. meliloti* Nod factors. Control roots are transformed with the empty pRedRoot binary vector.

Histochemical analysis and microscopy

Histochemical GUS staining was performed according to (*26*) with few modifications. Plant material was incubated in 0.05% (w/v) X-Gluc (Duchefa) in 0.1M sodium phosphate buffer (pH 7) with 3% sucrose, 5µM potassium-ferrocyadine and 5µM potassium. Roots were infiltrated for 30 min. under vacuum and further incubated at 37^{0}C. For sectioning roots or nodules were fixed for 1h in 2.5% glutaraldehyde buffered in 0.1M sodium phosphate buffer (pH 7), dehydrated in an alcohol series and embedded in Technovit 7100 (Heraeus Kulzer). 5 µm-thick nodule sections were made using a Leica microtome, stained with 0.04% toluidine blue or 0.1% ruthemium red and viewed with a Nikon Optiphot-2 microscope. Imaging of *Ds*RED1 or GFP fluorescence was done using the Leica MZIII fluorescence stereomicroscope and a Nikon Optiphot-2 coupled to a mercury-lamp.

References

1 Geurts R, Bisseling T: ***Rhizobium*** **Nod factor perception and signalling.** *Plant Cell* 2002, **14** (suppl): S239-S249.

2 Ardourel M, Demont N, Debellé F, Maillet G, De Billy F, Promé JC, Dénarié J, Truchet G: ***Rhizobium meliloti*** **lipoligosaccharide nodulation factors: different structural requirements for bacterial entry into target root hair cells and induction of plant symbiotic developmental responses.** *Plant Cell* 1994, **6**: 1357-1347.

3 Cooper JB, Long SR: **Morphogenetic Rescue of Rhizobium meliloti Nodulation Mutants by trans-Zeatin Secretion.** *Plant Cell.* 1994, **6**: 215-225.

4 Stougaard J: **Genetics and genomics of root symbiosis.** *Curr Opin Plant Biol* 2001, **4**: 328-335.

5 Tsyganov VE, Voroshilova BA, Priefer UB, Borisov AY, Tikhonovich IA: **Genetic dissection of the initiation of the infection process and nodule tissue development in the *Rhizobium*-pea (*Pisum sativum* L.) symbiosis.** *Ann Bot* 2002, **89**: 357-366.

6 Limpens E, Bisseling T: **Signaling in symbiosis.** *Curr Opin Plant Biol* 2003, **6**: 343-350.

7 Endre G, Kereszt A, Kevei Z, Mihacea S, Kaló P, Kiss GB: **Cloning of a receptor kinase gene regulating symbiotic nodule development.** *Nature* 2002, **417**: 962-966.

8 Catoira R, Galera C, De Billy F, Penmetsa RV, Journet EP, Maillet F, Rosenberg C, Cook D, Gough C, Dénarié J: **Four genes of *Medicago truncatula* controling components of a Nod factor transduction pathway.** *Plant Cell* 2000, **12**: 1647-1666.

9 Wais RJ, Galera C, Oldroyd G, Catoira R, Penmetsa RV, Cook D, Gough C, Dénarié J, Long SR: **Genetic analysis of calcium spiking responses in nodulation mutants of *Medicago truncatula.*** *Proc Natl Acad Sci USA* 2000, **97**: 13407-13412.

10 Bucher M, Brunner S, Zimmermann P, Zardi GI, Amrhein N, Willmitzer L, Riesmeier JW: **The expression of an extensin-like protein correlates with cellular tip growth in tomato.** *Plant Physiol* 2002, **128**: 911-923.

11 Mirabella R, Franken C, van der Krogt GNM, Bisseling T, Geurts R: **Use of the "fluorescent timer" DsRED-E5 as reporter to monitor dynamics of gene activity in plants.** *Plant Physiol* 2004, in press.

12 Journet EP, El-Gachtouli N, Vernoud V, de Billy F, Pichon M, Dedieu A, Arnould C, Morandi D, Barker DG, Gianinazzi-Pearson V. ***Medicago truncatula ENOD11*: a novel RPRP-encoding early nodulin gene expressed during mycorrhization in arbuscule-containing cells.** *Mol Plant Microbe Interact* 2001, **14**: 737-748.

13 Spaink HP, Sheeley DM, van Brussel AA, Glushka J, York WS, Tak T, Geiger O, Kennedy EP, Reinhold VN, Lugtenberg BJ: **A novel highly unsaturated fatty acid moiety of lipo-oligosaccharide signals determines host specificity of *Rhizobium*.** *Nature* 1991, **354**: 125-130.

14 Haywood V, Kragler F, Lucas WJ: **Plasmodesmata: pathways for protein and ribonucleoprotein signalling.** *Plant Cell* 2002, **14** (suppl): S303-S325.

15 Clark SE: **Cell signalling at the shoot meristem.** *Natl Rev Mol Cell Biol* 2001, **2**: 276-284.

16 Ryan CA, Pearce G, Scheer J, Moura DS: **Peptide hormones.** *Plant Cell* 2002, **14** (suppl): S251-S264.

17 Golz JF, Hudson A: **Signaling in plant lateral organ development.** *Plant Cell* 2002, **14** (suppl): S277-S288.

18 Lucas WJ, Bouche-Pillon S, Jackson DP, Nguyen L, Baker L, Ding B, Hake S. **Selective trafficking of KNOTTED1 homeodomain protein and its mRNA through plasmodesmata.** *Science* 1995, **270**: 1980-1983.

19 Kim JY, Yuan Z, Jackson D: **Developmental regulation and significance of KNOX protein trafficking in Arabidopsis.** *Development* 2003, **130**: 4351-4362.

20 Sessions A, Yanofsky MF, Weigel D: **Cell-cell signalling and movement by the floral transcription factor LEAFY and APETALA1.** *Science* 2000, **289**: 779-781.

21 Ruiz-Medrano R, Xoconostle-Cazares B, Lucas WJ: **Phloem long-distance transport of *CmNACP* mRNA: Implications for supracellular regulation in plants.** *Development* 1999, **126**: 4405-4419.

22 Goedhardt J, Hink MA, Visser AJ, Bisseling T, Gadella TW jr: ***In vivo* fluorescence correlation microscopy (FCM) reveals accumulation and immobilization of Nod factors in root hair cell walls.** *Plant J* 2000, **21**: 109-119.

23 Limpens E, Franken C, Smit P, Willemse J, Bisseling T, Geurts R: **LysM domain receptor kinases regulating rhizobial Nod factor-induced infection.** *Science* 2003, **302**: 630-633.

24 Sonti RV, Chiurazzi M, Wong D, Davies CS, Harlow GR, Mount DW, Signer ER: **Arabidopsis mutants deficient in T-DNA integration.** *Proc Natl Acad Sci USA* 1995, **92**: 11786-11790.

25 Ehrhardt DW, Atkinson EM, Long SR: **Depolarization of alfalfa root hair membrane potential by *Rhizobium meliloti* Nod factors.** *Science* 1992, **256**: 998-1000.

26 Jefferson AR, Kavanagh TA, Bevan MW: **Gus fusions: *β-glucuronidase* as a sensitive and versatile gene fusion marker in higher plants.** *EMBO J.* 1987, **6**: 3901-3907.

Chapter 6

NODULATION RECEPTOR KINASE controlling the switch from infection thread growth to release of bacteria in nodule cells

---

Erik Limpens, Rossana Mirabella, Carolien Franken, Elena Federova, Ton Bisseling and René Geurts

The formation of nitrogen-fixing root nodules is triggered by the perception of rhizobial signaling molecules, named Nod factors, in the epidermis of the root. The key-players of the Nod factor-signaling pathway have been identified and are characterized by the fact that mutations in these genes block nodulation at an initial stage of the interaction. One of the key-players is the *Medicago truncatula NODULATION RECEPTOR KINASE* (*NORK*). Here we show that the expression pattern of *NORK* in the nodule coincides with the region where rhizobial *nod* genes are active in the nodule. This corresponds to the place where the bacteria are released in the plant host cells. By mimicking allelic series of *NORK* by RNA interference and by ectopic expression of *NORK* in the mutant background we show that NORK controls the switch from infection thread growth to release of bacteria in the nodule. This suggests a role for the Nod factor perception and signaling machinery in this process in the nodule.

Introduction

Rhizobial signaling molecules, called Nod factors, play a pivotal role in the establishment of a successful nitrogen-fixing root nodule through the activation of a conserved Nod factor-signaling pathway (*1,2*). Genetic analysis in model legumes formed the basis to identify and clone the key-players of this Nod factor-signaling pathway. Based on these studies it is hypothesized that Nod factors are recognized by LysM domain containing receptor kinases (*3-5*). In the model legume *Medicago truncatula* (Medicago), these include *LYK3* and *LYK4* (*3*) and *NFP*, which is the putative ortholog of the *Lotus japonicus NFR5* gene (*4*; Gough and Geurts, unpublished). Other essential components of the Nod factor signal transduction pathway include the *DOES NOT MAKE INFECTIONS 1* gene *(DMI1), DMI3* and NODULATION *RECEPTOR-LIKE KINASE (NORK),* which encode, respectively, a putative cation channel, a calcium/calmodulin-dependent kinase and a leucine-rich repeat (LRR) containing receptor kinase (*6-10*). Upon perception of Nod factors these components are all involved in the formation of infection threads in the root hairs, by which the bacteria gain entry into the root, as well as in the induction of responses in the inner cell layers leading to the formation of the nodule organ.

The Nod factor-signaling components have been identified in genetic screens that were based on a search for loss of nodulation, and as a result all the characterized mutant alleles cause a block of nodulation at the initial steps. For example, the only morphological respons that is observed after inoculation with rhizobia in the 4 different mutant alleles of *NORK* that are characterized to date, is the induction of root hair swellings (*6,11*). Similar phenotypes have been reported for mutants of *SYMRK* in *Lotus japonicus*, *NORK* in alfalfa and *SYM19* in pea, which represent orthologs of Medicago *NORK* (*7,12*). Although it is obvious that Nod factor signaling is essential at initial stages of the interaction, several observations indicate that the Nod factor perception and signaling machinery also plays a role in the nodule. By

fusions of the *nod* genes with the *gusA* reporter gene it has been shown that the rhizobial *nod* genes -involved in Nod factor biosynthesis- are expressed by rhizobia throughout the infection zone of the nodule (*13*). Highest GUS activity was observed in the distal part of the infection zone and GUS activity diminished towards the proximal regions. *In situ* hybridizations detected *nod* gene expression more specifically in the distal region of the infection zone, and led to the conclusion the rhizobial *nod* genes are switched off as soon as bacteria are released into the nodule cells (*14*). The involvement of Nod factor perception and signaling in the nodule is further supported by the fact that several of the Nod factor perception and signaling genes (e.g. *LYK3* and *DMI3* in Medicago and *SYM10* in pea) are transcribed in the nodule, although their expression pattern is unknown (*3,4,9*). If the Nod factor signaling genes would play a role in Nod factor perception and transduction in the nodule we hypothesized that their expression pattern would coincide with that of *nod* genes. Therefore we determined the expression pattern of *NORK* in the nodule. We show that *NORK* is highly expressed in the distal part of the infection zone of the nodule, which coincides with the region where the rhizobial *nod* genes are expressed. This is the region where bacteria are released from the infection threads into the plant host cells and start to divide (*15*). These bacteria remain surrounded by a plant-derived membrane and are called symbiosomes (*16*). By mimicking allelic series of *NORK* using RNA interference and by expression of *NORK* in the mutant background we show that high expression levels of *NORK* are required to restrict growth of infection threads in the nodule and to facilitate the release of bacteria in the plant host cells. This suggests a role for the Nod factor perception and transduction machinery in these processes in the nodule.

Results

NORK expression is highly upregulated in the distal region of the infection zone

To determine whether Nod factor signaling could occur in nodules we examined whether the expression pattern of the Nod factor signaling component, *NORK*, coincides with the region where the rhizobial *nod* genes are expressed. The rhizobial *nod* genes are most strongly expressed in the distal part of the infection zone of the nodule (*13,14*). Quantitative RT-PCR (qPCR) showed that *NORK* expression was mainly detected in roots and in nodules (Fig. 1). Very low NORK expression levels were detected in the aerial parts of the plant (e.g. stem, leaves and flowers), which suggests that *NORK* has a specific role in the root system. Upregulation of *NORK* expression was observed in roots upon inoculation with *Sinorhizobium meliloti* and in root nodules, when compared to un-inoculated roots.

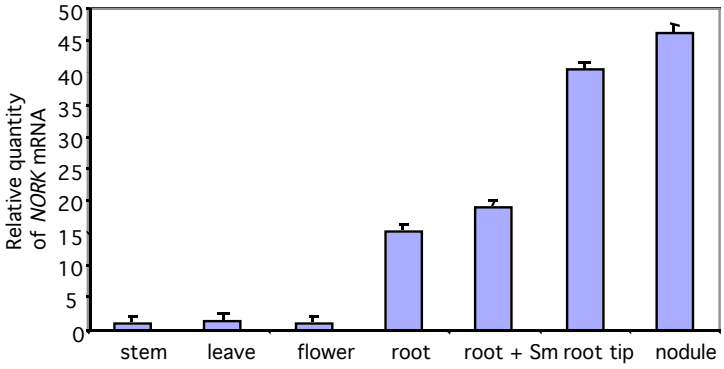

Figure 1. Quantification of *NORK* mRNA levels in stem, leaves, flowers, roots, roots 48 h post-inoculation with *S. meliloti*, root tips and 2-week-old nodules. Relative transcript levels were determined by qRT-PCR, and normalized using *MtACTIN2* that is constitutively expressed in all tissues tested.

To determine in which nodule cell types *NORK* is expressed we conducted *in situ* hybridizations on 2-week old nodules using *NORK* anti-sense RNA as probe. These studies showed that *NORK* is highly expressed in the distal region of the infection zone, in the 2 - 3 cell layers adjacent to the meristem (Fig. 2A). *NORK* expression levels rapidly diminished towards to proximal region of the infection zone. This indicates that regions where *nod* genes are active and *NORK* is expressed are coincide (*13,14*). The distal part of the infection zone is the place where bacteria are released from the infection threads into the plant host cells and division of symbiosomes starts (*15*).

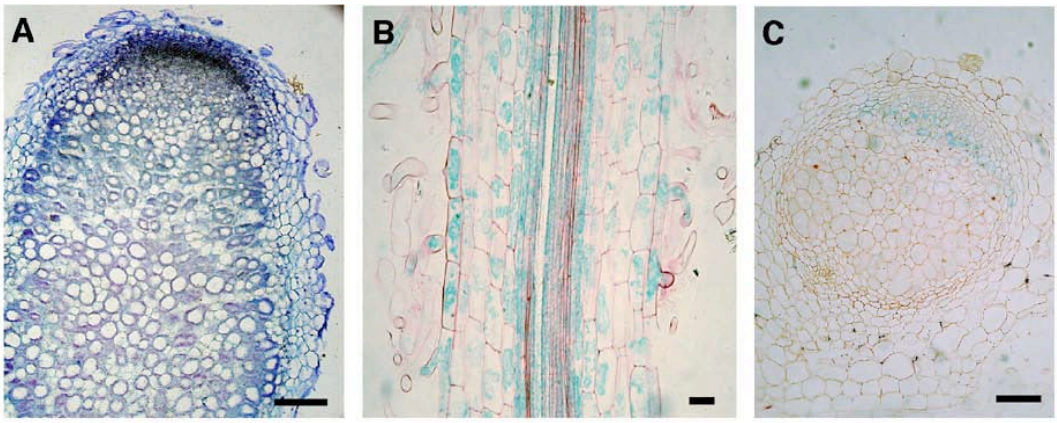

Figure 2. *NORK* expression profiling. (A) *In situ* hybridization of a longitudinal section hybridized with ^{35}S-UTP labeled anti-sense *NORK* probes; signal appears as silver grains. Section is counterstained with toluidine blue. Strong hybridization is observed in the distal part of the infection zone adjacent to the meristem and rapidly declines towards more proximal regions. (B) Histochemical localization of GUS activity in semi-thin (5 μm) longitudinal section of *NORKp::GUS* transformed roots. (C) Localization of *NORKp::GUS* expression in a longitudinal section (5 μm) of a 2-week-old nodule. GUS activity is observed in the infection zone (zone II) of the nodule. Sections in (B) and (C) are stained with 0.1% ruthemium red. Bars in (A) and (C) = 200 μm; Bar in (B) = 25 μm.

NORK controls the switch from infection thread growth to release of bacteria in the nodule

To gain insight into the function of *NORK* and probably Nod factor signaling in the infection zone of the nodule we used two strategies. First we mimicked allelic series of *NORK* by using RNA interference (RNAi) and second, the gene was over-expressed using the *CaMV* 35S promoter.

RNAi is a powerful tool to knock-down the expression of genes in order to study their function and it has been shown that RNAi can result in phenotypes that mimic allelic series due to partial knock-down of the target mRNA (*17,18*). Previously, we have shown that gene knock-down by RNAi via *A. rhizogenes* mediated root transformation in Medicago is very effective (*3,18*). In the case of *NORK,* 75% of the RNAi roots displayed a phenotype identical to the described knock-out mutants (*3*). So only in 25% of the cases some nodules were formed on roots where the silencing construct was introduced. We decided to examine such nodules to determine whether a weak knock-down phenotype could reveal a function of NORK in the nodule. In total 57 roots, homogeneously transformed with a *NORK* hairpin construct, were inoculated with *S. meliloti* 2011-pHC60 expressing *GFP*. Fourteen days after inoculation 25 nodules were observed on 9 homogeneously transformed roots. Histological examination by analyzing sections of 12 of these nodules with light microscopy revealed in 6 of the nodules the presence of numerous wide infection threads in the central tissue of the nodule with no, or very few bacteria in the nodule cells (Fig. 3A). The remaining 6 nodules showed infected cells filled with released bacteria similar to control nodules (data not shown). Control nodules, transformed with an empty binary vector, all showed a normal histology, typical for indeterminate nodules, with infected plant host cells containing bacteroids (Fig. 3B) (*15*). This suggests that partial knock down of *NORK* expression causes extensive infection thread growth in the nodule with no, or very inefficient, release of bacteria from the infection threads.

In addition to knock-down of *NORK* expression, we over-expressed *NORK* by introducing the *NORK* coding sequence into wild-type roots under the control of the *CaMV* 35S promoter (*35S::NORK*) via *A. rhizogenes* mediated root transformation. To check whether the construct was functional we introduced the *NORK* coding sequence under the control of the *CaMV* 35S promoter into the *nork* mutant TR25 and under the control of a 2200 bp *NORK*-upstream putative promoter region (*NORKp::NORK*) (*6*). To determine whether this *NORK* upstream region truly represents the endogenous *NORK* promoter we cloned the 2200 bp *NORK* upstream-region also into a binary vector containing the *uidA* reporter gene encoding β-glucoronidase (GUS). The resulting plasmid was introduced into the plant by *Agrobacterium rhizogenes* mediated root transformation.

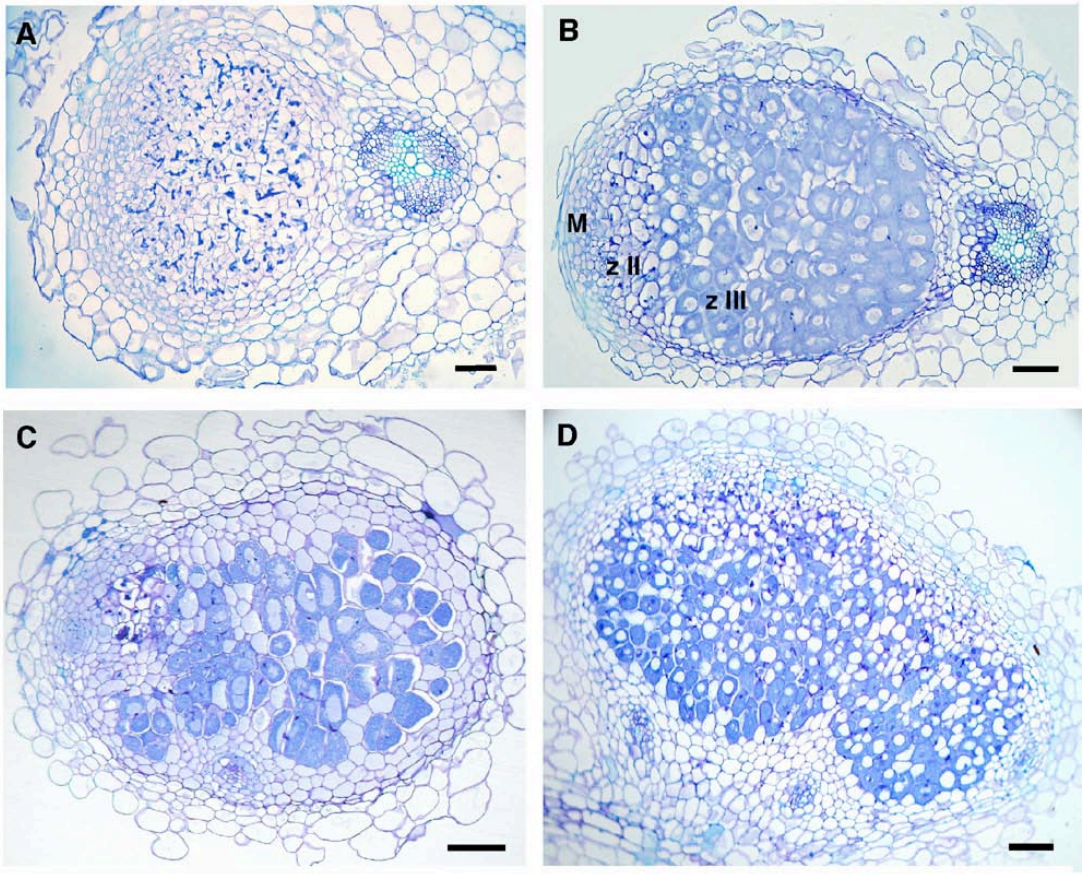

Figure 3. Histochemical analysis of nodules by light microscopy. Longitudinal sections (5 μm) of 2-week-old nodules formed on (A) *NORK* knock-down (RNAi) roots, (B) wild type (A17) roots transformed with an empty binary vector, (C) *35S::NORK* transformed wild type roots and (D) *NORKp::NORK* transformed TR25 roots. Sections are stained with toluidine blue. M = meristem; z II = zone II or infection zone; z III = zone III or fixation zone with infected cells containing bacteroids. Bars in (A) to (D) = 100 μm.

Histological GUS staining revealed that under non-symbiotic conditions the *NORK* promoter was active in all tissues of the root (Fig. 2B). Stronger GUS activity was detected in the root apex containing dividing cells and in lateral root primordia. Quantitative RT-PCR on RNA isolated from root tips (excised ~3mm behind the tip) confirmed the strong expression of *NORK* in the root apex (Fig. 1). Upon inoculation with rhizobia *NORK* promoter activity was up-regulated in nodule primordia and root nodules. In 2-week-old nodules GUS activity was especially observed in the infection zone of the nodule, which is consistent with the expression pattern of *NORK* observed by the *in situ* hybridisations and indicates that the 2200 bp *NORK* upstream-region indeed represents the endogenous *NORK* promoter (Fig 2C).

Inoculation of *NORKp::NORK* transformed TR25 roots resulted in on average 7 nodules / transformed root (n=22), that showed a wild type histology including fully infected cells (Fig. 3D). This shows that the *NORK* cDNA construct was functional and could complement the TR25 mutant. Introduction of *35S::NORK* into wild type roots did not affect nodule

development. Fourteen days after inoculation with *S. meliloti* 2011-pHC60 on average 8 nodules were formed per transformed root (n=8) and these nodules showed a normal histology (Fig. 3C). This shows that over-expression of *NORK* does not negatively affect nodulation. Introduction of *35S::NORK* into the TR25 mutant effectively complemented early Nod factor induced responses (data not shown), however, the nodulation efficiency was reduced. On average 2 nodules formed on a transformed TR25 root (n=43). Strikingly, histological examination of these nodules revealed a similar phenotype as observed in the *NORK* knock-down nodules; extensive infection thread growth in the central tissue of the nodule with no, or very few bacteria in the nodule cells.

Cytology of 35S::NORK transformed TR25 nodules

Introduction of *NORK* under the control of the 35S promoter into the *nork* mutant resulted in nodules with a similar histology as that of nodules obtained by RNAi. Because of higher nodule numbers and consistency of the phenotypes in the *35S::NORK* transformed TR25 roots, we studied the cytology of *35S::NORK* transformed TR25 nodules in more detail. Based on light microscopic analysis of semi-thin sections of the 2-week-old *35S::NORK* transformed TR25 nodules we divided the nodules into two groups. Group I consisted of small nodules (12-18 cell layers in longitudinal sections) showing very wide infection threads in many cells of the central tissue of the nodule as well as big intercellular bacterial colonies. The infection threads penetrated and traversed the cells and no release of bacteria into the nodule cells was observed (Fig. 4A-C). In sections of wild type nodules only a few infection threads are typically seen in cells of the central tissue (Fig 4D). Since the thickness (0.6-1 μm) of semi-thin sections represents less than 1/20 -1/50 of the diameter of nodule cells, the occurrence of infection threads in almost every cell in a thin section of the *35S::NORK* TR25 nodules, indicates that the infection threads almost completely fill these cells. Further, infected cells are interspersed by small groups of uninfected cells that have a function in the nitrogen assimilation process. These uninfected cells often form small clusters in wild type nodules. Since several small groups of cells without infection threads could be observed in thin sections of the *35S::NORK* TR25 nodules, this suggests that the uninfected cell type can still be formed and are not penetrated by infection threads. Transmission electron microscopy showed that infection threads had a similar morphology as wild type infection threads with the bacteria embedded in a matrix with a low electron density surrounded by a fibrillar wall and a membrane (Fig. 6A). The only difference with wild-type infection threads was their length and diameter, with some threads accommodating up to 100 bacteria compared to 10-15 bacteria observed in cross-sections of infection threads in *35S::NORK* TR25 nodules and wild type nodules, respectively. The second group showed nodules that were bigger in size (22-30 cell layer long central tissue), and these also contained numerous (wide) infection threads and large intercellular bacterial colonies in the central tissue (Fig 5A). However, in these nodules intracellular bacteria were occasionally observed in the proximal cell layers (Fig. 5B).

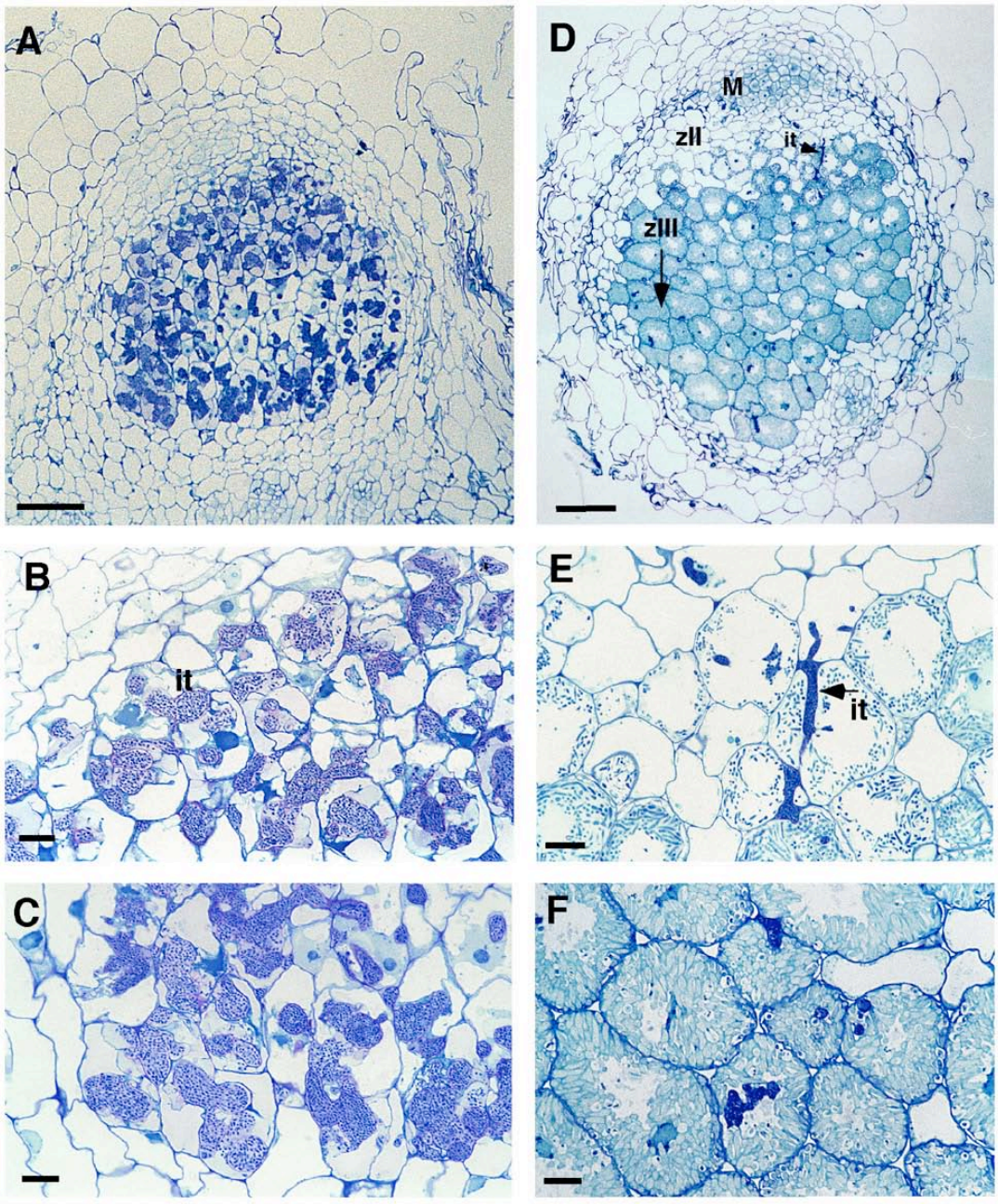

Figure 4. Histology of 2-week-old *35S::NORK* transformed TR25 group I nodules compared to control nodules. (A) Longitudinal section of a small *35S::NORK* transformed TR25 group I nodule shows that most cells of the central tissue contain an infection thread. These threads are very wide. (B,C) Magnification of (A) in the apical part and basal part of the nodule, respectively. No release of bacteria is observed. (D) Longitudinal section of a control nodule (transformed with an empty binary vector). A typical zonation of indeterminate nodules can be seen, with M = meristem; z II = infection zone and z III = zone III or fixation zone with infected cells containing elongated bacteroids. (D,E) Magnification of (D) in the infection zone and basal part of the nodule, respectively. Sections (0.6-1 μm) are stained with 0,5% toluidine, 0,5% methylene blue. It = infection thread. Bars in (A,D) = 100 μm, Bars in (B,C,E,F) = 20 μm.

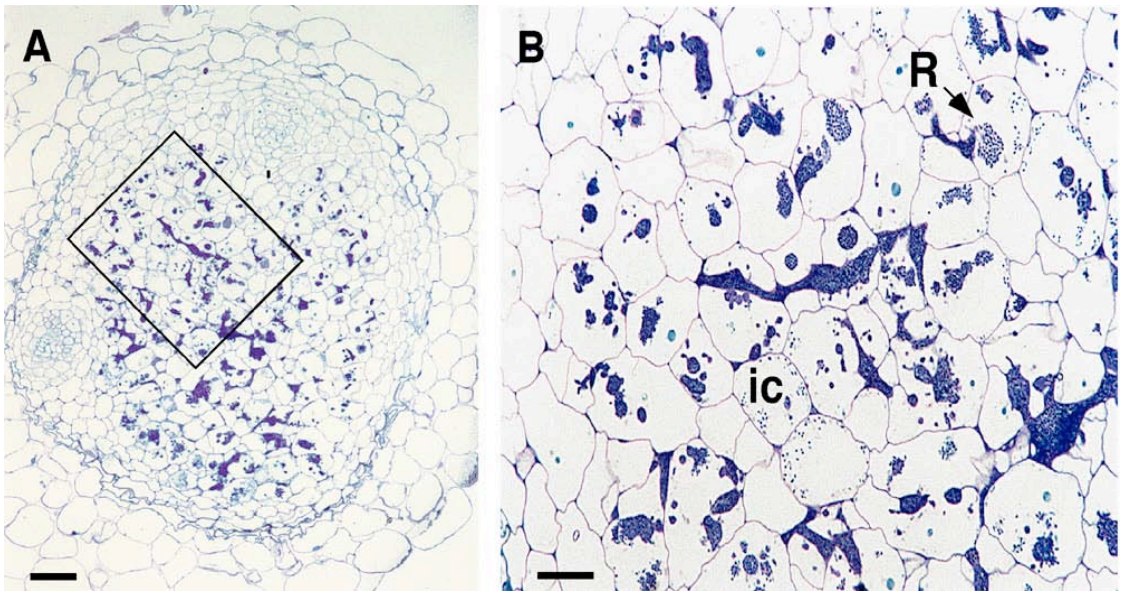

Figure 5. Light microscopic analysis of 2-week-old *35S::NORK* transformed TR25 group II nodules. (A) Longitudinal section of a *35S::NORK* transformed group II TR25 nodule. (B) Magnification of boxed area in (A) showing release of bacteria from the infection threads (R and arrow) and several infected cells (ic) containing few bacteroids in the cytoplasm. Bar in (A) = 100 μm, Bar in (B) = 31 μm.

In wild type nodules infection thread growth is directed towards the meristem and bacteria are normally released in the first 2 – 3 cell layers adjacent to the meristem after which they start to multiply (Fig. 4D-F). In most of the 2-week old *35S::NORK* transformed TR25 nodules no meristem was observed, and release of bacteria, as judged by the presence of unwalled infection droplets, appeared to occur in the more proximal cell layers. Such events are rare and most infection threads invaded and traversed the cells without release of bacteria. In the cases where bacterial release was observed division of the bacteria was limited as only a few symbiosomes where observed in the cytoplasm of the infected cells and these infected cells did not show an increase in cell size, which is typically observed (3 - 4x) in wild type infected cells (Fig. 4D). Transmission electron microscopy revealed that bacteria where released inside the living cells from unwalled infection droplets. From these unwalled droplets single bacteria emerged that were surrounded by a plant-derived membrane, the symbiosome membrane (Fig. 6B) (*16,19*). However, the released bacteria did not elongate as observed in wild type infected cells (*15*) (Fig. 6C). Some of the symbiosomes revealed typical features of premature senescence, having an electron dense cytoplasm, abnormal morphologies and some symbiosomes seemed to fuse, forming vacuole-like structures causing lysis of bacteroids entrapped inside (Fig. 6D). In several *35S::NORK* transformed TR25 nodules, especially older nodules, the host cells in the central and basal part of the nodule also showed premature senescence with loss of cytoplasm and without visible nuclei. These cells appeared to be repopulated by saprophytic bacteria (data not shown).

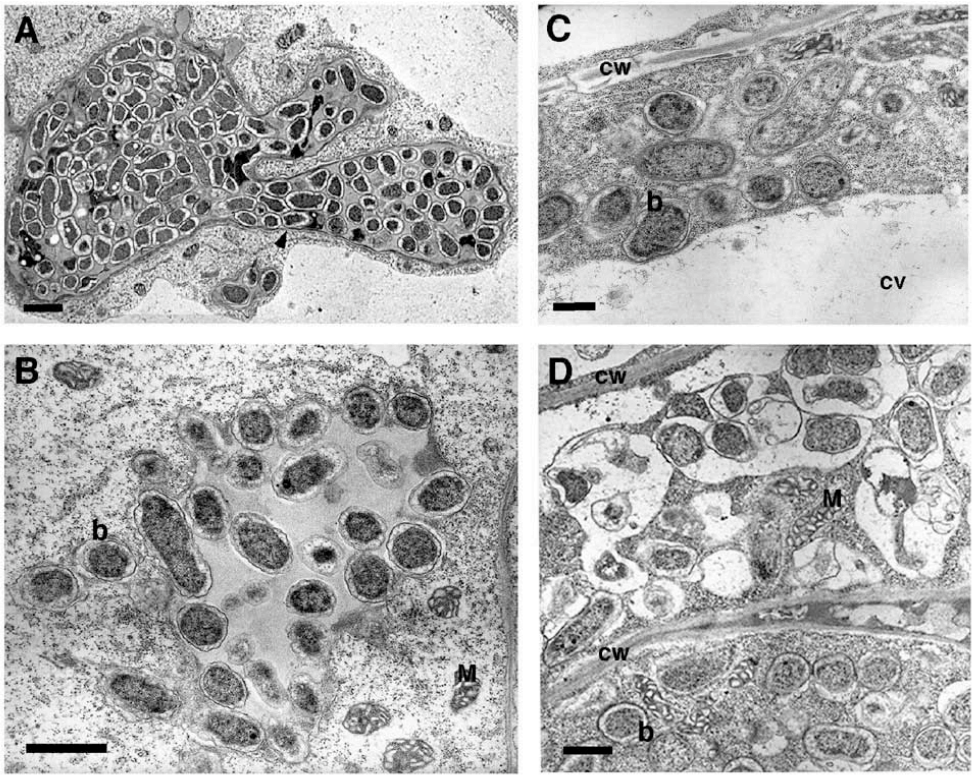

Figure 6. Transmission electron microscopy of *35S::NORK* transformed TR25 nodules. (A) Section showing a nodule cell with an infection thread without releasing bacteria. The infection thread has a fibrillar wall and is surrounded by a membrane (arrow). (B) Release of bacteria from an unwalled infection droplet. Note that the released bacteria (b) are surrounded by a membrane. (C) Released bacteria do not elongate and are located in a thin layer of cytoplasm surrounding the big central vacuole. (D) Two cells containing bacteria at different stages of senescence. Some symbiosomes have a big peribacteroid space and symbiosome membranes have fused to form vacuole-like structures, some ghost membranes probably of lysed bacteria are present. CW = cell wall, M = mitochondria, b = bacteroid, cv = central vacuole. Bars in (A to C) = 1 μm, Bar in (D) = 0.5 μm.

Discussion

The *NORK* gene was shown to be required for the induction of many Nod factor induced epidermal responses, such as the induction of early nodulin genes, infection thread formation and also the induction of cortical cell divisions (*6*). Here we show that a high *NORK* expression level in the distal part of the infection zone of the nodule is required to restrict infection thread growth in the nodule and to facilitate the release of bacteria into the plant host cells. Since NORK is an essential component of the Nod factor perception and signaling machinery this suggests a role for Nod factor signaling in these processes in the nodule.

In situ hybridisation revealed high *NORK* expression levels in 2 – 3 cell layers of the infection zone adjacent to the meristem. Previously, it has been shown that rhizobial *nod* genes are active in these cell layers (*13,14*). This suggests that Nod factor signaling takes place in this

zone. Whether the zone where Nod factor signaling takes place is larger than the first 3 cell layers of the infection zone will depend on the stability of the Nod factor signaling proteins. The *in situ* hybridization studies of Schlaman *et al.,* (*14*) indicate that *nod* gene expression coincides with the region where *NORK* is expressed. The studies of Sharma and Signer (*13*) suggest that the *nod*-expressing zone might be broader. However it seems probable that this is due to the stability of the GUS protein that has been used as reporter. Infection threads grow in the direction of and penetrate new cells that originate form dividing meristem cells. Bacteria are released from the infection threads in the 2-3 cell layers adjacent to the meristem after which the symbiosomes start to multiply (*15,20*). Thus the region where *NORK* is expressed in the nodule coincides with the place where the rhizobial *nod* genes are active and corresponds to the region where infection thread growth and release of bacteria from the infection threads and subsequent division take place. This suggests a role for Nod factor signaling via NORK in these processes.

Partial knock down of *NORK* expression via RNAi affected infection thread growth and release of bacteria in the nodule cells. In most roots knock-down of *NORK* expression by RNAi blocked nodulation at an initial step, since nodules are not formed. Therefore we expect that in RNAi knock down roots which still allow nodules to be formed, that *NORK* mRNA levels are less reduced. This indicates that the observed nodule phenotypes are the result of partial knock down of *NORK* expression. As other Nod factor responses appeared to be induced in these partial knock down roots this suggests that the switch form infection thread growth to release of bacteria (and possibly division of symbiosomes) requires a higher threshold level of *NORK* than do other Nod factor responses. Fifty percent of the *NORK* RNAi nodules did not show an aberrant nodulation phenotype, indicating that *NORK* expression levels in these nodules still reached the threshold level. In line with the hypothesis that relatively high expression levels of NORK need to be reached to facilitate bacterial release is the observation that over-expression of *NORK* in wild type roots under the control of the 35S promoter did not negatively affect nodulation. It further indicates that expression of *NORK* in the proximal cell layers does not affect nodulation. Introduction of *35S::NORK* into the mutant background resulted in similar nodule phenotypes as observed in the knock-down nodules. This suggests that the phenotypes observed in the *35S::NORK* transformed TR25 nodules are also the result of *NORK* mRNA levels that are below the threshold value needed to induce bacterial release.

The most markedly affected processes in these "*NORK* mutant" nodules was the release of bacteria from the infection threads and the sustained growth of infection threads that continually invaded and traversed cells without releasing bacteria. The observation of clusters of cells that are not invaded by infection threads in the semi-thin sections suggests that, although the infection threads appear to be numerous, still uninfected cells are present. This indicates that in the RNAi and *35S::NORK* TR25 nodules not more cells are infected by

rhizobia, but rather that in the infected cells the switch from infection thread growth to bacterial release is disturbed by which infection threads occupy large parts of these cells. Occasionally, release of bacteria was observed in the more proximal cell layers of the *35S::NORK* transformed TR25 nodules. However, only a few bacteria occur in these nodule cells, which indicates that the symbiosomes do not efficiently divide. As a result no increase in cell size of the infected cells was observed, which is typical for wild type infected cells (*15,20*). The fact that release occurs in older cells that are in a different developmental stage could be a reason for the impaired division of the bacteria in the proximal cell layers of the *35S::NORK* TR25 nodules. However, it cannot be excluded that Nod factor signaling plays a role in this process as well.

The release of bacteria from an infection thread coincides with the stop of growth of this thread. Infection thread growth involves the deposition of plant cell wall material to the growing infection thread, while release of bacteria from the infection thread involves the formation of unwalled infection droplets that extrude from the infection threads (*16,19,21*). From such unwalled infection droplets single bacteria are released into the cytoplasm that stay surrounded by a plant derived symbiosome membrane (*16,22*). Although the molecular basis of bacterial release is unknown, it is thought to be related to the process of endocytosis (*16,23*). It is clear that the symbiosomal membrane and the membrane surrounding the infection droplets have no associated plant cell wall (*16,23*). Thus the release of bacteria from the infection thread seems to involve a change in the kind of vesicles, and their cargo, that fuse with the tip of the infection thread by which infection thread growth is not sustained, but instead unwalled droplets are formed. Nod factor signaling via NORK appears to be involved in inducing this switch in infection thread growth. The continued growth of infection threads and large intercellular bacterial colonies, as observed in the “NORK mutant” nodules, could both be a consequence of continued secretion of infection thread matrix to the tip of the infection thread and into the intercellular spaces allowing the bacteria to proliferate there. It can thus be hypothesized that sustained infection thread growth and suppressed release of bacteria are interlinked processes. Further, Nod factor signaling involving high threshold levels of NORK is essential in the switch from infection thread growth to release of bacteria in the nodule.

Infection thread growth and “endocytosis” of the bacteria both require continuous and extensive membrane proliferation, cytoskeletal rearrangements as well as targeted vesicle transport (*23,24*). The underlying molecular mechanism of a switch from infection thread growth to release of bacteria is therefore expected to involve regulation of cytoskeletal organization (microtubuli and/or actin) and targeting of vesicle insertions to the tip of infection threads. The observation that redirecting and sustaining polar growth of root hairs in response to Nod factors is impaired in the *NORK* knock-out mutants supports the idea that NORK facilitates cytoskeletal re-organization and vesicle transport (*6*). Examination of the actin

cytoskeleton and microtubule structure in response to Nod factor treatment in root hairs of the NORK knock-out mutants and in nodule cells of the knock-down mutants, should give insight into Nod factor signaling to the cytoskeleton. As small GTPases (e.g. ROPs) are known to be key regulators of the cytoskeletal organization and vesicular transport (*25*), these might represent likely downstream targets of Nod factor signaling via NORK.

Release of bacteria into the nodule cells appears to require higher *NORK* mRNA levels than Nod factor induced epidermal responses and induction of cortical cell divisions. This could indicate that NORK associates in different (Nod factor perception) complexes in the nodule cells. As infection thread growth, which depends on Nod factor signaling in the epidermis, still occurs in "*NORK* mutant" nodules it shows that infection thread growth and release of bacteria in the nodule require different threshold levels of NORK. Therefore, it cannot be excluded that Nod factor signaling plays additional roles in the nodule, e.g. in infection thread growth. However, since the rhizobial *nod* genes appear to be switched off as soon as bacteria are released into the cells it is unlikely that Nod factor signaling plays a role in the subsequent cell layers of the nodule.

Materials and Methods

Plasmids and vectors

To isolate the *NORK* promoter a 2200 bp region upstream from the ATG startcodon was PCR amplified from Medicago A17 genomic DNA using primers that introduce HindIII and BamHI restriction sites and cloned into pGEM-t (Promega): 5' AAGCTTCAAATTTGGACCGAACTG 3' and 5' GGATCCAACTTGAATCCATGCTAACTAACT 3'. This fragment was cloned HindIII-BamHI into the pCambia1304 binary vector from which all *CaMV 35S* sequences were deleted, resulting in the *NORKp::GUS* fusion construct. The full length *NORK* coding sequence was PCR amplified from Medicago root cDNA using primers containing NheI and SacI restriction-sites: 5' CTAGCTAGCATGATGGAGTTACAAGTTATTAAG 3' and 5' TCCGAGCTCTATAGCTCTGTTGAAGTGTC 3'.The 3103 bp fragment was subsequently cloned into pGEM-t (Promega). After sequence analysis, the full length *NORK* cDNA was cloned NheI-SacI into a modified pBluescriptII SK+ vector, which contains the *CaMV 35S* promoter from pMON999 (Monsanto) or the *NORK* promoter and a NOS-terminator sequence with an introduced PacI restriction-site and subsequently cloned HindIII-PacI into the binary vector pRedRoot (*18*), resulting in *d35S::NORK* and *NORKp::NORK*.

Plant material and rhizobial strain

Medicago accession Jemalong A17 and *nork* mutant TR25 containing *MtENOD11::GUS* (*6*) were used for transformations. The Medicago A17 line containing *ENOD11::GUS* was kindly provided by David Barker/Annemie Emons.*Sinorhizobium meliloti* 2011.pHC60 (*3*) was used to inoculate plants.

A. rhizogenes mediated transformation and RNAi

Agrobacterium strain MSU440 containing the pRi plasmid pRiA4 (*26*) was used to transform Medicago. The binary vectors were introduced into MSU440 by electrotransformation and grown for two days at 28^{0}C under kanamycin selection (50 µg/ml). *A. rhizogenes* mediated root transformation of 5 day old Medicago seedlings was performed according to Limpens *et al.* (*3*). *A. rhizogenes* mediated RNAi of *NORK* was performed as described in Limpens et al. (*3*).

Plant assays

Medicago seeds were surface sterilized by incubating for 10 min. in concentrated Sulfuric acid, 6x washing in sterile water, 10 min incubation in 4% hyper chlorite (commercial bleach) and 7x washing in sterile water and subsequently plated on Färhaeus medium (*3*). Seeds were vernalized for 1 day at 4^{0}C and germinated at 25^{0}C for 24 hours in darkness. For mass-inoculation with *S. meliloti* 2011.pHC60 composite Medicago plants were starved for nitrate for 3 days (22^{0}C; 16h light-8h darkness) on agra-perlite (Maasmond-Westland, The Netherlands) saturated with Färhaeus medium (without $Ca(NO3)_2$). Plants were inoculated with 1 ml culture of *S. meliloti* 2011.pHC60 (OD600: 0.1) per plant and grown for two weeks (22^{0}C; 16h light-8h darkness). Root hair deformation studies were performed with 10^{-9} M *S. meliloti* Nod factors added directly to transformed plants growing on BNM medium (*27*) with 1.2% agar and 0.1 µM AVG. 6 hours after treatment with 10^{-9} M *S. meliloti* Nod factors *A. rhizogenes* transformed roots were stained for *ENOD11::GUS* activity. Root hair deformations were checked 16h post inoculation after staining with 0.002% methylene blue. To examine cortical cell divisions *A. rhizogenes* transformed roots were grown on BNM medium and spot inoculated with ~0.3 µl *S. meliloti* 2011.pHC60 (OD600: 0.1).

Histochemical analysis and microscopy

Histochemical GUS staining was performed according to Jefferson *et al.* (*28*), with few modifications. Plant material was incubated in 0.05% (w/v) X-Gluc (Duchefa) in 0.1M sodium phosphate buffer (pH 7) with 3% sucrose, 5µM potassium-ferrocyadine and 5µM potassium. Roots were infiltrated for 30 min. under vacuum and further incubated at 37^{0}C.

For sectioning, roots or nodules (Fig. 2 and 3) were fixed for 1h in 2.5% glutaraldehyde buffered in 0.1M sodium phosphate buffer (pH 7), dehydrated in an alcohol series and embedded in Technovit 7100 (Heraeus Kulzer). 5 µm-thick sections were made using a Leica microtome, stained with 0.04% toluidine blue or 0.1% ruthemium red and mounted on glass slided with Euparal (Agar Scientific LTD.).

For electron microscopy, nodules were fixed for 3,5h in a mixture of 4% paraformaldehyde and 3% glutaraldehyde in 50 mM potassium phospate buffer, pH 7.4. The nodules were postfixed for 3h with 1% osmium tetroxide, dehydrated through an ethanol series and embedded in London Resin White. Ultrathin sections (60 nm) were obtained with a Reichert Untracuts Leica ultratome, stained with with 2% of uranil acetate and Reinolds lead citrate solution, and observed with a Philips EM208 electron microscope (Eindhoven, the Netherlands). For light microscopy semithin sections (1-0,6 mm) (Fig. 4 and 5) were stained with 1:1 mix of 1% toluidine blue and 1% methylene blue solution and embedded in Paraplast (EMS). Sections were viewed with a Nikon Optiphot-2 microscope. Images where processed electronically using Adobe Photoshop 6.0. Imaging of *Ds*RED1 or GFP fluorescence was done using the Leica MZIII fluorescence stereomicroscope and a Nikon Optiphot-2 coupled to a mercury-lamp.

RNA extraction and qPCR

Total RNA was extracted from un-inoculated roots, roots inoculated with *S. meliloti* 2011 48h dpi, root tips (excised ~3mm behind the tip), leaves, stem, flowers and 2-week-old nodules according to Pawlowski *et al.,* (*29*) followed by DNAseI (Promega) treatment. cDNA was made from 1 µg total RNA using the Taqman Gold RT-PCR kit (Perkin-

Elmer Applied Biosystems) in a total volume of 50 μl using the supplied hexamer primers. qPCR reactions were performed in triplo on 6,5 μl cDNA using the SYBR-GreenR PCR Master kit (Perkin-Elmer Applied Biosystems) (40 cycles of 95°C for 10 s, 60°C for 1 min) and real-time detection was performed on the ABI 7700 and analyzed using the GeneAmp 5700 SDS software (Perkin-Elmer Applied Biosystems). The specificity of the PCR amplification procedures was checked with a heat dissociation step (from 60°C-95°C) at the end of the run and by agarose gel electrophoresis. Results were standardized to the *MtACTIN2* expression levels. Primers used:

MtACTIN2: 5' TGGCATCACTCAGTACCTTTCAACAG 3' and 5' ACCCAAAGCATCAAATAATAAGTCAACC 3'

MtDMI-2: 5' TGGACCCCTTTTGAATGCCTATG 3' and 5' TCCACTCCAACTCTCCAATGCTTC 3'

In situ hybridization

Nodules were harvested 14 days post-inoculation and fixed in 4% paraformaldehyde supplemented with 0.25% gluteraldehyde in 10 mM sodium phosphate buffer (pH 7.4) for 3 h (*30*). Fixed nodules were dehydrated, by passing through a series of grade ethanol, and embedded into paraffin (Paraclean; Klinipath, Duiven, The Netherlands) by routine methods (*30*). Sections (7 μm) were dried on polylysine-coated slides at 37° C overnight, deparaffinized with xylene and rehydrated via a graded ethanol series. Hybridisation pre-treatment, hybridisation and washing were performed as described by Cox (*31*) and adapted by Van de Wiel (*30*). For preparing antisense *NORK* RNA probes the fragments 373-617 bp, 784-1039 bp, 1200-1453 bp, 1610-1864 bp and 1964-2219 bp within the *NORK* coding region, were PCR amplified and subcloned into a pGEM-t vector (Promega). An ApaI restriction site in the 3' end primer (see below) allowed the removal of polylinker sequences from the vector. Subsequently, the fragments were amplified by PCR using M13-forward and 5' end primers specific for the *NORK* fragments. The amplified fragments were used as substrate to synthesise antisense RNA probes with T7 RNA polymerase (Promega), in the presence of [^{35}S]-UTP (1000-1500 Ci mmol^{-1}, Amersham). For the hybridisation a mixture containing 2×10^6 cpm of each probe was used. After washing, the slides were coated with microautoradiography emulsion LM-1 (Amersham) and exposed for 3 weeks at 4° C. They were developed for 5 min in Kodak D-19 developer (East-man Kodak, Rochester, NY) and fixed in Kodak fixative. Sections were counterstained with toluidine blue and subsequently mounted. For imaging a Nikon (Tokyo, Japan) optiphot-2 bright field microscope was used. Primers used for *NORK* fragments (ApaI restriction-site underlined):

373-617 bp: 5' TCATGATGGAGTTACAAGTTATTA 3' and 5' GGGCCCTTTTTATTGCTTCTGTGG 3'

784-1039 bp: 5' GAGGACTTGGAAATTGAGGGAG 3' and 5' GGGCCCATGTTGGAGTTGAAGTT 3'

1200-1453 bp: 5' CTTTCTTGAACTAAATGGCACTGT 3' and 5' GGGCCCTTTTTGGTTGGTCTCTTCA 3'

1610-1864 bp : 5' ATCTTTCTTCCAATAATCTCAAGGG 3' and 5' GGGCCCTTGTTGTATCTTCGTCACTC 3'

1964-2219 bp: 5' CACTTTTGATTACTTTGGCTGTTG 3' and 5' GGGCCCTCTAGAGTGCCCCTGTAAAC 3'

References

1 Oldroyd GED: **Dissecting symbiosis: Development in Nod factor signal transduction.** *Ann Bot* 2001, **87**: 709-718.

2 Limpens E, Bisseling T: **Signaling in Symbiosis.** *Curr Opin Plant Biol* 2003, **6**: 343-350.

3 Limpens E, Franken C, Smit P, Willemse J, Bisseling T, Geurts R: **LysM domain receptor kinases regulating rhizobial Nod factor-induced infection.** *Science* 2003, **302**: 630-633.

4 Madsen EB, Madsen LH, Radutoiu S, Olbryt M, Rakwalska M, Szczyglowski K, Sato S, Kaneko T, Tabata S, Sandal N, Stougaard J: **A receptor kinase gene of the LysM type is involved in legume perception of rhizobial signals.** *Nature* 2003, **425**: 637-640.

5 Radutoiu S, Madsen LH, Madsen EB, Felle HH, Umehara Y, Gronlund M, Sato S, Nakamura Y, Tabata S, Sandal N, Stougaard J: **Plant recognition of symbiotic bacteria requires two LysM receptor-like kinases.** *Nature* 2003, **425**: 585-592.

6 Catoira R, Galera C, De Billy F, Penmetsa RV, Journet EP, Maillet F, Rosenberg C, Cook D, Gough C, Dénarié J: **Four genes of *Medicago truncatula* controling components of a Nod factor transduction pathway.** *Plant Cell* 2000, **12**: 1647-1666.

7 Endre G, Kereszt A, Kevei Z, Mihacea S, Kaló P, Kiss GB: **Cloning of a receptor kinase gene regulating symbiotic nodule development.** *Nature* 2002, **417**: 962-966.

8 Ané JM, Kiss GB, Riely BK, Penmetsa RV, Oldroyd GE, Ayax C, Levy J, Debellé F, Baek JM, Kaló P, Rosenberg C, Roe BA, Long SR, Dénarié J, Cook DR: ***Medicago truncatula DMI1* required for bacterial and fungal symbioses in legumes.** *Science* 2004, **303**: 1364-1367.

9 Levy J, Bres C, Geurts R, Chalhoub B, Kulikova O, Duc G, Journet EP, Ané JM, Lauber E, Bisseling T, Dénarié J, Rosenberg C, Debellé F: **A putative Ca2+ and calmodulin-dependent protein kinase required for bacterial and fungal symbioses.** *Science* 2004, **303**: 1361-1364.

10 Mitra RM, Gleason CA, Edwards A, Hadfield J, Downie JA, Oldroyd GE, Long SR: **A Ca2+/calmodulin-dependent protein kinase required for symbiotic nodule development: Gene identification by transcript-based cloning.** *Proc Natl Acad Sci USA* 2004, **101**: 4701-4705.

11 Wais RJ, Galera C, Oldroyd G, Catoira R, Penmetsa RV, Cook D, Gough C, Dénarié J, Long SR: **Genetic analysis of calcium spiking responses in nodulation mutants of *Medicago truncatula.*** *Proc Natl Acad Sci USA* 2000, **97**: 13407-13412.

12 Stracke S, Kistner C, Yoshida S, Mulder L, Sato S, Kaneko T, Tabata S, Sandal N, Stougaard J, Szczyglowski K, Parniske M: **A plant receptor-like kinase required for both bacterial and fungal symbiosis.** *Nature* 2002, **417**: 959-962.

13 Sharma SB, Signer ER: **Temporal and spatial regulation of the symbiotic genes of *Rhizobium meliloti* in planta revealed by transposon *Tn5-gusA*.** *Genes Dev* 1990, **4**: 344-356.

14 Schlaman HR, Horvath B, Vijgenboom E, Okker RJ, Lugtenberg BJ: **Suppression of nodulation gene expression in bacteroids of *Rhizobium leguminosarum biovar viciae.*** *J Bacteriol* 1991, **173**: 4277-4287.

15 Vasse J, de Billy F, Camut S, Truchet G: **Correlation between ultrastructural differentiation of bacteroids and nitrogen fixation in alfalfa nodules.** *J Bacteriol* 1990, **172**: 4295-4306.

16 Brewin NJ: **Development of the legume root nodule.** *Annu Rev Cell Biol* 1991, **7**: 191-226.

17 Chuang C, Meyerowitz M: **Specific and heritable genetic interference by double-stranded RNA in *Arabidopsis thaliana.*** *Proc Natl Acad Sci USA* 2000, **97**: 4985-4990.

18 Limpens E, Ramos J, Franken C, Raz V, Compaan B, Franssen H, Bisseling T, Geurts R: **RNA interference in *Agrobacterium rhizogenes* transformedroots of Arabidopsis and *Medicago truncatula*** *J Exp Bot* 2004, **55**: 983-992.

19 Roth LE, Stacey G: **Bacterium release into host cells of nitrogen-fixing soybean nodules: the symbiosome membrane comes from three sources.** *Eur J Cell Biol* 1989, **49**: 13-23.

20 Kijne JW: **The *Rhizobium* infection process.** In: Stacey G, Burris RH, Evans HJ, eds. *Biological Nitrogen Fixation*. New York: Chapman and Hall, 1992: 349-398.

21 Callaham DA, Torrey JG: **The structural basis for infection of root hairs of *Trifolium repens* by *Rhizobium.*** *Can J Bot* 1981, **59**: 1647-1664.

22 Rae AL, Bonfante-Fasolo P, Brewin NJ: **Structure and growth of infection threads in the legume symbiosis with *Rhizobium leguminosarum.*** *Plant J* 1992, **2**: 385-395.

23 Brewin NJ: **Tissue and cell invasion by *Rhizobium:* The structure and development of infection threads and symbiosomes.** In: Spaink HP, Kondorosi A, Hooykaas PJJ, eds. *The Rhizobiaceae*. Dordrecht: Kluwer Academic Publishers, 1998: 417-429.

24 Verma DP, Hong Z: **Biogenesis of the peribacteroid membrane in root nodules.** *Trends Microbiol* 1996, **4**: 364-368.

25 Yang Z: **Small GTPases: versatile signaling switches in plants.** *Plant Cell* 2002, **14** Suppl: S375-S388.

26 Sonti RV, Chiurazzi M, Wong D, Davies CS, Harlow GR, Mount DW, Signer ER: **Arabidopsis mutants deficient in T-DNA integration.** *Proc Natl Acad Sci USA* 1995, **92**: 11786-11790.

27 Ehrhardt DW, Atkinson EM, Long SR: **Depolarization of alfalfa root hair membrane potential by *Rhizobium meliloti* Nod factors.** *Science* 1992, **256**: 998-1000.

28 Jefferson AR, Kavanagh TA, Bevan MW: **Gus fusions: *β-glucuronidase* as a sensitive and versatile gene fusion marker in higher plants.** *EMBO J.* 1987, **6**: 3901-3907.

29 Pawlowski K, Kunze R, de Vries S, Bisseling T: **Isolation of total, poly(A) and polysomal RNA from plant tissues.** In: Gelvin, SB Schilperoort RA (eds) *Plant Molecular Biology Manual*. Kluwer Academic Publishers. Dordrecht 1994, pp D5 1-13.

30 Van De Wiel C, Norris JH, Bochenek B, Dickstein R, Bisseling T: **Nodulin gene expression and *ENOD2* localization in effective, nitrogen-fixing and ineffective, bacteria-free nodules of alfalfa.** *Plant Cell* 1990, **2**: 1009-1017.

31 Cox KH, Goldberg RB: **Analysis of plant gene expression.** In: *Plant Molecular Biology*: A practical approach, C.H. Shaw, ed. Oxford: IRL Press 1988, pp 1-34.

Chapter 7

Concluding Remarks

Rhizobial Nod factors are important signalling molecules that induce developmental processes leading to the formation of a nitrogen fixing root nodule and function as major host-specificity determinants in this symbiosis (Chapter 1). The major goal of the research described in this thesis, was to unravel the molecular basis of Nod factor perception. To achieve this we used a genetic approach in which we focussed on the pea *SYM2* gene, which was proposed to be involved in Nod factor perception (*1-4*). In the wild pea variety Afghanistan a $SYM2^A$ allele was identified, which controls rhizobial infection in a Nod factor structure dependent manner. Only *Rhizobium leguminosarum* bv *viciae* strains that contain a specific bacterial nodulation gene, *nodX*, are able to successfully infect $SYM2^A$ containing plants. *nodX* encodes an acetyl transferase, which specifically acetylates the reducing terminal sugar residue of pentameric Nod factors, suggesting that $SYM2^A$ is involved in recognizing these *nodX* modified Nod factors. However, positional cloning in pea is severely hampered because of its large genome size (~5000 Mb) and further it is difficult to transform this legume. Therefore we decided to adopt a synteny based positional cloning approach in the phylogenetically closely related model legume *Medicago truncatula* (Medicago) (*5*). We studied the level of microsynteny between pea and Medicago in the *SYM2* region (Chapter 2). A pea marker tightly linked to *SYM2* was identified by differential RNA display on near-isogenic pea lines and used to construct a BAC physical contig (~ 450 kb) in Medicago. From this region, eight gene-specific markers were generated to construct a comparative genetic map of the *SYM2* orthologous region in pea and Medicago. This allowed us to delimitate the *SYM2* orthologous region in Medicago to ~350 kb. The two genomic regions appeared to contain the same gene content, which supports the idea that Medicago can be used as an intergenomic cloning vehicle to clone pea genes.

We survey-sequenced the Medicago *SYM2* orthologous region to identify candidate genes that might be involved in Nod factor perception (Chapter 4). A total of 21 putative genes were identified and annotated based on sequence homologies and EST data. Strikingly, several genes encoding receptor-like proteins appeared to be present, including one gene homologous to the tobacco mosaic virus (TMV) resistance gene *N*, 7 LRR type of receptors homologous to *Cladosporium fulvum* resistance genes, and 7 LysM domain containing receptor-like kinases. To identify potential *SYM2* candidates we first selected those genes that were expressed in roots and root hairs, as *SYM2* appeared to be only essential in the root epidermis (*4*). Since *SYM2* represents a natural occurring allelic variation in pea, sequence analysis could not be used to identify *SYM2*. Instead we decided to examine which of the candidate genes in Medicago played a role in the rhizobial infection process, using a reverse genetics approach.

RNA interference as reverse genetics tool

Since its discovery, RNA interference (RNAi) has developed into a powerful tool to knock-down gene expression in order to study gene function. The most commonly applied way to trigger RNAi in plants is by stably transforming plants with gene-specific hairpin constructs (*6*). However, for plants that are difficult to transform or have (relatively) long regeneration times (e.g. Medicago), this is not always a feasible option. As an alternative we investigated whether *Agrobacterium rhizogenes* mediated root transformation could be used to trigger RNAi (Chapter 3). *A. rhizogenes* mediated root transformation is a commonly used (fast) method, especially in legumes, that generates adventitious genetically transformed roots at the site of inoculation. We show (Chapter 3) that *A. rhizogenes* mediated RNAi is a fast and efficient tool to knock-down genes in roots of both Medicago and Arabidopsis. Furthermore, we found that the silencing signal did not spread systemically to non-cotransformed roots and only inefficiently to the non-transgenic shoot. Similar observations were also made in *Lotus japonicus* (*7*). The lack of systemic transport to the non-cotransformed roots is most likely due to the suggested uni-directional transport of the silencing signal via the phloem (*8*). In the root epidermis we observed that RNAi was even triggered cell-autonomously, most likely due to the fact that these cells become symplastically isolated very early during development (*9*). These findings have serious implications for the correct interpretation of *A. rhizogenes* mediated RNAi experiments. *A. rhizogenes* mediated root transformation results in the formation of adventitious roots that are co-transformed with the gene of interest as well as roots lacking this gene. Furthermore, chimaeric roots can be formed, which most likely contain both co- and non co-transformed tissues. Especially in Medicago a high percentage of the newly formed roots (up to 50%) appeared to be chimaeric. Because of the apparent cell autonomous nature in the epidermis and lack of systemic spread of the silencing signal to non co-transformed roots it is important to identify those roots (and tissues) that are homogeneously co-transformed with the hairpin construct. For this purpose we developed the binary vector, pRedRoot, which allows the non-destructive selection of co-transformed roots (and tissues) based on *Ds*RED1 fluorescence. At the same time the lack of systemic spreading of the silencing signal could offer the opportunity to use tissue specific or inducible promoters to more specifically regulate RNAi. Furthermore, by targeting the Arabidopsis *KOJAK* gene (Chapter 3), involved in root hair development (*10,11*), we observed that RNAi can lead to phenotypes resembling weak alleles as a result of partial knock-down of the mRNA, which has also been reported for *A. tumefaciens* mediated RNAi (*6*). This could be exploited to analyse the function of genes with otherwise lethal knock-out phenotypes or could give additional insight into their function.

LysM domain receptor kinases controlling nodulation

We used *A. rhizogenes* mediated RNAi as reverse genetic tool to knock-down candidate genes from the Medicago *SYM2* orthologous region and examined their involvement in the rhizobial infection process (Chapter 4). The use of *Rhizobium* strains expressing *GFP* allowed us to visualize infection thread morphology. Efficient nodulation of pea $SYM2^A$ lines requires the presence of *R. leguminosarum* bv *viciae* Nod factors that are *nodX* acetylated at the reducing terminal C6-residue. At the reducing terminal residue in *Sinorhizobium meliloti* Nod factors a sulphate group is present, and it is absolutely required for the induction of most symbiotic responses in Medicago (*12*). However, a complete block of nodulation in pea $SYM2^A$ lines was only observed when in addition to the absence of *nodX*, also *nodE* was mutated. Therefore we also used a *nodFE* mutated *S. meliloti* strain to screen for infection phenotypes in Medicago. On wild-type plants *S. meliloti* 2011-*ΔnodFE* is able to nodulate as efficiently as the wild-type strain. Targeting of 11 candidate genes in Medicago by *A. rhizogenes* mediated RNAi resulted in an infection phenotype with two genes, *LYK3* and *LYK4*, both encoding LysM domain containing receptor-like kinases (LYKs)(Chapter 4). Knock-down of *LYK3* caused a severe reduction in nodulation efficiency, specifically when plants were inoculated with *S. meliloti* 2011-*ΔnodFE*. The vast majority of the infection threads were blocked at the micro-colony stage. Knock-down of *LYK4* did not clearly affect nodulation, but did affect infection thread morphology. Most infection threads that formed on *LYK4* knock-down roots contained sac-like structures along their length. As infection threads are thought to be tip-growing structures this is most likely due to the temporal loss-and-regain of polar growth (*13*). The fact that *LYK3* controls rhizobial infection in a similar Nod factor structure dependent manner as the pea $SYM2^A$ gene and is located in a similar genomic environment, suggests that allelic variations in a pea *LYK3/4* homolog causes the Nod factor structure dependent *SYM2* phenotype in pea. However, characterization of these allelic variants will be required to show that this is indeed the case. The *LYK3* and *LYK4* genes are composed of 12 exons and encode proteins containing a serine/threonine kinase domain with two extracellular LysM domains. LysM domains were originally identified in bacterial lysins and enzymes associated with bacterial cell walls, and are thought to have a general peptidoglycan binding function (*14*). In eukaryotes LysM domain have also been found in some chitinases (*15*). The structural homology between chitin, peptidoglycan subunits and the *N*-acetylglucosamine backbone of the Nod factor supports the hypothesis that *LYK3/4* indeed encode Nod factor receptors. However, it remains to be shown whether, and how, Nod factors and LysM receptor kinases interact physically. Two recent studies in *Lotus japonicus* (Lotus) also identified two LysM domain containing receptor-like kinases involved in Nod factor perception (*16,17*). Plants with mutations in these genes, *Nod Factor Receptor 1* (*NFR1)* and *NFR5*, do not show any symbiotic response to Nod factor treatment or rhizobia. *NFR5* is composed of a single exon and encodes a receptor-like protein with three extracellular LysM domains and an intracellular kinase domain that typically lacks an

activation loop. *NFR5* was shown to be the ortholog of the pea *SYM10* gene (*16,18*), and in Medicago the *nod factor perception (nfp*) mutant (*19*) represents the Medicago ortholog of *NFR5* (Gough and Geurts, unpublished). Based on similarities in sequence and genomic environment (Fig. 1) *NFR1* most likely represents the *Lotus* ortholog of *LYK3.* However, the phenotype observed in *nfr1* mutants markedly differs from that of *LYK3* knock-down plants. The block of all Nod factor induced responses in both the *nfr1* and *nfr5* mutants clearly shows that they are required during the earliest stages of nodulation and suggests that they function as a heterodimer. LYK3/4 appears to play a role specifically in the infection process, since early responses such as root hair deformation and curling still take place. However, a possible explanation for this difference could be that residual LYK3 protein is sufficient to induce some of these early Nod factor induced responses, since *LYK3* mRNA could still be detected in the knock-down lines. Alternatively, since extensive genetic screens in both pea and Medicago have never identified mutants blocked for all Nod factor induced responses other than the *NFR5* orthologs, the Nod factor perception mechanism may have diversified between Lotus and Medicago (and pea), putting a more stringent demand on Nod factor structure to allow bacterial entry in the latter two. This might reflect a difference in the formation of determinate (Lotus) versus indeterminate nodules (pea and Medicago). Studies on the nodulation efficiency of rhizobial mutants producing altered Nod factors in pea, vetch, *Medicago sativa* and Medicago led to a model proposing two types of Nod factor receptors: a signalling receptor with less stringent structural requirements, and an entry receptor with stringent requirements to specifically control bacterial entry (*20*). The phenotypes of the Medicago *nfp* mutant and *LYK3/4* knock-out lines are consistent with such a model; with NFP representing the signalling receptor and LYK3/4 controlling bacterial entry. However, the fact that knock-down of *LYK3/4* still allows wild-type *S. meliloti* to the form infection threads suggests that either other *LYK* genes are involved that have a higher affinity for wild type C16:2 acyl chain containing Nod factors or that LYK3/4 has a lower affinity for C18:1 Nod factors (*nodFE* mutant) by which residual protein in the knock-down lines still allows infection thread formation by wild type bacteria but not by *S. meliloti* 2011-*ΔnodFE*. Characterization of true *LYK3* and *LYK4* knock-outs will help to distinguish between these possibilities. Nod factors are major host specificity determinants and phylogenetically closely related plants can differ substantially in their Nod factor structural requirement, which suggests that recognition specificity evolved rapidly. The observation that *LYK* genes appear to be located in clusters in both Medicago and Lotus (Fig. 1) could reflect this rapid evolution of Nod factor specificity. A similar rapid evolution has been reported for resistance genes, which are also often clustered in tandem arrays. Such clusters show a high frequent rearrangements and recombinations between diversified copies is thought to drive the fast generation of novel recognition specificities (*21*).

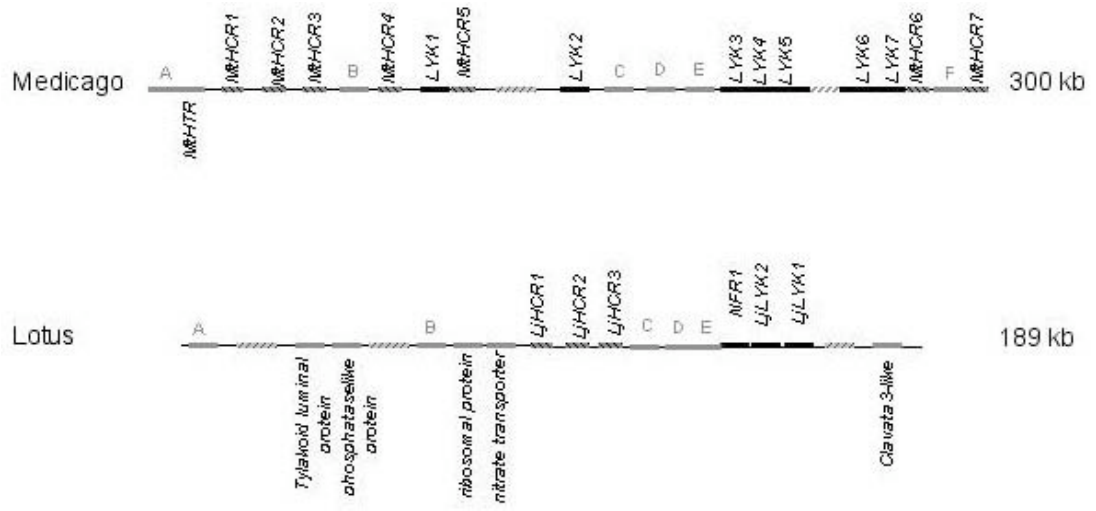

Figure 1. Comparison of the genomic regions around *LYK3* and *NFR1* in Medicago (Mt) and Lotus (Lj), respectively. Annotation of genes is based on sequence information from the Medicago *SYM2* orthologous region as described in Chapter 4, and Lotus TAC clones: LjT05B16, LjT02D13 and LjT211O12 (*17)*, using different gene annotation programs (http://www.arabidopsis.org/links/gene_id.html) and BLAST analysis. Homologous genes in the two genomic regions are placed above the schematic representations. *HCR* = homolog of tomato *Cladosporium fulvum* resistance gene; *LYK* = LysM domain receptor kinase; *NFR1* = *NOD FACTOR RECEPTOR 1* (*17*), the putative ortholog of *LYK3*; *HTR* = homolog of *TMV* resistance gene *N* of tobacco; A = gene encoding a protein homologous to a ubiquitin carboxyl-terminal hydrolase; C = gene homologous to *UFD1* of Arabidopsis; B,D,E,F = genes of unknown function. Putative retroelements are shown as a shaded box.

Genetic studies have shown that part of the signaling pathway activated by rhizobia (Fig. 2, Chapter 1) is shared in the establishment of the more ancient arbuscular mycorrhizal interaction (*22,23*). This suggests that arbuscular mycorrhizal (AM) fungi secrete molecules that activate this common pathway. This signal molecule, the so-called Myc factor, has not yet been characterized, but recent studies demonstrate that AM fungi indeed produce a diffusible signal molecule that can induce responses in the legume host (*24*). It is tempting to speculate that LysM domain receptor kinases, other than those specific for the *Rhizobium* interaction, could play a role in recognizing this fungal factor.

The Medicago *SYM2* orthologous region contains 7 *LYK* genes, but *A. rhizogenes* mediated RNAi only indicated a function in symbiosis for *LYK3* and *LYK4*, both of which are highly homologous in their extracellular domains. Expression analysis revealed that *LYK1* is exclusively expressed in shoots and *LYK6* and *LYK7* are expressed in both roots and shoots (Chapter 4). These genes most likely have a non-symbiotic function, either in plant development or disease resistance, and it is tempting to speculate that Nod factor-like molecules play a role in these processes. The hypothesis that certain *LYK* genes are involved in non-symbiotic processes is further supported by the fact that LysM domain containing receptor-like kinases are also present in non-legume species such as Arabidopsis, which besides being unable to establish a nitrogen fixing symbiosis, is also unable to establish a symbiotic interaction with arbuscular mycorrhiza.

The Nod factor-signalling pathway

Genetic studies in pea, Lotus and Medicago have identified a small, but similar set of genes that control Nod factor signal transduction (*18,23,25,26*). These genes appear to be symbiosis-specific and genetically dissect the Nod factor-signalling pathway as summarized in Figure 2 of Chapter 1. Several of these genes have recently been cloned and it is probable that the remaining genes will be cloned in the near future. *DOES NOT MAKE INFECTIONS 1, DMI1,* encodes a protein with homology to a cation channel (*27*); *NODULATION RECEPTOR KINASE, NORK,* encodes a receptor-like kinase with an extracellular domain containing three leucine rich repeats (LRRs) (*28*); and *DMI3* was shown to encode a calcium and calmodulin dependent kinase (*29*). Based on their mutant phenotypes and sequence homologies a model can be made for the mode of action of these components in Nod factor signalling in Medicago. Plant receptor kinases are usually part of protein complexes (*30,31*). The organization of such signalling complexes is dynamic and complexes are often locally assembled in response to signal input (*32*). It can therefore be speculated that the LysM domain receptor kinases, NFP and LYK3/4, form complexes with or activate a complex containing DMI1 and NORK, since *dmi1* and *nork* mutants have the same phenotype. This activation in turn induces cytoplasmic calcium oscillations as well as other responses. As discussed above, it is possible that LYK3/4 play a role in Nod factor perception specifically inducing infection thread formation and growth. The induced calcium “signatures” are in turn perceived and interpreted by DMI3, which is required for further signal transduction. From studies in the animal field, especially neuronal development, it is known that calcium/calmodulin dependent kinases (e.g. CAMKII) play a key role in many cellular processes (*33*). Especially the activation dependent subcellular targeting of CAMKII appears to play a pivotal role in the localized formation and regulation of receptor complexes in the neuronal synaps (*34,35*). It is tempting to speculate that DMI3 also plays such a dynamic role in the establishment or regulation of the early receptor complexes involved in Nod factor signal transduction, which also could be highly localized. Misregulation of these complexes could be an explanation for the observed increase in Nod factor sensitivity of the calcium spiking response in the *dmi3* mutant (*36*). Pharmacological studies have further implied the involvement of phospholipid based signalling (e.g. phosphatidic acid) at a very early step in the Nod factor-signalling pathway (*37*). Phosphatidic acid represents a novel second messenger in plant cells (*38*). Phospholipids also play important roles in controlling vesicle transport to specific domains in the plasmamembrane. The formation of specific lipid microdomains at the membrane could be involved in the localized organization and regulation of receptor complexes and their cross-talk (*39*). This model remains speculative. Identification of interacting partners of the Nod factor signalling proteins and studies on their dynamic subcellular localization will be required to show how these different components work together to control the different steps of nodulation.

Intercellular communication during nodulation

A successful nitrogen-fixing symbiosis requires a tight coordination of the infection process by the bacteria, which is initiated in the root hairs, and the formation of the nodule organ from root cortical cells. In all symbiotic legume mutants characterized so far, the loss of (all) Nod factor responses in the epidermis is always correlated with the loss of mitotic activation of the cortical cells, which led to the hypothesis that secondary signals are generated upon Nod factor perception in the epidermis and these subsequently trigger cortical cell divisions (26,40,41; Chapter 1). This would imply that a legume mutant only able to recognize Nod factors in its epidermis would be able to respond with cortical cell divisions despite the lack of a functional Nod factor perception and transduction machinery in the cortical cells. To test this we introduced the essential Nod factor-signalling component *NORK* under the control of a root hair specific promoter into the *nork* mutant background (Chapter 5). This showed that the presence of *NORK* in the epidermis is sufficient to trigger Nod factor induced responses in the inner cell layers (Chapter 5). It implies that cortical cell divisions are induced by Nod factors in a non cell-autonomous manner. Such non cell-autonomous signalling requires an intercellular communication between the epidermis and the cortical cells. Intercellular communication is a common mechanism used to coordinate developmental processes. It involves the transport of signals, such as small peptides, phytohormones, transcription factors and RNA, either via the extracellular space or through plasmodesmata (*42-44*). Since NORK is an essential component of the Nod factor-signalling pathway, our data imply that upon Nod factor perception in the epidermis secondary signals are generated, which subsequently trigger responses in the inner cell layers. This seems to represent the molecular mechanism underlying the strict coupling of the two spatially separated responses. The generation of secondary signals upon Nod factor perception is in agreement with the observation that Nod factors are immobile in cell walls (*45*). The involvement of secondary signals was also suggested by studies on Nod factor induced cortical cell divisions and early nodulin expression in *Vicia sativa* (*46*). Here, external Nod factor application induced the mitotic reactivation of cortical cells and expression of *ENOD12,* but did not induce *ENOD5*. *ENOD5* was only induced in cells that are in direct contact with the Nod factor, e.g. infected cells, whereas *ENOD12* was induced in primordial cells without direct contact with Nod factors. Further, the generation and long distance transport of secondary signals has been indicated by mutants that are impaired in the auto-regulation of nodule numbers (*47-49*). Physiological studies with such mutants showed that autoregulation involves a long distance communication between shoot and root. This was based on grafting studies showing that in several cases a mutated shoot grafted on a wild type root causes hypernodulation of this wild type root. This shoot-control of nodule number was shown to require an LRR receptor-like kinase, which is most likely involved in perception of a signal from the root and generation of an autoregulation signal by which nodulation is stopped. The identified LRR receptor-like kinase shows a striking homology to CLAVATA1, which controls shoot apical meristem

organization in response to the small peptide CLAVATA3 (*50*). Furthermore, several other receptors involved in the perception of small peptides, such as the systemin receptor SR160/BRI1 (*44*) and the phytosulfokine receptor PSKR (*51*), show a similar protein structure. This might suggest that small peptides are involved in the long distance communication between shoot and root to control nodule numbers. It is conceivable that the autoregulation signals affect components of the Nod factor-signalling pathway, which would bring these two fascinating areas together. Which molecules are involved in the different intercellular communication steps during nodulation remains to be elucidated.

Nod factor signalling in the later steps of nodulation

The earlier discussed Nod factor signalling genes have been identified in genetic screens that searched for loss-of-nodulation mutants, and as a result all the characterized mutant alleles show a block of nodulation at the initial stage. However, several observations suggest that the Nod factor perception and transduction machinery also plays a role in the later steps of nodule development. The effect of *LYK3/4* knock-down (Chapter 4) and inoculation with rhizobial strains producing aberrant Nod factors (*18,20*; Chapter 4) on infection thread growth, shows that Nod factor perception and signalling plays a role during infection thread growth in the epidermis. Furthermore, it was shown that the bacterial *nod* genes -involved in Nod factor biosynthesis- remain active during infection thread growth in the nodule primordium and in the infection zone of the nodule, where bacteria are released from the infection threads into the plant host cells (*52,53*). This suggests that Nod factor perception and signalling also plays a role in the nodule, which is supported by the fact that several of the Nod factor-signalling genes, e.g. *LYK3* and *DMI3* in Medicago and *SYM10* in pea, are transcribed in the nodule (*16,29*; Chapter 4). If Nod factor perception and signalling would occur in the nodule, we hypothesized that expression of the Nod factor signalling genes would coincide with the place where Nod factors are produced. By studying the expression profile of the essential Nod factor-signalling component *NORK*, we showed that the region where *NORK* is highly expressed coincides with the place where the rhizobial *nod* genes are active in the distal part of the infection zone of the nodule (Chapter 6). This is the place where the bacteria are released from the infection threads. By mimicking allelic series via RNAi and by expression of *NORK* under the control of the *CaMV* 35S promoter in the mutant background we showed that insufficient *NORK* expression levels impair the release of bacteria from the infection threads and cause sustained growth of these threads (Chapter 6). These data led to the hypothesis that sustained infection thread growth and suppressed release of bacteria are interlinked processes and that Nod factor signalling involving high threshold levels of NORK is essential in the switch from infection thread growth to release of bacteria in the nodule. The underlying molecular mechanism of this switch is unknown. However, it is likely that cytoskeletal rearrangements and targeted vesicle transport play a role in this process, as release of bacteria from the infection thread seems to involve a change in the kind of vesicles,

and their cargo, that fuse with the tip of the infection thread (*54*). The observation that redirecting and sustaining polar growth of root hairs in response to Nod factors is impaired in the *NORK* knock-out mutants supports the idea that NORK facilitates cytoskeletal re-organization and vesicle transport (*23*). As small GTPases (e.g. ROPs) are known to be key regulators of the cytoskeletal organization and vesicular transport (*55)*), these might represent likely downstream targets of Nod factor signaling via NORK. Whether Nod factor perception and signalling plays additional roles in the nodule remains to be determined.

Since the start of this thesis research several of the Nod factor signaling genes that were identified genetically have now been cloned. On one hand this has provided first insight in the molecules that play key regulatory roles in symbiosis but additionally they provide the toolbox to further unravel the mechanism controlling the *Rhizobium*-legume symbiosis. Examples of such research are given in chapters 5 and 6, where we addressed the question how events at spatially separate places can be coordinated and study the role of Nod factor signaling in nodules, respectively. It seems probable that the Nod factor signaling proteins activate modules/networks that are derived from non-symbiotic processes. Examples include those controlling vesicle targeting and cytoskeletal organization as discussed in chapter 6. Also the identification of nodulation mutants that show pleiotropic effects, such as the *har1* and *crinkle* mutants in Lotus (*56-58*) and the *sunn* and *sickle* mutants in Medicago (*59,60*), support the idea that the nodulation process is integrated into non-symbiotic networks. How the non-symbiotic networks are modified and when and where they are activated by Nod factor signaling proteins will be an interesting and challenging area to study in the future.

References

1 Lie TA: **Host genes in Pisum sativum L. conferring resistance to European *Rhizobium leguminosarum* strains.** *Plant Soil* 1984, **82**: 462-465.

2 Firmin JL, Wilson KE, Carlson RW, Davies AE, Downie J: **Resistance to nodulation of c.v. Afghanistan peas is overcome by *nodX*, which mediates an *O*-acetylation of the *Rhizobium leguminosarum* lipo-oligosaccharide nodulation factor.** *Mol Microbiol* 1993, **10**: 351-360.

3 Kozik A, Heidstra R, Horvath B, Kulikova O, Tikhonovich I, Ellis THN, Van Kammen A, Bisseling T: **Pea lines carrying *sym1* or *sym2* can be nodulated by *Rhizobium* strains containing *nodX*; *sym1* and *sym2* are allelic.** *Plant Sci* 1995, **108**: 41-49.

4 Geurts R, Heidstra R, Hadri AE, Downie A, Franssen H, Van Kammen A, Bisseling T: ***Sym2* of *Pisum sativum* is involved in a Nod factor perception mechanism that controls the infection process in the epidermis.** *Plant Physiol* 1997, **115**: 351-359.

5 Cook DR: ***Medicago truncatula* – a model in the making!** *Curr Opin Plant Biol* 1999, **2**:301-304.

6 Chuang C, Meyerowitz M: **Specific and heritable genetic interference by double-stranded RNA in *Arabidopsis thaliana.*** *Proc Natl Acad Sci USA* 2000, **97**: 4985-4990.

7 Kumagai H, Kouchi H: **Gene silencing by expression of hairpin RNA in *Lotus japonicus* roots and root nodules.** *Mol Plant-Microbe Interact* 2003, **8**: 663-668.

8 Palauqui J-C, Elmayan T, Pollien JM, Vaucheret H: **Systemic acquired silencing: Transgene-specific post-transcriptional silencing is transmitted by grafting from silenced stocks to non-silenced scions.** *EMBO J* 1997, **16**: 4738-4745.

9 Duckett CM, Oparka KJ. Prior DAM, Dolan L, Roberts K: **Dye-coupling in the root epidermis of *Arabidopsis* is progressively reduced during development.** *Development* 1994, **120**: 3247-3255.

10 Favery B, Ryan E, Foreman J, Linstead P, Boudonck K, Steer M, Shaw P, Dolan L: ***KOJAK* encodes a cellulose synthase-like protein required for root hair cell morphogenesis in Arabidopsis.** *Genes and Development* 2001, **15**: 79-89.

11 Wang X, Cnops G, Vanderhaegen R, De Block S, Van Montagu M, Van Lijsebettens M: ***AtCSLD3*, a cellulose synthase-like gene important for root hair growth in Arabidopsis.** *Plant Physiol* 2001, **126**: 575-586.

12 Gressent F, Drouillard S, Mantegazza N, Samain E, Geremia RA, Canut H, Niebel A, Driguez H, Ranjeva R, Cullimore J, Bono JJ: **Ligand specifictiy of a high-affinity binding site for lipo-oligosaccharidic Nod factors in *Medicago* cell suspension cultures.** *Proc Natl Acad Sci USA* 1999, **96**: 4704-4709.

13 De Ruijter NCA, Rook MB, Bisseling T, Emons AMC: **Lipochito-oligosaccharides re-initiate root hair tip growth in *Vicia sativa* with high calcium and spectrin-like antigen at the tip.** *Plant J* 1998, **13**: 341-350.

14 Bateman A, Bycroft M: **The structure of a LysM domain from *E. coli* membrane-bound lytic murein transglycosylase D (MltD).** *J Mol Biol* 2000, **299**: 1113-1119.

15 Amon P, Haas E, Sumper M: **The sex-inducing pheromone and wounding trigger the same set of genes in the multicellular green alga *Volvox*.** *Plant Cell* 1998, **10**: 781-789.

16 Madsen EB, Madsen LH, Radutoiu S, Olbryt M, Rakwalska M, Szczyglowski K, Sato S, Kaneko T, Tabata S, Sandal N, Stougaard J: **A receptor kinase gene of the LysM type is involved in legume perception of rhizobial signals.** *Nature* 2003, **425**: 637-640.

17 Radutoiu S, Madsen LH, Madsen EB, Felle HH, Umehara Y, Gronlund M, Sato S, Nakamura Y, Tabata S, Sandal N, Stougaard J: **Plant recognition of symbiotic bacteria requires two LysM receptor-like kinases.** *Nature* 2003, **425**: 585-592.

18 Walker SA, Viprey V, Downie JA: **Dissection of nodulation signaling using pea mutants defective for calcium spiking induced by Nod factors and chitin oligomers.** *Proc Natl Acad Sci USA* 2000, **97**: 13413-13418.

19 Amor BB, Shaw SL, Oldroyd GE, Maillet F, Penmetsa RV, Cook D, Long SR, Dénarié J, Gough C: **The *NFP* locus of *Medicago truncatula* controls an early step of Nod factor signal transduction upstream of a rapid calcium flux and root hair deformation.** *Plant J* 2003, **34**: 495-506.

20 Ardourel M, Demont N, Debellé F, Maillet G, De Billy F, Promé JC, Dénarié J, Truchet G: ***Rhizobium meliloti*** **lipoligosaccharide nodulation factors: different structural requirements for bacterial entry into target root hair cells and induction of plant symbiotic developmental responses.** *Plant Cell* 1994, **6**: 1357-1347.

21 Parniske M, Hammond-Kosack KE, Golstein C, Thomas CM, Jones DA, Harrison K, Wulff BB, Jones JD: **Novel disease resistance specificities result from sequence exchange between tandemly repeated genes at the *Cf-4/9* locus of tomato.** *Cell* 1997, **91**: 821-832.

22 Albrecht C, Geurts R, Bisseling T: **Legume nodulation and mycorrhizae formation; two extremes in host specificity meet.** *EMBO J* 1998, **18**: 281-288.

23 Catoira R, Galera C, De Billy F, Penmetsa RV, Journet EP, Maillet F, Rosenberg C, Cook D, Gough C, Dénarié J: **Four genes of *Medicago truncatula* controling components of a Nod factor transduction pathway.** *Plant Cell* 2000, **12**: 1647-1666.

24 Kosuta S, Chabaud M, Lougnon G, Gough C, Dénarié J, Barker DG, Bécard G: **A diffusible factor from arbuscular mycorrhizal fungi induces symbiosis-specific *MtENOD11* expression in root of *Medicago truncatula*.** *Plant Physiol* 2003, **131**: 952-962.

25 Wais RJ, Galera C, Oldroyd G, Catoira R, Penmetsa RV, Cook D, Gough C, Dénarié J, Long SR: **Genetic analysis of calcium spiking responses in nodulation mutants of *Medicago truncatula.*** *Proc Natl Acad Sci USA* 2000, **97**: 13407-13412.

26 Stougaard J: **Genetics and genomics of root symbiosis.** *Curr Opin Plant Biol* 2001, **4**:328-335.

27 Ané JM, Kiss GB, Riely BK, Penmetsa RV, Oldroyd GE, Ayax C, Levy J, Debellé F, Baek JM, Kaló P, Rosenberg C, Roe BA, Long SR, Dénarié J, Cook DR: ***Medicago truncatula DMI1*** **required for bacterial and fungal symbioses in legumes.** *Science* 2004, **303**:1364-1367.

28 Endre G, Kereszt A, Kevei Z, Mihacea S, Kaló P, Kiss GB: **Cloning of a receptor kinase gene regulating symbiotic nodule development.** *Nature* 2002, **417**: 962-966.

29 Levy J, Bres C, Geurts R, Chalhoub B, Kulikova O, Duc G, Journet EP, Ané JM, Lauber E, Bisseling T, Dénarié J, Rosenberg C, Debellé F: **A putative Ca2+ and calmodulin-dependent protein kinase required for bacterial and fungal symbioses.** *Science* 2004, **303**: 1361-1364.

30 Becraft PW: **Receptor kinase signaling in plant development.** *Annu Rev Cell Dev Biol* 2002 **18**: 163-192.

31 Tichtinsky G, Vanoosthuyse V, Cock JM, Gaude T: **Making inroads into plant receptor kinase signalling pathways.** Trends Plant Sci 2003, **8**: 231-237.

32 Jordan JD, Landau EM, Iyengar R: **Signaling networks: the origins of cellular multitasking.** *Cell* 2000, **103**: 193-200.

33 Hudmon A, Schulman H: **Neuronal Ca2+/calmodulin-dependent protein kinase II: the role of structure and autoregulation in cellular function.** *Ann Rev Biochem* 2002, **71**: 473-510.

34 Fox K: **Synaptic plasticity: the subcellular location of CaMKII controls plasticity.** *Curr Biol* 2003, **13**: R143-145.

35 Colbran RJ: **Targeting of calcium/calmodulin-dependent protein kinase II**. *Biochem J* 2004, **378**: 1-16.

36 Oldroyd GE, Mitra RM, Wais RJ, Long SR: **Evidence for structurally specific negative feedback in the Nod factor signal transduction pathway.** *Plant J* 2001, **28**: 191-199.

37 Den Hartog M, Musgrave A, Munnik T: **Nod factor-induced phosphatidic acid and diacylglycerol pyrophosphate formation: A role for phospholipase C and D in root hair deformation.** *Plant J* 2001, **25**: 55-65.

38 Munnik T: **Phosphatidic acid: an emerging plant lipid second messenger.** *Trends Plant Sci* 2001, **6**: 227-233.

39 Hur EM, Park YS, Lee BD, Jang IH, Kim HS, Kim TD, Suh PG, Ryu SH, Kim KT: **Sensitization of epidermal growth factor-induced signaling by bradykinin is mediated by c-Src. Implications for a role of lipid microdomains.** J Biol Chem 2004, **279**: 5852-5860.

40 Cooper JB, Long SR: **Morphogenetic Rescue of *Rhizobium meliloti* Nodulation Mutants by trans-Zeatin Secretion.** *Plant Cell.* 1994, **6**: 215-225.

41 Tsyganov VE, Voroshilova BA, Priefer UB, Borisov AY, Tikhonovich IA: **Genetic dissection of the initiation of the infection process and nodule tissue development in the *Rhizobium*-pea (*Pisum sativum* L.) symbiosis.** *Ann Bot* 2002, **89**: 357-366.

42 Ruiz-Medrano R, Xoconostle-Cazares B, Lucas WJ: **The phloem as a conduit for inter-organ communication.** *Curr Opin Plant Biol* 2001, **4**: 202-209.

43 Haywood V, Kragler F, Lucas WJ: **Plasmodesmata: pathways for protein and ribonucleoprotein signalling.** *Plant Cell* 2002, **14** (suppl): S303-S325.

44 Ryan CA, Pearce G, Scheer J, Moura DS: **Peptide hormones.** *Plant Cell* 2002, **14** (suppl): S251-S264.

45 Goedhardt J, Hink MA, Visser AJ, Bisseling T, Gadella TW jr: ***In vivo* fluorescence correlation microscopy (FCM) reveals accumulation and immobilization of Nod factors in root hair cell walls.** *Plant J* 2000, **21**: 109-119.

46 Vijn I, Yang WC, Pallisgård N, Østergaard EJ, Van Kammen A, Bisseling T: ***VsENOD5*, *VsENOD12* and *VsENOD40* expression during *Rhizobium* induced nodule formation on *Vicia sativa* roots. *Plant* Mol *Biol* 1995, **28**: 1111-1119.

47 Krusell L, Madsen LH, Sato S, Aubert G, Genua A, Szczyglowski K, Duc G, Kaneko T, Tabata S, de Bruijn F, Pajuelo E, Sandal N, Stougaard J**: Shoot control of root development and nodulation is mediated by a receptor-like kinase.** *Nature* 2002, **420**: 422-426.

48 Nishimura R, Hayashi M, Wu G-J, Kouchi H, Imaizumi-Anraku H, Murakami Y, Kawasaki S, Akao S, Ohmori M, Nagasawa M, Harada K, Kawaguchi M: ***HAR1* mediates systemic regulation of symbiotic organ development.** *Nature* 2002, **420**: 426-429.

49 Searle IR, Men AE, Laniya TS, Buzas DM, Iturbe-Ormaetxe I, Carroll BJ, Gresshoff PM: **Long-distance signaling in nodulation directed by a *CLAVATA1*-like receptor kinase.** *Science* 2003, **299**: 109-112.

50 Clark SE: **Cell signalling at the shoot meristem.** *Natl Rev Mol Cell Biol* 2001, **2**: 276-284.

51 Matsubayashi Y, Ogawa M, Morita A, Sakagami Y: **An LRR receptor kinase involved in perception of a peptide plant hormone, phytosulfokine.** *Science* 2002, **296**:1470-2.

52 Sharma SB, Signer ER: **Temporal and spatial regulation of the symbiotic genes of *Rhizobium meliloti* in planta revealed by transposon *Tn5-gusA*.** *Genes Dev* 1990, **4**: 344-356.

53 Schlaman HR, Horvath B, Vijgenboom E, Okker RJ, Lugtenberg BJ: **Suppression of nodulation gene expression in bacteroids of *Rhizobium leguminosarum biovar viciae.*** *J Bacteriol* 1991, **173**: 4277-4287.

54 Brewin NJ: **Tissue and cell invasion by *Rhizobium:* The structure and development of infection threads and symbiosomes.** In: Spaink HP, Kondorosi A, Hooykaas PJJ, eds. *The Rhizobiaceae*. Dordrecht: Kluwer Academic Publishers, 1998: 417-429.

55 Yang Z: **Small GTPases: versatile signaling switches in plants.** *Plant Cell* 2002, **14** Suppl: S375-S388.

56 Wopereis J, Pajuelo E, Dazzo FB, Jiang Q, Gresshoff PM, de Bruijn FJ, Stougaard J, Szczyglowski K: **Short root mutant of *Lotus japonicus* with a dramatically altered symbiotic phenotype.** *Plant J* 2000, **23**: 97-114.

57 Nishimura R, Hayashi M, Wu G-J, Kouchi H, Imaizumi-Anraku H, Murakami Y, Kawasaki S, Akao S, Ohmori M, Nagasawa M, Harada K, Kawaguchi M: ***HAR1* mediates systemic regulation of symbiotic organ development.** *Nature* 2002, **420**: 426-429.

58 Tansengco ML, Hayashi M, Kawaguchi M, Imaizumi-Anraku H, Murooka Y: ***Crinkle*, a novel symbiotic mutant that affects the infection thread growth and alters the root hair, trichome, and seed development in *Lotus japonicus*.** *Plant Physiol* 2003, **131**: 1054-1063.

59 Penmetsa RV, Cook DR: **A legume ethylene-insensitive mutant hyperinfected by its rhizobial symbiont.** *Science* 1997, **275**: 527-530.

60 Penmetsa RV, Frugoli JA, Smith LS, Long SR, Cook DR: **Dual genetic pathways controlling nodule number in Medicago truncatula.** *Plant Physiol* 2003, **131**: 998-1008.

Nederlandse Samenvatting

Vlinderbloemige planten, zoals erwt, soja, boon en klaver, zijn in staat een symbiontische interactie aan te gaan met stikstofbindende *Rhizobium* bacteriën. Deze interactie leidt tot de ontwikkeling van een compleet nieuw orgaan, de wortelknol, waar de bacteriën in gastheercellen van de plant gehuisvest worden en de juiste omstandigheden vinden om atmosferische stikstof om te zetten in ammonia. Deze gebonden vorm van stikstof kan vervolgens gebruikt worden door de plant, die op zijn beurt koolhydraten levert aan de bacterie. Stikstof is een essentieel element van bijna alle bouwstenen van het leven (DNA, RNA en eiwitten) en de symbiose met *Rhizobium* bacteriën stelt vlinderbloemige planten in staat om te groeien op grond waarin weinig tot geen gebonden stikstof aanwezig is zonder dat extra bemest dient te worden. Vanuit landbouwkundig en ecologisch oogpunt is de *Rhizobium*-symbiose dus een zeer belangrijke interactie.

De vorming van een functionele wortelknol kan grofweg verdeeld worden in twee processen: (1) de ontwikkeling van het knol orgaan door het herprogrammeren van de ontwikkeling van corticale cellen in de wortel en (2) het binnendringen van de bacteriën in de gastheerplant via infectiedraden (het infectieproces). Zodra plant en bacterie elkaar herkennen, hecht de bacterie zich aan een wortelhaar waarna deze zich om de bacterie heen krult en de bacterie insluit. Vanuit de zo ontstane afgesloten holte wordt een buisvormige structuur aangelegd, de infectiedraad, waardoorheen de bacteriën naar binnen groeien richting de cortex. Voordat de infectiedraad de cortex bereikt, worden cellen in de cortex geactiveerd en tot delen aangezet, wat leidt tot de vorming van een knolprimordium. In de cellen van het knolprimordium aangekomen komen de bacteriën vrij uit de infectiedraden waar ze zich, omgeven door een membraan afkomstig van de plant, vermenigvuldigen in de gastheercellen. Het knolprimordium ontwikkelt zich vervolgens verder tot een knol en de bacteriën differentiëren tot hun stikstofbindende vorm.

De initiatie en coördinatie van deze processen vereist een "moleculaire dialoog" tussen de twee partners. De plant scheidt o.a. flavonoïden uit die de bacterie aanzetten tot het produceren van specifieke signaalmoleculen, de nodulatie factoren (Nod factoren), die op hun beurt een essentiële rol spelen bij zowel knolprimordiumvorming als het infectieproces. Hoe Nod factoren het complexe proces van knolvorming reguleren is een van de kernthema's in het onderzoek naar de plant-*Rhizobium* interactie (zie hoofdstuk 1). Nod factoren bestaan uit 4 of 5 chitine-eenheden (β-1,4-verbonden *N*-acetylglucosamine groepen) met een vetzuurketen gekoppeld aan de eindstandige niet-reducerende glucosamine. De exacte structuur varieert per *Rhizobium* soort en er kunnen specifieke decoraties aan de eindstandige glucosamine-eenheden aanwezig zijn, zoals een acetaat- of sulfaat-groep. Deze decoraties spelen een belangrijke rol in de gastheerspecificiteit van de plant-*Rhizobium* interactie. Alleen bepaalde combinaties van *Rhizobium* bacteriën en vlinderbloemige planten

zijn in staat een succesvolle symbiose aan te gaan. Bijvoorbeeld, *Rhizobium leguminosarum* biovarieteit *viciae* bacteriën kunnen knolvorming induceren op erwt, maar niet op klaver. Terwijl *Rhizobium leguminosarum* bv. *trifolii* bacteriën wel knolvorming induceren op klaver maar niet op erwt. Van alle responsen die Nod factoren induceren in de plant, blijkt het infectieproces de meest stringente eisen te stellen aan de Nod factor structuur. Het feit dat de activiteit van Nod factoren afhankelijk is van hun structuur en het feit dat ze in zeer lage concentraties (nano- tot picomolair) actief zijn suggereert dat Nod factoren herkend worden door specifieke receptoren van de gastheerplant.

Het ontrafelen van de moleculaire basis van deze specifieke Nod factor herkenning vormde het hoofddoel van het onderzoek beschreven in dit proefschrift. Hiervoor is er gebruik gemaakt van een natuurlijke variatie in erwt, waar het *SYM2* gen van een wilde erwtensoort uit Afghanistan is gevonden dat knolvorming op een Nod factor structuur afhankelijke manier reguleert. Erwten met het *SYM2* gen van Afghanistan erwt (*SYM2*^{A}) kunnen alleen knollen maken wanneer de bijbehorende *Rhizobium* bacteriën het *nodX* gen bevatten. Dit bacteriële gen koppelt een acetaat groep aan het reducerende uiteinde van de Nod factoren. *Rhizobium leguminosarum* bv. *viciae* bacteriën die het *nodX* gen niet bevatten blijken op Afghanistan erwt specifiek geblokkeerd in het infectieproces. De aanwezigheid van het *SYM2* gen van Afghanistan is dus gecorreleerd aan een specifieke Nod factor structuur nodig voor infectiedraadvorming. Dit suggereert dat het SYM2^{A} eiwit betrokken is bij de herkenning van *nodX* gemodificeerde Nod factoren en mogelijk een specifieke Nod factor receptor is.

Positionele klonering in erwt wordt echter gehinderd door het feit dat erwt een groot genoom heeft (~1,5x groter dan het menselijk genoom) en moeilijk te transformeren is. Daarom is gekozen voor een op synteny gebaseerde positionele klonering in de evolutionair nauwverwante vlinderbloemige model plant *Medicago truncatula* (Medicago). Deze strategie is gebaseerd op het feit dat overeenkomstige genen (orthologen) in dichtverwante organismen vaak op overeenkomstige locaties in de genomen te vinden zijn. In hoofdstuk 2 is de mate van synteny tussen erwt en Medicago in het *SYM2* gebied onderzocht. Dit heeft geleid tot de identificatie en afbakening van een ~350 kb grote regio in Medicago die het *SYM2*-orthologe gebied representeert. De genetische kartering van 8 gen-specifieke markers uit dit *SYM2*-orthologe gebied wijst erop dat de genomen van erwt en Medicago in deze regio een geconserveerde gen-inhoud hebben. Deze resultaten ondersteunen het idee dat Medicago gebruikt kan worden als model-organisme om genen te kloneren uit erwt.

Aangezien *SYM2* een natuurlijke variatie in een wilde erwtensoort vertegenwoordigt, kan een vergelijking van de basepaarvolgorde (sequentie) van het DNA uit het *SYM2* gebied tussen *SYM2*^{A}-wel en -niet bevattende erwtensoorten niet zomaar gebruikt worden om het betreffende gen te identificeren. Daarom is gezocht naar een efficiënte manier om te achterhalen welke genen uit het *SYM2*-orthologe gebied van Medicago een rol spelen bij het

infectieproces. Een effectieve manier om de functie van genen op te helderen is de zogenaamde RNA interference (RNAi) techniek. Deze techniek is gebaseerd op het feit dat introductie van dubbelstrengs RNA leidt tot een sequentie-specifieke afbraak van het overeenkomstige boodschapper RNA (mRNA), waardoor het gecodeerde gen-product (gedeeltelijk) uitgeschakeld wordt. In hoofdstuk 3 wordt aangetoond dat de introductie van zogenaamde haarspeld-constructen, die leiden tot de vorming van dubbelstrengs RNA, via *Agrobacterium rhizogenes* gebaseerde transformatie een effectieve manier is om genen uit te schakelen in de wortels van zowel Medicago als *Arabidopsis thaliana* (zandraket). *Agrobacterium rhizogenes* gebaseerde transformatie heeft als voordeel dat het een relatief snelle methode is om genetisch gemodificeerde (transgene) wortels te maken.

In hoofdstuk 4 wordt deze methode gebruikt om kandidaat genen uit het *SYM2*-orthologe gebied van Medicago uit te schakelen en hun rol in het infectieproces te bestuderen. In dit gebied blijken opvallend veel genen te liggen, die coderen voor eiwitten welke een rol zouden kunnen spelen in de herkenning (receptoren) van signaalmoleculen. Twee van deze genen, *LYK3* en *LYK4*, blijken specifiek betrokken te zijn bij infectiedraad vorming. Door gebruik te maken van een *Sinorhizobium meliloti* stam die een Nod factor maakt met een veranderde vetzuurketen, kon worden aangetoond dat de blokkade van infectiedraadvorming als gevolg van het (gedeeltelijk) uitschakelen van *LYK3/4* gecorreleerd is aan de afwijkende structuur van de Nod factor. Dit suggereert dat *LYK3/4* betrokken is bij Nod factor herkenning. *LYK3* en *LYK4* lijken sterk op elkaar en coderen voor zogenaamde receptor kinases, die een signaal van buiten de cel kunnen waarnemen en verder signaleren naar effector-eiwitten in de cel. In het gedeelte van het eiwit dat betrokken is bij de herkenning van signalen van buiten de cel bevatten LYK3 en LYK4 twee karakteristieke LysM domeinen. Van LysM domeinen is gepostuleerd dat ze betrokken zijn bij de binding van chitine-achtige verbindingen. Deze karakteristiek, samen met de Nod factor structuur afhankelijke regulatie van infectiedraad vorming, suggereert dat LYK3/4 Nod factoren bindt en daarmee een van de lang gezochte Nod factor receptoren is. Deze functioneert als het ware als een slot op de plant waarvoor de sleutel van de bacterie, de Nod factor, nodig is om de plant binnen te komen.

Om een functionele knol te maken moeten de vorming van het knolorgaan en het infectieproces door de bacteriën nauwkeurig op elkaar afgestemd zijn. In alle vlinderbloemige mutanten die tot dusver gekarakteriseerd zijn is het verlies van Nod factor geïnduceerde responsen in de wortelharen altijd gekoppeld aan verlies van het vermogen om een knolprimordium te vormen. Dit heeft geleid tot de hypothese dat Nod factor perceptie in de epidermis een secundair signaal genereert dat vervolgens corticale cellen aanzet tot deling. Dit zou inhouden dat een plant die alleen in de epidermis een functioneel Nod factor signaleringsmechanisme bezit, maar niet in de cortex, toch instaat zou zijn om corticale cellen te activeren. Om dit te toetsen is in hoofdstuk 5 een essentiële component van het Nod factor signaleringsmechanisme, de NODULATIE RECEPTOR KINASE (*NORK*), exclusief in de

epidermis tot expressie gebracht. Deze planten bevatten dus geen functioneel Nod factor signaleringsmechanisme in de binnenste cellagen. Het blijkt dat *Rhizobium* bacteriën instaat zijn om corticale celdelingen te induceren in de wortels van deze planten. Dit toont aan dat Nod factor perceptie en signalering in de epidermis leidt tot de aanmaak van secundaire signaalmoleculen die vervolgens responsen induceren in de binnenste cellagen. Op deze manier is een strikte koppeling tussen een succesvolle infectie en de ontwikkeling van het knolorgaan mogelijk. Wat voor soort secundaire signalen hierbij betrokken zijn is nog niet bekend.

Er waren verschillende aanwijzingen dat Nod factor perceptie en signalering, behalve betrokken te zijn bij de initiële stappen van het knovormingsproces, ook een rol speelt in de knol. Zo was er bijvoorbeeld aangetoond dat de bacteriële *nod* genen, die verantwoordelijk zijn voor het maken van de Nod factoren, actief zijn in de knol in het gebied waar de bacteriën vrijkomen uit de infectiedraden en zich beginnen te vermenigvuldigen. Om inzicht te krijgen in de rol die Nod factor signalering in de knol speelt is gebruik gemaakt van de essentiële Nod factor signaleringscomponent *NORK*. In hoofdstuk 6 wordt aangetoond dat *NORK* sterk tot expressie komt in de knol en dat de plek waar dit gebeurt samenvalt met de plaats waar de bacteriële *nod* genen actief zijn. Omdat volledige uitschakeling van *NORK* leidt tot een blokkade van het knolvormingsproces in een heel vroeg stadium, moest een alternatief gevonden worden om de functie van dit gen in de knol te achterhalen. Door gebruik te maken van het feit dat RNAi kan leiden tot een gedeeltelijke uitschakeling van een gen en door *NORK*-expressie onder een ander controle-mechanisme te zetten kon worden aangetoond dat NORK een rol speelt bij de overgang van infectiedraadgroei naar het vrijlaten van de bacteriën uit de infectiedraad in de cellen van de knol. Dit suggereert dat Nod factor perceptie en signalering een rol speelt in dit proces.

Aan het eind van dit proefschrift, in hoofdstuk 7, worden de belangrijkste resultaten van het beschreven onderzoek samengevat en bediscussieerd.

Dankwoord

Het proefschrift dat u zojuist heeft doorgelezen is het resultaat van vier jaar AIO-schap bij de vakgroep Molbi. Dit proefschrift was natuurlijk nooit geworden tot wat het is zonder de hulp en steun van anderen. Ik wil dan ook iedereen bedanken die hieraan op enige manier heeft bijgedragen en een aantal mensen in het bijzonder. Allereerst mijn directe begeleider en co-promotor René Geurts. René, jouw kennis en enthousiasme voor het onderwerp en vernieuwende kijk op het onderzoek hebben mij altijd erg gemotiveerd en jouw inbreng heeft er waarschijnlijk het meest toe bijgedragen dat ik gekomen ben tot waar ik nu ben. Bedankt! Verder wil ik mijn promotor Ton Bisseling bedanken voor de mogelijkheid om dit onderzoek uit te voeren, voor je kritische blik en de nuttige discussies, niet in de laatste plaats bij het schrijven van de artikelen en het proefschrift.

Daarnaast wil ik ook Carolien Franken bedanken voor haar hulp bij de proeven, zoals de vele transformaties en het maken van oneindig vele coupes. Zonder jouw hulp had ik nooit de resultaten kunnen bereiken die dit boekje maken tot wat het is. Ook de vijf studenten die ik heb mogen begeleiden tijdens mijn AIO-periode zou ik willen bedanken voor hun inbreng en prettige samenwerking. Koen, Paul en Max bedankt en veel succes met jullie verdere carrière. Ram and Xiaoxiao, thanks a lot for your help with the experiments and the best of luck in your future life and careers. I would also like to thank Jun for her contribution to the research during her stay at the lab. The best of luck to you. Verder bedank ik uiteraard ook de mensen die als co-auteur en in de acknowledgements bij de diverse hoofdstukken genoemd staan voor hun bijdrage aan dit boekje. Met name Mark Hink en Jan-Willem Borst voor hun assistentie bij de fluorescentie microscopie; Rossana thanks for doing the *in situ* hybridisation and Elena Federova for her expertise and willingness to make the EM pictures. Naast mijn twee paranimfen Jeroen en Patrick wil ik verder iedereen bij Molbi bedanken voor hun hulp op wat voor manier dan ook en vooral voor de gezellige tijd op het lab, bij de koffie en op de borrels!

Niet onbelangrijk was er naast het werk ook nog de nodige ruimte voor ontspanning, waarvoor ik alle vrienden, en met name de Jugend, wil bedanken voor de vele avonden in de Vlaam, de feesten, de BBQ's en het gamen. Ik hoop dat er nog vele gezellige tijden, met bier en vlees, mogen volgen!

In het bijzonder wil ik ook mijn ouders van harte bedanken voor mijn fijne jeugd en dat ze me de mogelijkheid hebben gegeven om met te ontwikkelen tot wie ik nu ben. Pap en mam, van harte bedankt voor alle steun tijdens al die jaren!

Als laatste gaat mijn dank natuurlijk uit naar Mandy. Lieve Mandy, ik vind het geweldig zoals jij je hebt weten aan te passen aan het Wageningse leven sinds het begin van mijn AIO-

periode toen we zijn gaan samenwonen in het toen nog zover van Stein gelegen Wageningen. Met jouw liefde en zorg heb je me door de soms moeilijke tijden van het AIO-schap heen gesleept en ondanks het feit dat de nabije toekomst nog niet helemaal helder is hoop ik dat we nog lang bij elkaar mogen zijn om van mekaar te genieten!

Thanks!

Erik

Curriculum vitae

Erik Hubert Maria Limpens werd op 6 april 1976 geboren in het Steinerbos te Stein. Na de RK basisschool Kerensheide in Stein, ging hij naar het gymnasium aan de Scholengemeenschap St. Michiel te Geleen. In 1994 behaalde hij hier met lof het VWO-diploma en in september van datzelfde jaar begon hij met de studie Moleculaire Wetenschappen aan de Wageningen Universiteit. In november 1999 werd met lof het ingenieursdiploma behaald met afstudeervakken bij de vakgroep Fokkerij en Genetica (onder begeleiding van dr. J. Herbergs en prof. dr. E.W. Brascamp) en de vakgroep Moleculaire Biologie (onder begeleiding van dr. H. Franssen en prof. dr. T. Bisseling) en een stage bij het Department of Plant Pathology and Microbiology aan de Texas A&M University in de Verenigde Staten (onder begeleiding van dr. DJ Kim en prof. dr. D. Cook). In januarie 2000 keerde hij terug als AIO bij de vakgroep Moleculaire Biologie aan de Wageningen Universiteit waar hij, onder begeleiding van dr. R. Geurts en prof dr. T. Bisseling, het onderzoek uitvoerde dat leidde tot dit proefschrift.

List of publications

Ruyter-Spira CP, Herbergs J, Limpens E, Marsh JA, van der Poel JJ, Ayoubi TA, Groenen MAM: **Nucleotide sequence of the chicken *HMGI-C* cDNA and expression of the *HMGI-C* and *IGF1* genes in autosomal dwarf chicken embryos.** *Biochim Biophys Acta* 1998, **1399**: 83-87.

Gualtieri G, Kulikova O, Limpens E, Kim DJ, Cook DR, Bisseling T, Geurts R: **Microsynteny between pea and *Medicago truncatula* in the *SYM2* region.** *Plant Mol Biol* 2002, **50**:225-235.

Limpens E, Bisseling T: **Signaling in symbiosis.** *Curr Opin Plant Biol* 2003, **6**:343-350.

Limpens E, Franken C, Smit P, Willemse J, Bisseling T, Geurts R: **LysM domain receptor kinases regulating rhizobial Nod factor-induced infection.** *Science* 2003, **302**:630-633.

Choi HK, Kim D, Uhm T, Limpens E, Lim H, Mun JH, Kalo P, Penmetsa RV, Seres A, Kulikova O, Roe BA, Bisseling T, Kiss GB, Cook DR: **A sequence-based genetic map of *Medicago truncatula* and comparison of marker colinearity with *M. sativa*.** *Genetics* 2004, **166**:1463-1502.

Limpens E, Ramos J, Franken C, Raz V, Compaan B, Franssen H, Bisseling T, Geurts R: **RNA interference in *Agrobacterium rhizogenes* transformed roots of Arabidopsis and *Medicago truncatula*.** *J Exp Bot* 2004, **55**: 983-992.